NEUROPLASTICITY MECHANISMS IN RAT AND HUMAN CORTEX

CHARACTERIZATION AND COMPARISON OF NEUROPLASTICITY MECHANISMS IN RAT AND HUMAN CORTEX

By

JOSHUA G.A. PINTO, MBA, B.S

A Thesis Submitted to the School of Graduate Studies in Partial Fulfillment of the Requirements for the Degree Doctor of Philosophy

DOCTOR OF PHILOSOPHY (2013) McMaster University
(Neuroscience) Hamilton, Ontario

Title: Proteomic evaluation of the mechanisms that control visual system plasticity

AUTHOR: Joshua G.G. Pinto, MBA (McMaster University), B.S. (Centenary College of Louisiana)

SUPERVISOR: Professor Kathryn M. Murphy

NUMBER OF PAGES: xii, 159

ABSTRACT

Neuroplasticity describes the capacity and mechanisms underlying experience driven changes in function and organization of neural connections. Animal models have uncovered many mechanisms that control neuroplasticity, such as the E-I balance and structural brakes, and have identified the timing of critical periods in development when the degree of plasticity is high. Ocular dominance plasticity in visual cortex is the preeminent model for studying plasticity. Its a useful paradigm because it links from molecular mechanisms to anatomical and physiological changes, to visual perception and the human visual disorder of lazy-eye (amblyopia). Treatments for amblyopia have traditionally had poor efficacy (~50%), but recently, a number of interventions have shown they are able to re-instate ocular dominance plasticity in older rats. Little is known, however, about developmental translation of the mechanisms that control the critical period plasticity between rat and human. To address this, I conducted a series of experiments in human and rat cortices to characterize and compare development of a set of proteins involved in regulating neuroplasticity. First, I used Western blot analysis to quantify the development of Synapsin, Synaptophysin, PSD-95, and Gephyrin in rat and human cortex, compared the development of these proteins between species and determined the translation from rat to human cortical development. These studies revealed that total protein expression is comparable in rat and human visual cortex during early development, and that synaptic age is similar between species at comparable stages of visual system development. Second, I quantified development of GABAergic mechanisms in human visual cortex across the lifespan. I found complex and prolonged changes in these mechanisms that help to highlight stages of human cortical development. Third, I quantified the effects of reinstating ocular

dominance plasticity in adult rats using fluoxetine on the mechanisms known to facilitate the onset and closure of the critical period. This study showed that fluoxetine reduces the brakes on plasticity, and re-set the E-I balance. The results from my Ph.D. thesis experiments provide detailed characterization of synaptic development in human visual cortex, and a new comparison for studying humans and rat cortical development. Together my studies have found new insights about the capacity for neuroplasticity in human visual cortex, a new way to translate cortical developmental stages between species, and that re-instating plasticity in adult cortex effects both the brakes and plasticity promoting mechanisms..

ACKNOWLEDGEMENTS

There are a number of people I would like to thank who supported me throughout my PhD, but I will keep this brief since I am typically a man of few words. First of all, I would like to thank Kathy for her support and guidance through the process. Your mentorship has helped me develop into the leader that I am today. Dave, thank you for all of your help, in particular the data analysis, I could not have done it without you. To Ram, Bruce, and more recently, Joe, thank you for your support. I would like members of the the murphy lab for always making it an fun and enjoyable environment to work in. In particular, I want to thank Kate for all of the help she has provided over the last number of years. Thank you to my parents for supporting me through the PhD, and my brother David who was always there to help me take my mind off science. I want to thank all of my friends from the minds program, the phoenix and beersby kept it enjoyable over the years. Last, and certainly not least, I would like to thank Alison and Scout. Alison, you are the reason that I always strive to be the best, and I am confident that I will achieve all of my goals with you by my side. Finally Scout, I want to thank you for always putting my work life in perspective, reminding me that my work was inconsequential, and that I should just take you for a walk instead of getting anything productive accomplished.

Table of Contents

LIST OF FIGURES

LIST OF TABLES

LIST OF ABBREVIATIONS

BDNF	Brain derived neurotrophic factor
E-I	Excitatory-Inhibitory
EM	Electron Microscopy
EPSC	Excitatory Post-Synaptic Current
GABA	Gamma-aminobutyric acid
GAD65	Glutamic acid decarboxylase 65
GAD67	Glutamic acid decarboxylase 67
GAPDH	Glyceraldehyde 3-phosphate dehydrogenade
GluA	α-amino-3-hydroxy-5-methyl-4-isoxazolepropionic acid
GluN	N-Methyl-D-aspartic acid
IPSC	Inhibitory Post-Synaptic Current
KCC2	Potassium-chloride transporter
MD	Monocular Deprivation
mGlu	Metabotropic glutamate
NKCC1	Sodium-potassium-chloride transporter
PCA	Principal Component Analysis
PSD-95	Post-Synaptic Density 95
SVD	Singular Value Decomposition
VGlut	Vesicular glutamate transporter
VAchT	Vesicular acetylcholine transporter
VGAT	Vesicular GABA transporter

PREFACE

This thesis is partly comprised of a paper (Chapter 2) that is in review in Frontiers in Neural Circuits. This chapter was a collaboration between myself, David Jones, and Kathryn Murphy. I was the lead on formulating and performing the experiments, analyzing the data, and preparing the manuscript.

This thesis is partly comprised of a paper (Chapter 3) that is in preparation for submission to Science Translational Medicine. This chapter was a collaboration between myself, David Jones, and Kathryn Murphy. I was the lead on formulating and performing the experiments, analyzing the data, and preparing the manuscript.

This thesis is partly comprised of a paper (Chapter 4) that is published in Frontiers in Cellular Neuroscience. This chapter was a collaboration between myself, Kyle Hornby, David Jones, and Kathryn Murphy. I was the lead on formulating and performing the experiments, analyzing the data, and preparing the manuscript.

Chapter 1.

General Introduction

Development of human cerebral cortex is a complex process that is shaped by interactions between the nervous system and our environment. There are known periods early in life when development is accelerated, and neural connections are readily formed and refined. Our understanding of the basic neural mechanisms that govern cortical development is predominantly based on work from animal models, while our understanding of the development of behavior is dominated by human studies. In this introduction, I will discuss theories of cortical development, synaptic complexity, and synaptic plasticity during development and in adult visual cortex. This will build the foundation for the studies in my thesis which aim to characterize basic neural mechanisms of plasticity, and compare those mechanisms between animals and humans.

Theories of Cortical Development

Neural connections transmit the information that allow us to perceive and react to our environment. At the center of every connection is a synapse, where information is transmitted from one neuron to another. There are a number of theories synaptic development in the cortex, and these theories have shaped our understanding of the perceptual and cognitive developmental processes. The two most influential theories of cortical synaptic development are the cascade theory, and the integrated network theory. These two theories analyzed different, yet complementary components of the synapse, to quantify the timing of synaptic development across the cortex.

The Cascade Theory

The cascade theory of synaptic development was proposed by Huttenlocher et al. (1990, 1997). It suggests that the cortex develops in a wave-like manner, with primary sensory areas

developing first, followed by higher-order cognitive areas. These studies used electron microscopy (EM) of human cortical areas to count the number of anatomical synapses, which were defined as the presence of a pre- and post-synaptic terminal, and the presence of at least 2 synaptic vesicles. This theory complements behavioral observations of sensory skills that indicate sensory skills showing that these perceptions develop well before higher order skills such as language acquisition and social skills. As such, it has shaped the way cognitive neuroscientists think about synaptic development. This theory, however, does have its limitations. First, EM is extremely time consuming, making it difficult to collect a large sample. Second, it measures the structural appearance of synapses, and it is known that structurally mature synapses can be functionally silent (Beique et al., 2006). The cascade theory of development has had a pronounced effect on the understanding of developmental neuroscience, but it must be placed into context with its known methodological limitations.

The Integrated Network Theory

The integrated network theory of synaptic development was proposed by Lidow et al., (1991). It suggests that the cortical areas develop in concert with one another, or as an integrated network. The study used autoradiography to quantify the expression levels of a number of receptor classes (Serotonergic, Dopaminergic, GABAergic, etc.) across sensory, motor, and association cortices in rhesus monkey. Unlike the cascade theory, the integrated network theory does not support the timeline for the development of behavioral skills, and, therefore, has not had as much influence on our understanding of developmental neuroscience. Although Lidow et al, (1991) quantified multiple synaptic markers, the study is not without limitation. The study only analyzed post-synaptic receptors, which make up a small part of the total synaptic proteome. It

is known that maturation of both pre- (Renger et al., 2001) and post-synaptic (Beique et al., 2006) transmission is required for normal synaptic function.

Taken together, these theories demonstrated that components of the synapse may follow different developmental trajectories during cortical maturation. This highlights a need to study both pre- and post-synaptic functional components, to gain a more comprehensive understanding of how synapses develop across the cortex. This approach will help to elucidate whether synaptic development in the cortex emerges as a cascade or an integrated network.

Synaptic Complexity

Synaptic connections transmit information from one neuron to another and link neurons together into neural circuits. Synapses are structurally complex, transmitting electrical and chemical information from an action potential by way of pre-synaptic to post-synaptic conductance. The pre- and post-synaptic terminals of electrical synapses are separated by only a couple of nanometers, whereas the terminals of chemical synapses are separated by 20-40 nm. Chemical synapses require the interaction of thousands of proteins to ensure the correct information is signaled from the pre-synaptic to post-synaptic terminals. The next sections will discuss synaptic complexity in the context of pre- and post-synaptic structure of the chemical synapse.

Pre-Synaptic Structure

There are hundreds of proteins contained in the pre-synaptic proteome (Bayes & Grant, 2009). These proteins interact with one another to transmit an action potential to the post-synaptic terminal through the release of neurotransmitters. Neurotransmitters are released by synaptic vesicles, compartments that contain neurotransmitters, which are constantly cycled

within the pre-synaptic terminal. The two major processes involved in synaptic vesicle cycling are exocytosis, which is the release of neurotransmitters from vesicles, and endocytosis, the process of vesicle re-uptake into the pre-synaptic terminal. There are a number of steps that mediate both exo- and endo-cytosis, and each step requires interactions between a number of proteins.

The first process involved in exocytosis is the loading of neurotransmitters into synaptic vesicles. A group of proteins called vesicular transporters load specific neurotransmitters into these vesicles. For example, VGlut loads glutamate (Wojcik et al., 2004), VAchT loads acetylcholine (Song et al., 1997), and VGAT loads GABA (McIntire et al., 1997; Sagne et al., 1997). Once synaptic vesicles are loaded, they cluster in the pre-synaptic terminal waiting to be released. Synapsin, the most abundant peripheral membrane protein (Huttner et al., 1983) is known to regulate the clustering (Bahler et al., 1990), and abundance (Bykhovskaia et al., 2011) of synaptic vesicles at the pre-synaptic terminal. Synapsin is also the most specific marker for pre-synaptic terminals, since it is present at all GABAergic and glutamatergic synapses (Micheva et al., 2010). Once the vesicles have been primed for release, they fuse with the active zone of the pre-synaptic terminal and are released into the synaptic cleft. For fusion to take place, SNARE complexes form between synaptic vesicle proteins such as SNAP25, syntaxin, and synaptobrevin (Lang & Jahn 2008), and the plasma membrane. Finally, neurotransmitters are released into the synaptic cleft, at a rate which is regulated by synaptotagmins through their action as calcium ion influx sensors (Sudhof, 2008).

Synaptic vesicle endocytosis occurs through a 5-step process mediated by clathrin, a protein that coats vesicles (Pearse, 1976). The first step in this process is initiation, when FCHO

proteins bind to the plasma membrane and recruit AP2 proteins (Henne et al., 2010). Next, the AP2 proteins select the cargo for the vesicles (Traub, 2003), then recruit clathrin to form a coat around the vesicle. Synaptic vesicle budding is then initiated by a fission complex that is composed of dynamin (Pucadyil & Schmid, 2009) and the vesicles are then endocytosed. Finally, the clathrin coat is removed by Auxilin when it recruits the ATPase, hsp70c (Ungewickell et al., 1995). The synaptic vesicle is once again ready for exocytosis and the clathrin complex is ready to endocytose another vesicle. Recent work has shown that endocytosis is regulated by Synaptophysin, the most abundant integral membrane protein on synaptic vesicles (Jahn et al., 1985; Wiedenmann & Franke, 1985; Takamori et al., 2006). Synaptophysin regulates the kinetics of synaptic vesicle endocytosis (Kwon & Chapman, 2011), as well as synaptic vesicle retrieval through interactions with synaptobrevin (Gordon et al., 2011). Synaptic vesicle cycling is a complex process that requires a number of precise protein interactions to ensure the correct information is transmitted, however, the potential for vesicle exo- and endo-cytosis can be captured by quantifying the expression of Synapsin and Synaptophysin, respectively.

Post-Synaptic Structure

There are approximately 2,000 distinct proteins contained within the post-synaptic density (Trinidad et al., 2008). These proteins are involved in creating the post-synaptic potential, which either initiates or inhibits a future action potential. Each synapse contains a subset of these 2,000 proteins, which help to form its synaptic identity. At the forefront of the post-synaptic terminal are the receptors. There are a number of classes of neuronal receptors, including adrenergic, serotonergic, dopaminergic, glycinergic, glutamatergic, GABAergic. These receptors differ in

what ions they selectively allow through. Each receptor class typically contains both fast acting ionotropic, as well as slower metabotropic receptors. When activated, the ionotropic receptors allow for the free flow of ions in and out of the post-synaptic membrane, whereas metabotropic receptors signal a second messenger cascade. The speed at which the flow of ions, and the second messenger cascade take place is what separates these receptor classes into mediating fast, and slow post-synaptic potentials. For example, the ionotropic $GABA_A$ receptors mediate fast GABA IPSCs, while the metabotropic $GABA_B$ receptors mediate slower IPSCs. The two main classes of receptors found in the cerebral cortex are excitatory glutamatergic, and inhibitory GABAergic receptors.

Glutamatergic synapses have tremendous receptor diversity, as well as a complex post-synaptic density, which are both required to formulate the post-synaptic potential. There are 3 classes of ionotropic glutamate receptors, GluA, GluN, and kainate, but only one class of metabotropic glutamate receptors, mGlu. Each of these receptor classes has a number of subunits, for example, GluA receptors have 4 subunits and GluN receptors have 3 subunit types (Jackson & Nicoll, 2011), which results in the functional receptors having tremendous stoichiometric diversity. These receptors are located on the surface of dendritic spines, and linked to the dendritic cytoskeleton through an array of protein-protein interactions in the post-synaptic density. The PSD-95/SAP family of proteins anchor the ionotropic GluN receptors directly (Kornaue et al., 1995), and GluA receptors through stargazin (Chen et al., 2000). The PSD95 family then binds to the GKAP family of proteins (Kim et al., 1997), which subsequently binds with the PDZ domain of SHANK proteins (Boeckers et al., 1999; Naisbitt et al., 1999). mGluRs are anchored by a protein class called HOMER that link this subset of glutamatergic

receptors with SHANK (Tu et al., 1999). SHANK proteins are then responsible for linking the post-synaptic density with the actin cytoskeleton (Boeckers et al., 2001). Clustering of post-synaptic glutamatergic receptors gives rise to the EPSCs, and requires the dynamic interaction between this array of proteins in the post-synaptic density.

GABAergic synapses have even more receptor diversity than their glutamatergic counterparts. The ionotropic $GABA_A$ receptors have 19 known subunits (Olsen & Sieghart, 2009), while the metabotropic GABAB receptor have 2 subunits (Bettler et al., 2004). Variations in $GABA_A$ receptor subunit composition, confer different kinetics, binding affinity, and channel gating properties . GABAergic receptors are present at a number of locations, including the cell body, dendritic shaft, and axon hillock, with different subunits being preferentially expressed at each location (Hensch, 2005). Much less is known about the structure and formation of the GABAergic post-synaptic density, relative to its glutamatergic counterpart. It is known that Gephyrin clusters $GABA_A$ receptors, analogous to PSD-95 clustering of glutamatergic receptors, but the mechanism by which Gephyrin clusters $GABA_A$ receptors is not well understood. Gephyrin could act in a manner similar to PSD-95, where it directly, and indirectly interacts with the receptor based on the subunit composition. There is also evidence that Gephyrin colocalizes with $GABA_A$ γ 2 receptors (Tretter et al., 2009), which would provide a direct interaction between Gephyrin and $GABA_A$ receptors. Gephyrin has also been shown to negatively regulate the diffusion of $GABA_A$ receptors (Jacob et al., 2005), suggestive of an indirect interaction between the pair. A better understanding of how the post-synaptic density links receptors to the cytoskeleton at GABAergic synapses is beginning to unfold (Tyagarajan & Fritschy, 2010), and

our limited knowledge of the protein-protein interactions that take place in GABAergic synapse should highlight their complexity.

There are close to 3,000 proteins that can form the identity of a synapse, and collections of synapses help to form functional neural circuits. The functioning of the human cortex is astonishing due to the complexity of the protein-protein interactions that take place within each of its 100-500 trillion synapses. There are, however, functionally relevant sets of synaptic proteins, that can provide new insight into the development of this complex network, and the mechanisms that control neural plasticity.

Developmental synaptic plasticity

Synaptic plasticity reflects the capacity for the connection between two neurons to change, either strengthen or weaken, depending on the activity of the neurons. During development, there are periods of heightened plasticity known as critical periods, when experience drives activity that shapes the maturation of the central nervous system. Sensory experience, including visual, auditory, and tactile stimulation, has the strongest effect on maturation of the cortical areas, whereas, non-sensory experience such as maternal care has been shown to have a different effect on cortical maturation. The timing of critical periods is well defined across sensory cortices in animal models, however, much less is known about these periods in non-sensory cortices, and in humans. To better understand this I will discuss models of the critical period, mechanisms that control the critical period, and disorders that can manifest during the critical period.

Models of Critical Period Plasticity

There are a number of models of critical period plasticity in sensory cortices that have been developed over the last half century, including ocular dominance plasticity in visual cortex, and layer 2/3 single whisker experience in somatosensory cortex (Stern et al., 2001). These models have built our understanding of the timing, duration, and magnitude of sensitive periods during development. Most of the work on critical periods has been conducted on sensory areas, however, experience can also drive the maturation of cortical connections in non-sensory areas. For example, maternal separation early in development adversely affects stress response later in life (Meaney, 2001; Liu et al., 1997; Monroy et al., 2010), but we know much less about the neural changes and plasticity mechanisms that underlie these stress-related changes.

The seminal work of Hubel and Wiesel (1963) built the foundation for ocular dominance plasticity as the preeminent model for studying developmental plasticity. For the purpose of this thesis I will focus on ocular dominance plasticity as the primary model of experience-dependent developmental plasticity.

Ocular dominance plasticity is an appealing paradigm for studying critical period development because of the:

A) **Ease of manipulation** - Monocular deprivation is a simple, highly reproducible manipulation

B) **Immediacy of response** - There are rapid physiological (Hubel & Wiesel, 1963; Hubel & Wiesel, 1970) and anatomical (Antonini & Stryker, 1993; Shatz & Stryker, 1978) changes after manipulation

C) **Link with disease** - Monocular deprivation is analogous to deprivation amblyopia, a disorder with a known onset during the critical period.

The critical period for ocular dominance plasticity has been well defined across a number of species; P20-45 in rodents (Fagiolini et al., 1994), 4-16 weeks in cats (Olsen & Freeman, 1980), and P35-60 in ferrets (Issa et al, 1999).

Although the timing of ocular dominance plasticity has been well characterized in a number of animal models, the timing of it in human visual cortex is less clear. Animal models have begun to fully elucidate the molecular biology that regulates critical period plasticity, which is an important step towards linking animal models of critical period plasticity to human development.

Mechanisms Controlling the Critical Period

Distinct mechanisms control the onset and closure of the critical period. Most of these mechanisms have been discovered through the study of ocular dominance plasticity in visual cortex of animals, but it is thought that the fundamental components are common among cortical areas and in different species.

The onset of the critical period is facilitated by a physiological balance between excitation and inhibition (E-I). Early in development the E-I balance is shifted in-favor of excitation, and the maturation of inhibition triggers the onset of the critical period by setting a balance between them (Maffei & Turrigiano, 2008; Morishita & Hensch, 2008). In support of inhibition as the trigger for critical period induction, a number of studies have shown that manipulation of inhibition before the critical period can delay or accelerate the timing of the critical period; knocking out the enzyme that produces the on-demand pool of GABA (GAD65) delays the onset

of the critical period (Fagiolini & Hensch, 2000), increasing BDNF accelerates inhibition and results in a precocious critical period (Hanover et al., 1999), dark rearing decreases BDNF and delays the critical period (Mower, 1991), and benzodiazepine infusion triggers the critical period (Iwai et al., 2003). There are a number of events that occur early in development that could trigger the required increase in inhibition that facilitates the onset of the critical period. The development shift in chloride co-transporters from more NKCC1 to more KCC2 is known to occur early in development, and shifts the response of GABA from depolarizing to hyperpolarizing (Ben-Ari, 2002). The maturation of the $GABA_A$ receptor scaffolding protein, Gephyrin, could also reflect a trigger since it represents the development of GABAergic synapses. Maturation of $GABA_A$ receptor subunit composition increases the speed of the receptor kinetics (Gingrich et al., 1995), which would allow for stronger and sustained inhibitory activity, producing the increase in physiological inhibition required to initiate the onset of the critical period. Studies have shown distinct GABAergic components are required for the onset of the critical period for ocular dominance, such as the GABA synthesizing enzyme GAD65 (Hensch, 2005), and the $GABA_A$ α 1 subunit (Fagiolini, 2004). Characterizing development of the GABAergic proteome and how it balances with mechanisms that control excitation, will provide valuable insights into what components of the system may trigger the onset of the critical period.

The factors that close the critical period for ocular dominance plasticity are not as clear, but recent studies support structural elements of the extracellular matrix as the brakes on plasticity (Bavelier et al., 2010). It has been shown that myelin related proteins inhibit axonal sprouting (McGee et al, 2005), while perineuronal nets form around GABA containing basket-cells

(Pizzorusso et al., 2006), both of which prevent the inhibitory activity necessary to initiate critical period plasticity. Perhaps that increased myelination restricts the formation of new connections, and thereby close the critical period. Understanding the molecular triggers that start the critical period, or that put the brakes on developmental plasticity is an important area of research because manipulating those mechanisms may be the keys to open up new windows of plasticity later in life.

Neuroplasticity Disorders

Neuroplasticity is at the root of a number of disorders including brain injury and stroke, neuropsychiatric, neurodegeneration, and neurodevelopmental disorders. Critical periods during development are times when the degree of plasticity is high and experience rapidly shapes the maturation of the cortex. During these periods, the cortex is in its most vulnerable state and a number of neurodevelopmental disorders manifest during this period. Amblyopia, more commonly called lazy-eye, is perhaps the best understood neurodevelopmental disorder. During the critical period for ocular dominance plasticity normal visual experience matches eye specific inputs to the cortex (Wang et al., 2010), while abnormal visual experience (e.g. cataract, strabismus, or anisometropia) causes amblyopia, which results in reduced visual acuity. Monocular deprivation during the critical period modifies physiological (Hubel & Wiesel, 1963; Hubel & Wiesel, 1970) and anatomical (Antonini & Stryker, 1993; Shatz & Stryker, 1978) connections in primary visual cortex, as neurons shift their responsiveness away from the deprived eye towards the non-deprived eye. This manifests as a loss of visual perceptual abilities including contrast sensitive, and acuity. If visual deprivation extends beyond the critical period

the neural changes become permanent, as do the perceptual deficits. For optimal recovery, vision must be corrected before, or during the critical period.

Autism is another prominent neurodevelopmental disorder whose origin links with the critical period (LeBlanc & Fagiolini, 2011). It is thought that sensory function in autism is adversely affected by an E-I imbalance during the critical period (Marco et al., 2011), which could be caused by either increased GABA concentrations (Dhossche et al., 2002), or decreased GAD expression (Fatemi et al., 2002). In addition, the degree of sensory impairment in children with autism is directly correlated with the degree of social impairment (Kern et al., 2007).

Critical periods during development are a double edge sword, on the one side they facilitate the normal maturation of the cortex, on the other side they allow for adverse events to negatively impact the refinement of connections. Development of more effective therapies to treat these disorders requires a deeper understanding of disease onset during critical periods in development, and the first step towards treatment is identifying interventions that can re-instate critical-period-like plasticity in adult cortex.

Adult Plasticity

Characterizing and comparing the mechanisms that regulate neural plasticity is an important area of study because it holds the promise of allowing neuroscientists to be able to harness neuroplasticity that will lead to better treatments for neurological and psychiatric disorders. Re-instating critical period like plasticity in the adult brain is one of the first steps in re-shaping the cortex, an action that has two clear benefits: First, it can help to promote recovery from neurodevelopmental, neurodegenerative, neuropsychiatric, and cortical injury disease.

Second, it can help to promote learning and memory in adulthood, which will improve healthy aging.

Models of adult plasticity

In recent years, a number of models have shown that environmental and pharmacological interventions can re-instate plasticity in adult visual cortex. Most of these models have focused on re-instating ocular dominance plasticity in rodent visual cortex. Interventions such as dark-rearing (He et al, 2007), chronic fluoxetine administration (Maya Vetencourt et al, 2008), environmental enrichment (Baroncelli et al, 2010), and food restriction (Spolidoro et al, 2011) have been effective in promoting plasticity in adult animals. Across these models, there is a consistent reduction of intracortical inhibition, which is interesting since an increase in inhibition triggers the critical period during development. It will be important to determine how these paradigms effect the E-I balance, as well as the structural elements of the extracellular matrix that put the brakes on plasticity. This will provide evidence on the targeted mechanism of action and help to guide effective translation of these interventions from rodents to humans.

Effectively translating interventions to humans

Translating these interventions from rodents to humans requires an understanding of how the mechanisms that control critical period plasticity develop in human cortex. It is known that there are a number of differences between rodent and human cortex that affect the efficacy of therapeutic interventions between the species (Geerts, 2009). Parallel studies that quantify the mechanisms that control critical period plasticity in rat and humans will begin to uncover the similarities and differences between the species and provide a framework for translating the therapeutic benefit of these interventions from rat to humans.

Summary of the chapters

This thesis builds the argument that with a conservative set of synaptic proteins, we can effectively capture synaptic development and the mechanisms that control critical period plasticity across species.

Chapter 2

- Quantifies changes in a conservative set of synaptic proteins (Synapsin, Synaptophysin, PSD-95, and Gephyrin) across rat visual, somatosensory, and frontal cortex

Chapter 3

- Quantifies the same conservative set of synaptic proteins in human visual cortex and translates protein expression between human and rat

Chapter 4

- Quantifies dev changes in GABAergic mech in human vis ctx

Chapter 5

- Quantifies conservative set of proteins to determine how fluoxetine re-instates ocular dominance plasticity

Chapter 2.

Comparing development of synaptic proteins in rat visual, somatosensory, and frontal cortex

Introduction

During the critical period, substantial changes in expression of pre- and post-synaptic proteins interact with experience to facilitate synaptic development, fine tuning of cortical circuits, and maturation of the cortical connectome. The nascent synaptic proteome provides the ready plasticity that underlies functional development of synapses and cortical circuits. Two influential theories have been proposed to describe how synaptic development proceeds across the cortex: the integrated network and the cascade of development. An integrated network of synaptic development, with cortical areas developing in unison, was proposed when autoradiography of a collection of post-synaptic receptors found common developmental trajectories in different cortical areas (Lidow et al., 1991). In contrast, a cascade of synaptic development, with a system-by-system wave of maturation, was proposed when electron microscopy counts of synapses showed changes starting in primary sensory areas and proceeding to higher order cortical areas (Huttenlocher et al., 1990; Huttenlocher et al., 1997). Those anatomical studies present opposing views on cortical development that raise challenges for current work aimed at comparing detailed maturation of the connectome among cortical areas. We have taken a different approach and quantified the available pool of a small set of pre- and post-synaptic proteins in different cortical areas to capture developmental changes in these building blocks of synapses.

There are nearly 3000 synaptic proteins (Filiou et al, 2010) that provide robust diversity and determine the function of individual synapses. The pre-synaptic proteome has hundreds of proteins (Bayes & Grant, 2009), many of which are directly involved with the cycling of synaptic vesicles. Synapsin and Synaptophysin are the most abundant synaptic vesicle proteins

and have distinct functional roles. They are also the most commonly used markers for pre-synaptic terminals (Micheva et al., 2010), which points to them as good candidates to capture pre-synaptic development. Synapsin is the most specific marker for pre-synaptic terminals (Micheva et al., 2010); it is the major peripheral membrane protein accounting for 6% of the total synaptic vesicle protein (Huttner et al., 1983), regulating the reserve pool of synaptic vesicles available for exocytosis (Bahler et al., 1990), and maintaining the organization and abundance of vesicles at pre-synaptic terminals (Bykhovskaia, 2011). Synaptophysin is the major integral membrane protein accounting for 6-10% of total synaptic vesicle protein (Jahn et al., 1985; Wiedenmann & Franke, 1985; Takamori et al., 2006), regulating the kinetics of synaptic vesicle endocytosis (Kwon & Chapman, 2011), and synaptic vesicle retrieval through its interaction with Synaptobrevin (Gordon et al., 2011). Synapsin is found at all glutamatergic and GABAergic synaptic boutons, while Synaptophysin levels are highest at glutamatergic and very low at GABAergic terminals (Gronborg et al., 2010; Micheva et al., 2010). Importantly, the development of Synapsin and Synaptophysin expression is required for the maturation of pre-synaptic function and stabilization of pre-synaptic boutons (Hopf et al., 2002). Furthermore, the balance between these proteins will effect vesicle cycling and likely impact the probability of transmitter release, especially after strong or sustained stimulation.

The post-synaptic proteome contains about 2,000 proteins (Collins et al., 2006; Trinidad et al., 2008) and in the cortex it is dominated by proteins for glutamatergic (GluA, GluN) and GABAergic ($GABA_A$) receptors. There is tremendous diversity in the subunit makeup of these classes of receptors, and the complexity is increased by the many intracellular components for receptor trafficking, functioning, and signaling. GluA receptors have 4 subunit types (Jackson &

Nicoll, 2011), GluN receptors have 3 subunit types, GluNR1, GluNR2, and GluNR3, with multiple variants and distinct isoforms (Jackson & Nicoll, 2011), and $GABA_A$R have 19 subunit types (Sieghart, 1995; Olsen & Sieghart, 2009). This post-synaptic complexity is reduced, however, at the level of scaffolding proteins where PSD-95 anchors GluA and GluN receptors, and Gephyrin anchors $GABA_A$ receptors. Furthermore, PSD-95 and Gephyrin are the most commonly used markers for excitatory and inhibitory synapses, which points to them as good markers to capture post-synaptic development.

PSD-95 is required for functional GluA and GluN containing synapses, and when knocked-out, there is an increase in the number of silent synapses (Beique et al., 2006). Gephyrin knock-down decreases the number of $GABA_A$ receptor clusters, showing that it is required for stabilization of GABAergic synapses (Yu et al., 2007). Both PSD-95 and Gephyrin are motile among a localized group of synapses (Dobie & Craig, 2011; Gray et al., 2006), with the total amount of PSD-95 or Gephyrin limiting the number of synapses (Keith and El-Husseini, 2008). At any given time, however, only a fraction of the protein is located at the synapse. In addition, interactions between PSD-95 and Gephyrin regulate the number of excitatory and inhibitory synapses and affect the physiological E-I balance (Keith and El-Husseini, 2008, Lardi-Studler et al., 2007, Prange et al., 2004). The E-I balance shifts during early development (Dorrn et al., 2010), and it is important for triggering the start of the critical period for ocular dominance plasticity in visual cortex (Hensch & Fagiolini, 2005). Taken together, these attributes point to PSD-95 and Gephyrin as good post-synaptic markers to capture development of excitatory and inhibitory synapses and the E-I balance.

Although there is remarkable diversity in the synaptic proteome, quantifying just a few markers, the pre-synaptic proteins Synapsin and Synaptophysin, plus the post-synaptic proteins PSD-95 and Gephyrin, can capture multiple aspects of synaptic development in rat cortex including developmental expression of each synaptic protein, the balance among all proteins, and the E-I balance. These are important measures for comparing synaptic development among cortical areas and we set out to study development of visual, somatosensory, and frontal cortex by quantifying the available pool of these four synaptic proteins. We found that development of the individual proteins overlapped among the 3 cortical areas, but the balance between proteins developed later in frontal cortex. We applied a neuroinformatics approach using principal component analysis (PCA) to characterize the multidimensional changes during development of these synaptic proteins. Developmental increases in the total protein expression were similar among the cortical areas, but the E-I balance emerged as waves, and the balance between pre- and post-synaptic proteins followed a different trajectory in somatosensory cortex. Together, these results give the most support for an integrated network of development, but also highlight more complex patterns of development that vary in timing and end point among the cortical areas.

Methods

Tissue Sample Collection

A total of 40 tissue samples were collected from primary visual (n=13), frontal (n=14), and somatosensory cortex (n=13) from Long-Evans rats ranging in age from 0 to 93 days (visual, range=P4-P93; frontal, range=P0-P93; somatosensory, range=P0-P74) (Table 1). The rats were euthanized with Euthanol (150mg/kg) and perfused transcardially with cold 0.1 M PBS (4 ºC) until circulating fluid was cleared. The brain was quickly removed and immersed in cold PBS, a sample was cut out from each of the cortical regions (approx. 3 mm X 2 mm) then quickly frozen on dry ice and stored at -80 ºC. Tissue samples from visual cortex were collected at P0, however, they did not contain enough synaptic protein to be measured by Western blotting.

All experimental procedures were approved by the McMaster University Animal Research Ethics Board.

Tissue Sample Preparation

To quantify the available pool of synaptic proteins, tissue samples (50-100 mg) were suspended in cold homogenization buffer (1 ml buffer:50 mg tissue -- 0.5mM DTT, 1mM EDTA, 2 mM EGTA, 10 mM HEPES, 10 mg/L leupeptin, 100nM microcystin, 0.1 mM PMSF, 50 mg/L soybean trypsin inhibitor) and homogenized in a glass-glass Dounce homogenizer (Kontes, Vineland, NJ). The homogenized sample was removed and added to 10% sodium-dodecyl-sulfate (SDS). Protein concentrations were determined using the bicinchonic acid (BCA) assay guidelines (Pierce, Rockford, IL). A control sample was made by combining a small amount of the prepared tissue sample from each of the 40 samples.

Table 1. Cortical Tissue Samples

Table 1. Cortical Tissue Samples

Postnatal Age (Days)	Visual	Somatosensory	Frontal
0		x	x
4	x	x	x
7		x	
11	x	x	x
14	x	x	x
17	x	x	x
21	x	x	x
25	x	x	x
28	x	x	x
31	x	x	x
35	x	x	x
45	x	x	x
64	x		x
74	x	x	x
93	x		x

For this study we used whole homogenate samples and not synaptopneurosomes to quantify the total pool of the synaptic proteins. We chose to use the homogenate for 2 reasons: first, the proteins we quantified have high abundances; second, during the first 7 days of postnatal development in the rat there is very low protein yield in the cortex, significant numbers of mature cortical synapses do not emerge until about P7 (Li et al., 2010) and neurons are still migrating, differentiating, and forming cortical layers early in development until about P20 (Hicks & D'Amato, 1968). These immaturities, especially the low protein yield, mean that the filtration and centrifugation steps used to concentrate synaptic proteins in the synaptoneurosome preparation will lead to different levels of synaptic enrichment in neonatal versus older tissue (Balsor & Murphy, Unpublished Observation).

Immunoblotting

The homogenate samples (25 μg) were separated on polyacrylamide (SDS–PAGE) mini-gels (Precise Protein Gels, Pierce Biotechnology Inc., Rockford, IL, USA) and transferred to polyvinylidene difluoride (PVDF-FL) membranes (Millipore, Billerica, MA). Each sample was run 2 or 3 times. Blots were pre-incubated in blocking buffer (Odyssey Blocking Buffer 1:1 with PBS) for 1 hour (Li-cor Biosciences; Lincoln, NE), then incubated in primary antibody overnight at 4°C using the following concentrations: Synapsin 1, 1:8000 (Invitrogen, Carlsbad, CA); Synaptophysin, 1:2000 (Sigma-Aldrich, St. Louis, MO); PSD-95, 1:32000 (Millipore, Billerica, MA); Gephyrin, 1:2000 (Millipore, Billerica, MA); GAPDH, 1:4000 (Imgenex, San Diego, CA). The blots were washed with PBS containing 0.05% Tween (Sigma, St. Louis, MO) (PBS-T) (3 x 10 min), incubated for 1 hour at room temperature with the appropriate IRDye labeled secondary antibody, (Anti-Mouse, 1:8000, Anti-Rabbit, 1:10,000) (Li-cor Biosciences; Lincoln,

NE), and washed in PBS-T (3 x 10 min). The bands were visualized using the Odyssey scanner (Li-cor Biosciences; Lincoln, NE). The combination of the IRDye secondary antibodies and Odyssey scanner system provides a wide linear dynamic range so that both strong and weak bands could be accurately quantified on the same blot. The blots were stripped and prepared to be re-probed with additional antibodies (Blot Restore Membrane Rejuvenation kit, Chemicon International, Temecula, CA).

Analysis

To analyze the bands, we scanned the blots (Odyssey Infrared Scanner) and quantified the bands using densitometry (Licor Odyssey Software version 3.0; Li-cor Biosciences; Lincoln, NE). The Odyssey system uses near infrared-dyes for antibody detection, providing a 16-250 fold wider linear range than chemiluminescence (Schutz-Geschwender et al., 2004). We determined that both the amount of protein loaded in each well and the concentration of each antibody was within that linear range. Density profiles were determined by performing a subtraction of the background, integrating the pixel intensity across the area of the band, and dividing the intensity by the width of the band to control for variations in lane width. GAPDH normalization was used as the loading control and for each sample the expression of the synaptic protein was divided by GAPDH expression. The control sample (a mixture of all the samples) was run on all of the gels and the density of each sample was measured relative to that control (sample density/control density).

The developmental trajectories for each of the 4 proteins in the 3 cortical areas were visualized by plotting the expression levels for all samples (light colored dots) as well as the average expression (dark colored dots) for each animal. Many of the developmental changes

followed a monotonic increase or decrease and we used a model fitting approach (Christopoulos & Lew, 2000) to fit curves that allowed us to describe and compare these developmental trajectories. Using the online tool ZunZun.com an exponential decay function ($y=yo+a*exp(-t/\tau)$) (solid lines), where t=age in days, was fit to the results from all samples. The best fitting curve was found by least squares and the goodness of fit (R), and the statistical significance of the fit (p) were determined. The time constant (τ) for the rise or fall of expression level was calculated from the exponential decay function. We defined the age when adult level was reached as 3τ. This provided an objective measure representing the age when protein expression reached 87.5% of the asymptotic level. In addition, we calculated 95% confidence intervals (CI) around the decay functions (dotted lines). To determine the upper and lower 95% confidence limits we assumed the data for each individual animal was normally distributed. We multiplied the standard error of the mean for each animal by 1.96 (0.975 quantile of the normal distribution) then added or subtracted that value from the mean of each individual animal providing us with upper and lower 95% confidence limits for each animal. We then fit exponential decay functions to the upper and lower limits of the 95% CIs to visualize the predicted range of protein expression at any given age. Gephyrin had a different developmental trajectory with a brief peak when there was rapid change in expression. This type of brief increase in inhibitory synapses has been found previously in electronmicroscopy counts (Blue & Parvavelas, 1983) so we fit a peak function ($y=a*exp(-0.5*(ln(t/b)/c)2)$) to the Gephyrin expression. The peak parameter (t) provided a measure of the timing of maximum Gephyrin expression for all three cortical areas. To determine if the timing of development for the four proteins was significantly different among

the 3 cortical areas, we performed a two-sample z-tests using 3τ or the peak parameter (t) and their respective standard errors.

We quantified the relationship between pre- and post-synaptic proteins by calculating 2 indices that measured the developmental differences between the pairs of pre-synaptic (Synapsin and Synaptophysin) or post-synaptic proteins (PSD-95 and Gephyrin). The indices provide an indication of synaptic development because each pair of proteins is functionally related: Synapsin and Synaptophysin expression is required for pre-synaptic function and stabilization of pre-synaptic boutons (Hopf et al., 2002); interactions between PSD-95 and Gephyrin regulate the number of excitatory and inhibitory synapses and affect the physiological E-I balance (Keith & El-Husseini, 2008; Lardi-Studler et al., 2007; Prange et al., 2004). In addition, this type of contrast index is common approach in signal processing to determine the quality of the signal and here provided an analysis of pre- or post-synaptic development. Pre-Synaptic Index -- [(Synapsin-Synaptophysin)/(Synapsin+Synaptophysin)], Post-Synaptic Index -- [(PSD-95-Gephyrin)/(PSD-95+Gephyrin)]. Exponential decay functions were fit to the indices, 95% CIs calculated and plotted as described above, and 2 sample z-tests were performed to quantify significant differences among the 3 cortical areas.

Principal Component Analysis

A multivariate analysis of the expression pattern for all proteins was done using principal component analysis (PCA). Protein expression was compiled into an mxn matrix. The rows (m=4) represent the proteins (Synapsin, Synaptophysin, PSD-95, Gephyrin), and the columns (n=40) represent protein expression levels for each of the 40 samples (Visual=13, Somatosensory=13, Frontal=14). The data were centered by subtracting the mean column

vector, and then a singular value decomposition (SVD) was applied to calculate the principal components in Matlab (The Mathworks, Inc., Natick, MA). The SVD represents the expression level for all proteins from one sample as a vector in high dimensional space. The PCA identifies the directions in "protein expression space" that represent the variance in the data across all cortical areas.

In this study, there were 4 principal components; the first 3 accounted for 99% of the variance in the data. A commonly used rule of thumb is that principal components accounting for up to 80% of the cumulative variance are considered significant. To be more precise, the data were analyzed using a bootstrapping method. We performed a Monte Carlo simulation with 100,000 repetitions. For each, the simulated data set had the same number of rows (proteins) and columns (samples), and the simulated protein expression levels were drawn randomly from a normal distribution with the same mean and standard deviation as the original data. For each iteration, a PCA was performed and we calculated how much of the residual variance each of the 4 principal components accounted for. Our experimental principal components were deemed to be statistically significant if they accounted for a much greater proportion of the residual variance than would be expected from random simulation. For example, a principal component was significant with $p<0.05$ if it accounted for more of the residual variance than was observed in 95% of the simulated iterations. To determine biological links and to aid interpretation of the significant principal components, we used an approach that we developed (Beston et al., 2010) and calculated correlations between each significant principal component and several biologically relevant measures. These included: expression levels of the four proteins, the pre- and post-synaptic index, total protein expression, and a Pre-Synaptic:Post-Synaptic index. The

significance level for identifying potential biological correlates was adjusted to $p<0.0021$ using the Bonferroni correction for multiple comparisons. The PCA results were visualized using scatterplots, with PCA coordinates on the y-axis, and age on the x-axis. We fit exponential decay and peak functions where appropriate, as well as a logistics functions ($y=a+b/(1+\exp(0.5*(x-t)))$) when there was an abrupt monotonic decrease in expression. The inflection point parameter (t) provides an objective measure of the timing of the abrupt decrease in expression. We performed 2-sample z-tests were performed to determine if there were any significant differences in the timing of development among the three cortical areas. To determine if there were significant differences in expression levels of principal component 3, we used an analysis of variance, and a Tukey's post-hoc test.

Quantification of total protein expression and a Pre-Synaptic:Post-Synaptic Index was done after PCA. Total protein expression was calculated by summing the expression of the 4 proteins for each sample. Total protein expression was the visualized using a scatterplot, with total protein expression on the y-axis, and age on the x-axis. We fit exponential decay functions to total protein expression for each cortical area, as previously described, and performed 2-sample z-tests to determine if there were significant differences in the timing of development among the 3 areas. The Pre-Synaptic:Post-Synaptic (Pre:Post) index ((Synapsin+Synaptophysin)-(PSD-95+Gephyrin)/(Synapsin+Synaptophysin+PSD-95+Gephyrin)) was calculated for each sample and then visualized using a scatterplot, with the Pre:Post index on the y-axis, and age on the x-axis. We fit exponential decay functions to the Pre:Post index for visual and frontal cortex, and performed a 2-sample z-test to determine if there was a significant difference in the timing of

development between the areas. We fit a weighted average curve to the Pre:Post index for somatosensory cortex.

Results

GAPDH loading control during cortical development

We used GAPDH expression as the loading control for this study and examined development of GAPDH expression in the cortex. During the first 14-20 days of postnatal development neurons are still migrating into the rat cortical plate, differentiating, and forming the cortical layers (Hicks & D'Amato, 1968) and we found that GAPDH expression also increased over that time period (Fig. 1). Thus, it was important to use GAPDH expression as the control for total protein levels so that subsequent quantification of pre- and post-synaptic proteins reflected specific development of the available pool of synaptic proteins rather than a non-specific increase in total cortical proteins.

Pre-synaptic development is led by Synapsin and happens first in somatosensory cortex

To examine pre-synaptic development we quantified the expression of pre-synaptic proteins, Synapsin and Synaptophysin, in rat visual, somatosensory, and frontal cortex. Both proteins are components of the synaptic vesicle membrane and are involved in organizing vesicles at pre-synaptic terminals (Bykhovskaia, 2011), but they have different functions: Synapsin regulates the pool of vesicles for exocytosis (Bahler et al., 1990); and Synaptophysin regulates the kinetics of vesicle endocytosis (Kwon & Chapman, 2011). In addition, Synapsin is the most specific pre-synaptic maker (Micheva et al, 2010). Together, the expression of Synapsin and Synaptophysin provides information about both function and number of pre-synaptic terminals.

In all 3 cortical areas, we found that Synapsin developed before Synaptophysin (Fig. 2, 4A) and all of the changes were well fit by τ decay functions. Initially, Synapsin expression was low

and

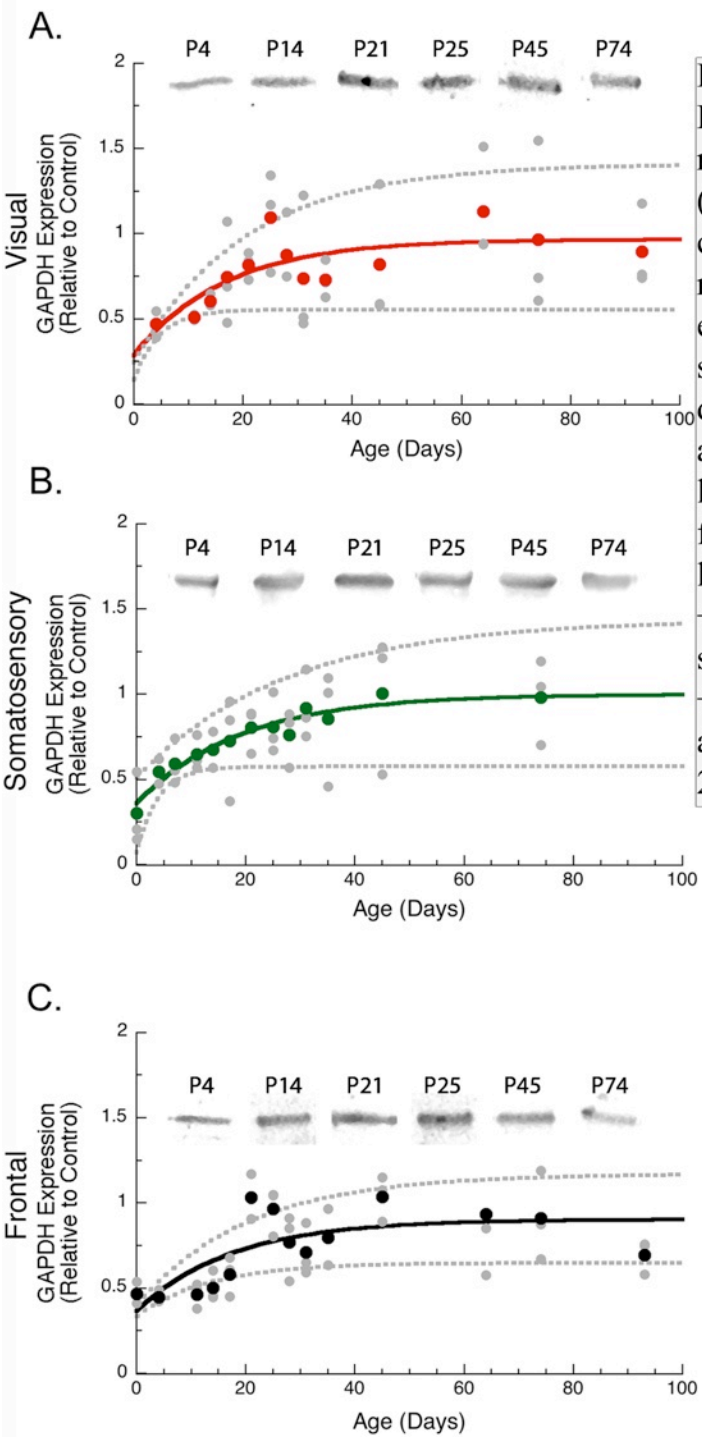

Figure 1.
Developmental changes in GAPDH in rat visual (red, A), somatosensory (green, B), and frontal (black, C) cortex. Grey dots are results from all runs, and color dots are the average for each animal. Example bands are shown above the graphs. Exponential decay functions were fit (solid lines), and 95% confidence intervals (dotted lines) were added, adult levels are defined as 3τ. GAPDH reached adult levels in visual (A) at P50 (3τ=P49.9 +/- 30.4; curve-fit R=0.50; $p<0.001$), somatosensory (B) at P57 (3τ=P57.1 +/- 26.9; curve-fit R=0.69; $p<0.0001$), and frontal (C) at P53 (3τ=P52.6 +/- 24.3; curve-fit R=0.69; $p<0.0001$).

then rose rapidly to reach adult levels. Somatosensory cortex developed first, increasing 2-fold

to reach adult levels at P19 (Fig. 2D, curve-fit $R=0.45$; $p<0.005$, 3τ=P19.0 +/- 14.9). Synapsin expression increased about 3-fold in visual and frontal cortex to reach adult levels at P37 and

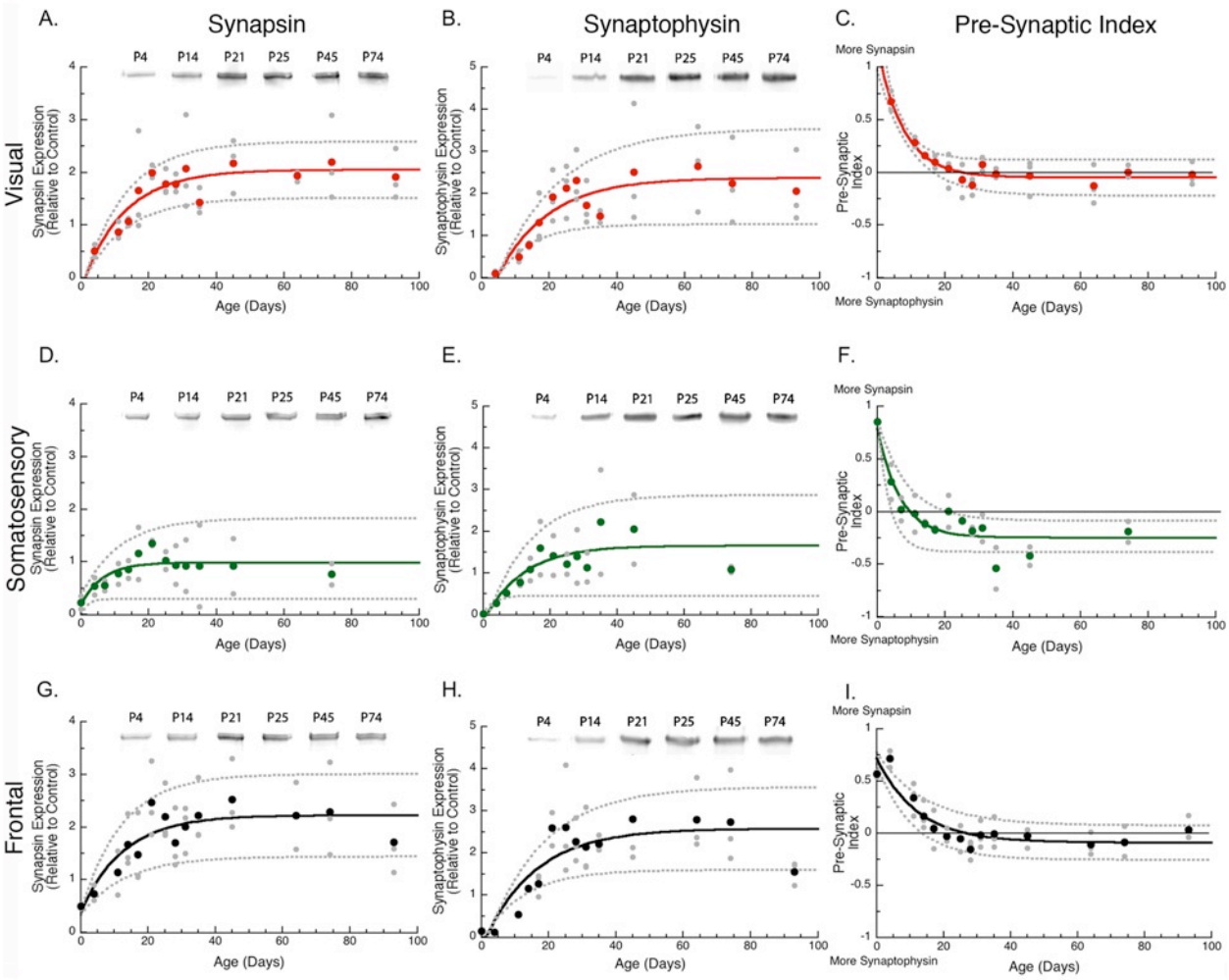

Figure 2.
Developmental changes in Synapsin (A, D, G), Synaptophysin (B, E, H), and the pre-synaptic index (C, F, I) in rat visual (red), somatosensory (green) and frontal (black) cortex. Grey dots are results from all runs, and color dots are the average for each animal. Example bands for each protein and area are shown above the graphs. Exponential decay functions were fit (solid lines), and 95% confidence intervals (dotted lines) were added, adult levels are defined a 3τ. Synapsin reached adult levels in visual (A) at P37 (3τ=P37.2 +/- 12.6; curve-fit R=0.70; p<0.0001), somatosensory (D) at P19 (3τ=P19.0 +/- 14.9; curve-fit R=0.45; p<0.005), and frontal (G) at P38 (3τ=P37.6 +/- 13.5; curve-fit R=0.70; p<0.0001). Synaptophysin reached adult levels in visual (B) at P45 (3τ=P44.8 +/- 15.1; curve-fit R=0.72; p<0.0001), somatosensory (E) at P35 (3τ=P34.7 +/- 22.2; curve-fit R=0.64; p<0.0001), and frontal (H) at P45 (3τ=P45.4 +/- 14.2; curve-fit R=0.75; p<0.0001). Pre-synaptic index reached adult levels in visual (C) at P24 (3τ=P23.5 +/- 4.2; curve-fit R=0.88; p<0.0001), somatosensory (F) at P20 (3τ=P20.2 +/- 6.0; curve-fit R=0.82; p<0.0001), and frontal (I) at P37 (3τ=P36.8 +/- 7.8; curve-fit R=0.85; p<0.0001).

P38, respectively (visual Fig. 2A, curve-fit R=0.70; p<0.0001, 3τ=P37.2 +/- 12.6) (frontal Fig. 2G, curve-fit R0.70; p<0.0001, 3τ=P37.6 +/- 13.5). To compare the ages when Synapsin

reached adult levels (3τ) among the 3 cortical areas we plotted the 3τ ages and their standard errors (Fig. 4) and ran a z-test to determine if there were any significant differences. We found a lot of overlap around the ages when adult-levels of Synapsin were reached and no significant (z-test) differences among the 3 cortical areas.

During the first few days of postnatal development (P0-P4) there was very little expression of Synaptophysin in any of the 3 cortical areas, but then it increased substantially. Synaptophysin reached adult levels (3τ) first in somatosensory cortex, increasing 3-fold (Fig. 2E, curve-fit $R=0.64$ $p<0.0001$) by P35 (3τ=P34.7 +/- 22.2). Between P11 and P45 Synaptophysin increased 4-fold in visual cortex, and 5-fold in frontal cortex when adult levels were reached (Fig. 2B, curve-fit $R=0.72$; $p<0.0001$; 3τ=P44.8 +/- 15.1) (Fig. 2H, curve-fit R0.75; $p<0.0001$, 3τ=P45.4 +/- 14.2). There was substantial overlap around the age when adult levels (3τ) were reached in the 3 areas with no significant differences among the areas(z-test, n.s; Fig. 4A).

The Synapsin:Synaptophysin balance is reached later in frontal cortex

The overlap among visual, somatosensory, and frontal cortex for the ages when either Synapsin or Synaptophysin expression reached adult-levels suggests that these pre-synaptic proteins develop at a similar rate in the 3 cortical areas. It is important to recall that the development of pre-synaptic function depends on both proteins (Hopf et al., 2002), and will be effected by the balance between proteins since they regulate different aspects of synaptic vesicle cycling (exo-cytosis, Synapsin endo-cytosis, Synaptophysin). To address the balance we calculated an index of Synapsin and Synaptophysin expression that had a value of +1 when only Synapsin was expressed, 0 when there was equal expression, and -1 when only Synaptophysin was expressed. We found rapid developmental shifts in this index from substantially more

Synapsin to either balanced expression or slightly more Synaptophysin that suggests a progressive development from dominance by vesicle exo-cytosis until reaching the adult balance of exo- and endo-cytosis regulation of synaptic vesicle cycling. In visual cortex, the pre-synaptic balance shifted to roughly equal expression reaching adult levels at P24 (Fig. 2C, curve-fit $R=0.88$; $p<0.0001$, 3τ=P23.5 +/- 4.2). In somatosensory cortex, the shift was to slightly more Synaptophysin by P20 (Fig. 2F, curve-fit $R=0.82$; $p<0.0001$, 3τ=P20.2 +/- 6.0). In frontal cortex, the shift was slower and adult levels were not reached until P37 (Fig 2I, curve-fit $R=0.85$; $p<0.0001$, 3τ=P36.8 +/- 7.8). The pre-synaptic balance developed later in frontal than somatosensory cortex (z-test, $p<0.05$), and there was a trend towards frontal developing later than visual cortex (z-test, $p=0.06$) (Fig. 4B). Together, these point to slower development of pre-synaptic function in frontal cortex.

PSD-95 expression increases progressively but Gephyrin has a brief period of rapidly changing expression

Both glutamatergic and GABAergic mechanisms are involved in developmental synaptic plasticity, and the physiological E-I balance is central to initiation of the critical period in visual cortex. We examined post-synaptic development of glutamatergic and GABAergic systems by quantifying expression of 2 proteins -- PSD-95 and Gephyrin -- that anchor excitatory glutamatergic and inhibitory GABAergic receptors, respectively. PSD-95 anchors the excitatory receptors GluA and GluN, and is required for functional GluA and GluN receptors (Beique et al., 2006). Gephyrin anchors the inhibitory $GABA_A$ receptor, and is required for the stabilization of GABAergic synapses (Yu et al., 2007). Together, the expression of PSD-95 and Gephyrin can provide information about the development of excitatory and inhibitory synapses (Keith and El-

Husseini, 2008) especially the E-I balance that is crucial for ocular dominance plasticity in visual cortex (Hensch & Fagiolini, 2005).

We found substantial increases in PSD-95 expression during development of all 3 cortical areas, starting from very little expression at P0-P4 to reach adult levels between P49-P62. In visual cortex, there was a 10-fold increase in PSD-95 expression (Fig. 3A, curve-fit $R=0.89$; $p<0.0001$) between P11 and P62 when adult levels were reached (3τ=P61.9 +/- 12.3). Expression of PSD-95 also rose substantially in somatosensory cortex with an 8-fold increase in expression between P7 and P61 (3τ=P61.2 +/- 21.4) (Fig. 3D, curve-fit $R=0.82$; $p<0.0001$). In frontal cortex, there was a 5-fold increase in PSD-95 expression (Fig. 3G, curve-fit $R=0.83$ $p<0.0001$) between P11 and P49 (3τ=P 49.1 +/- 11.8). There were no significant (z-test) differences among the 3 cortical areas in the age when adult levels were reached for PSD-95 expression (Fig. 4A).

The postnatal development of Gephyrin expression followed a different trajectory from the other synaptic proteins, with a bump in expression that was similar to earlier reports counting inhibitory synapses in developing visual cortex (Blue & Parnavelas, 1983). Gephyrin expression levels were similar early (P0, P4) and late (>P60) in development, but we noticed that each cortical area went through an intermediate period when Gephyrin expression was elevated (Fig. 3). The development of Gephyrin expression in frontal cortex was well fit by the peak function (curve-fit $R=0.60$; $p<0.0001$) (Fig. 3H), showing a 2-fold bump in expression around P20 (peak P20.4 +/- 1.1)(Fig. 3). Since Gephyrin expression appeared elevated during that intermediate period in the other cortical areas, and Blue & Parnavelas (1983) had found a transient increase in inhibitory synapses we fit the same peak function to visual and somatosensory cortex and found

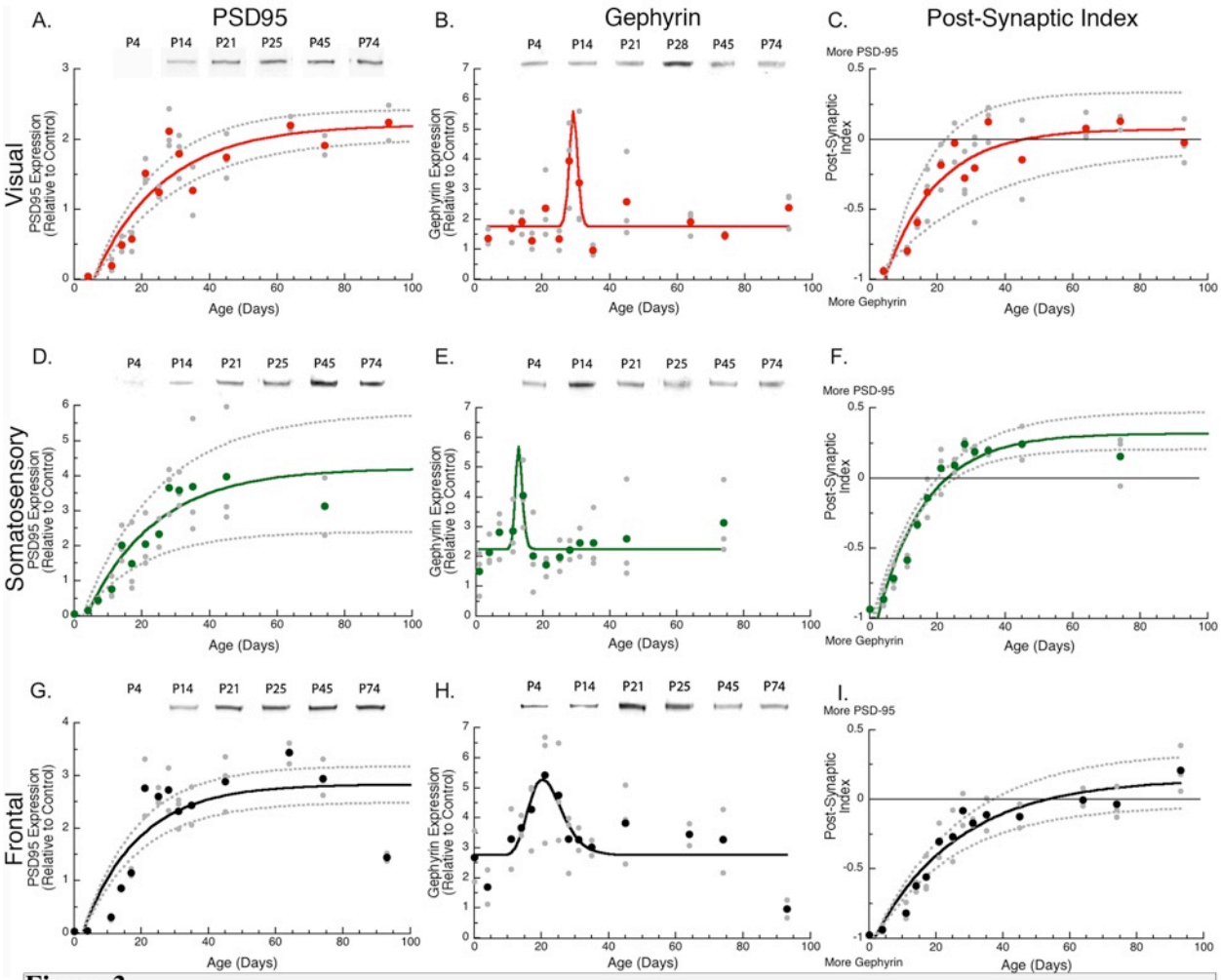

Figure 3.
Developmental changes in PSD-95 (A, D, G), Gephyrin (B, E, H), and the post-synaptic index (C, F, I) in rat visual (red), somatosensory (green) and frontal (black) cortex. Grey dots are results from all runs, and color dots are the average for each. Example bands for each protein and area are shown above the graphs. Exponential decay functions were fit (solid lines) to PSD-95 and the post-synaptic index, and 95% confidence intervals (dotted lines) were added, adult levels are defined as 3τ. Peak function was fit to Gephyrin expression. PSD-95 reached adult levels in visual (A) at P62 (3τ=61.9 +/- 12.3; curve-fit R=0.89; p<0.0001), somatosensory (D) at P61 (3τ=P61.2 +/- 21.4; curve-fit R=0.82; p<0.0001), and frontal (G) at P49 (3τ=P49.1 +/- 11.8; curve-fit R=0.83; p<0.0001). Gephyrin expression reached a peak in visual (B) at P29 (Peak=29.3 +/- 5.1; curve-fit R=0.61 p<0.0001), somatosensory (E) at P13 (Peak=12.8 +/- 5.1; curve-fit R=0.48 p<0.005), and frontal (H) at P20 (Peak=20.4 +/- 1.1; curve-fit R=0.60 p<0.0001). Post-synaptic index reached adult levels in visual (C) at P46 (3τ=P46.4 +/- 9.5; curve-fit R=0.86; p<0.0001), somatosensory (F) at P44 (3τ=P43.5 +/- 6.1; curve-fit R=0.95; p<0.0001), and frontal (I) at P76 (3τ=P75.6 +/- 11.2; curve-fit R=0.94; p<0.0001).

that the bump was more restricted in time. In visual cortex, the peak occurred at P29 (curve-fit R=0.61; p<0.0001, peak P29.3 +/- 5.1)(Fig. 3B), significantly later than the peak in frontal cortex

(z-test, $p<0.05$; Fig. 4A). In contrast, the peak in somatosensory cortex occurred at P13 (curve-fit $R=0.48$; $p<0.005$, peak P12.8 +/- 5.1)(Fig. 3E), which was significantly earlier than the peak in visual cortex (z-test, $p<0.05$; Fig. 4A). The brief elevations in Gephyrin expression in visual and somatosensory cortex indicate that additional studies with more samples targeted around the developmental ages we have identified, will be needed to obtain more precise estimates of the magnitude and timing of the Gephyrin bump.

The PSD-95:Gephyrin balance shifts from Gephyrin to roughly equal with PSD-95 and matures later in frontal cortex

The excitatory-inhibitory (E-I) balance is a key component of plasticity in the visual cortex (Maffei & Turrigiano, 2008; Morishita & Hensch; 2008). To examine development of the mechanisms involved in regulating the E-I balance we calculated an index of PSD-95:Gephyrin expression in visual, somatosensory, and frontal cortex. Interactions between PSD-95 and Gephyrin regulate the number of excitatory and inhibitory synapses that affect the physiological E-I balance (Keith & El-Husseini, 2008; Lardi-Studler et al., 2007; Prange et al., 2004). This post-synaptic index is calculated from the difference in expression of PSD-95 and Gephyrin divided by the sum (Post-Synaptic Index = (PSD-95 - Gephyrin)/(PSD-95 + Gephyrin) and can vary between -1 (only Gephyrin) and +1 (only PSD-95). We found significant developmental changes in the post-synaptic index for all 3 cortical areas with a progressive shift from much more Gephyrin to balanced expression or slightly more PSD-95 (Fig. 3). In visual cortex, the shift to a balanced post-synaptic index was reached at P46 (Fig. 3C, curve-fit $R=0.86$; $p<0.0001$, 3τ=P46.4 +/- 9.5). In somatosensory cortex, the shift to slightly more PSD-95 expression was mature at P45 (Fig. 3F, curve-fit $R=0.95$; $p<0.0001$; 3τ=P4.5 +/- 6.1). In frontal cortex, the shift

in the post-synaptic index was slower and did not reach adult levels until P76 (Fig. 3I, curve-fit R=0.94; p<0.0001; 3τ=P75.6+/- 11.2). The adult-level of the post-synaptic index was reached

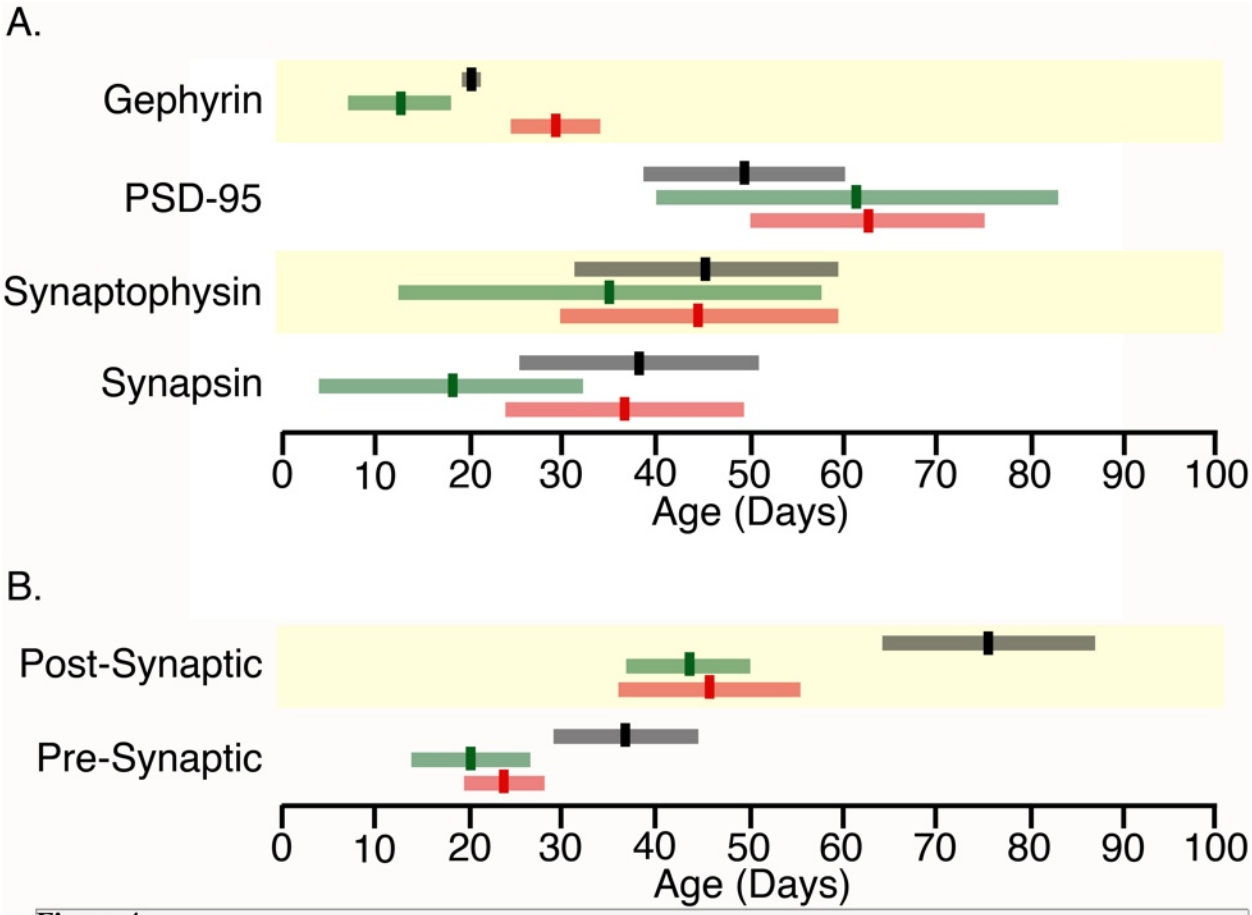

Figure 4.
Time lines for maturation of protein expression and pre- and post-synaptic indices in frontal (black), somatosensory (green) and visual cortex (red) showing the age when adult levels (3τ) or peak in expression were reached (bright bars) and the standard error (light bars) around the 3τs or peak (light bars) A) Adult levels of Synapsin expression overlapped among the 3 cortical areas(Visual,3τ=P37.2 +/- 12.6; Somatosensory cortex, 3τ=P19.0 +/- 14.9; Frontal,3τ=P37.6 +/- 13.5). Adult levels of Synaptophysin expression overlapped among the 3 cortical areas (Visual, 3τ=P44.8 +/- 15.1; Somatosensory, 3τ=P34.7 +/- 22.2; Frontal, 3τ=P45.4 +/- 14.2). Adult levels of PSD-95 expression overlapped among the 3 cortical areas ((Visual, 3τ=61.9 +/- 12.3; Somatosensory, 3τ=61.2 +/- 21.4; Frontal, 3τ=49.1 +/- 11.8). Peak in Gephyrin expression was significantly later in Visual (Peak=29.3 +/- 5.1), than Somatosensory (Peak=12.8 +/- 5.1, p<0.05) and Frontal (Peak=20.4 +/- 1.1, p<0.05) cortex. B) The pre-synaptic index reached adult levels earlier in the sensory areas (Visual, 3τ=P23.5 +/- 4.2, p=0.06; Somatosensory, 3τ=P20.2 +/- 6.0, p<0.05) than in frontal cortex (3τ=P36.7 +/- 7.8). The post-synaptic index reached adult levels earlier in the sensory areas (Visual, 3τ=46.4 +/- 9.5, p<0.05; Somatosensory, 3τ =43.5 +/- 6.1, p<0.005) than in frontal cortex (3τ=75.6 +/- 11.2).

significantly later in frontal cortex, than either visual (z-test, $p<0.05$), or somatosensory cortex (z-test, $p<0.005$) (Fig. 4B) and suggests slower maturation of the E-I balance in frontal cortex.

Principal Component Analysis highlights similarities and differences in development among the cortical areas

The synaptic proteome is a complex functional system. To address the multidimensional nature of the combined development of the 4 proteins in visual, somatosensory, and frontal cortex, we used a data-driven approach and analyzed all of the protein expression using singular value decomposition (SVD). This allowed us to quantify the underlying principal components that explain this multidimensional data-set. The SVD showed that there were 4 principal components, the first principal component (PCA 1) explained the greatest proportion of the variance (64%), the second (PCA 2) explained 22% of the variance, the third (PCA 3) explained 13%, and the fourth (PCA 4) explained 1 % (Fig. 5A). We ran a Monte Carlo simulation to determine which components accounted for a significant proportion of the residual variance in the data. The first 3 components (PCA 1, $p<0.0001$; PCA 2, $p<0.005$; PCA 3, $p<0.0001$) each accounted for a significant proportion and were used for the subsequent analyses.

Each principal component represents a linear combination of the expression of the 4 proteins and the influence that each protein had on a principal component was reflected by the relative amplitude of the basis vector (Fig. 5). Analyzing the basis vectors was an important, 2-step process, that we used to link the principal components with relevant biological mechanisms (Beston et al., 2010). First, we computed the basis vectors; this provided insights regarding the biological mechanisms driving the data. The basis vectors for PCA 1 (Fig. 5B) showed positive contributions from all 4 of the proteins, indicating that it is driven by total expression of

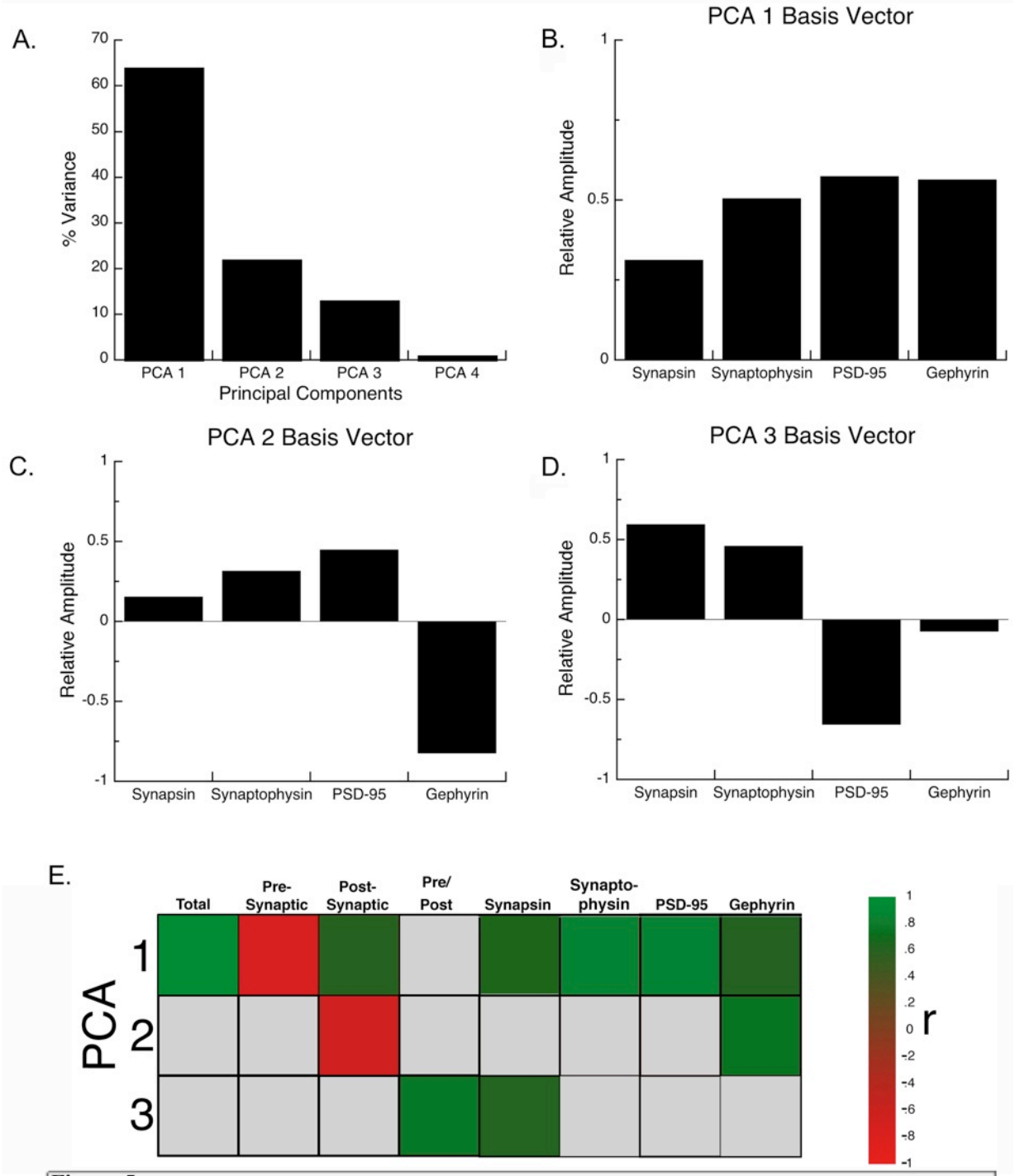

Figure 5.
Principal component analysis. (A) The percent variance captured by each component of the SVD analysis of protein expression in rat visual, somatosensory, and frontal cortex. The first three principal components represent the significant portion (99%) of the SVD. (B-D) The influence of each protein on the three principal components was reflected by the relative amplitude in the basis vectors. (E) Significant correlations (colored cells) between the three principal components and the combinations of proteins derived from the basis vectors. The color indicates the magnitude (represented by color intensity) and direction (green indicates positive, red indicates negative) of significant correlations (Bonferroni corrected, $p<0.0024$).

Synapsin, Synaptophysin, PSD-95, and Gephyrin. For PCA 2 (Fig. 5C) the basis vectors showed opposite directions for PSD-95 and Gephyrin, the markers for excitatory and inhibitory synapses, respectively, suggesting that this component is linked with the E-I balance. Finally, for PCA 3 (Fig. 5D) the basis vectors had opposite directions for the pre- versus post-synaptic proteins suggesting that it reflects differences in pre- versus post-synaptic development.

Second, we calculated a set of correlations between the 3 significant principal components and the 4 proteins, 2 indices, and 2 new measures identified by step one (Fig. 7A, Total Protein Expression; Fig. 7B, Pre-Synaptic:Post-Synaptic Index). To account for multiple comparisons, we performed a Bonferroni correction, and then displayed significant correlations between the 3 principal components and 8 measures (Fig. 5E; green and red squares, $p<0.0021$). The pattern of correlations provided information that described the biological links for each principal component (Table. 2). The first principal component was characterized by total protein expression ($R=0.9913$, $p<0.0001$). The second principal component captured changes in Gephyrin expression ($R=0.7594$, $p<0.0001$), and the post-synaptic index (E-I balance)

Table 2. PCA Correlation

r-value	Total Protein	Pre-Synaptic	Post-Synaptic	Pre/ Post	Synapsin	Synapto-physin	PSD-95	Gephyrin
PCA 1	0.9913	-0.7663	0.6713	0.2004	0.6992	0.8845	0.8931	0.6449
PCA 2	0.0755	0.3125	-0.6669	-0.4472	-0.0238	-0.2153	-0.3181	0.7594
PCA 3	0.1071	0.1135	-0.0548	0.8034	0.6911	0.3901	-0.3164	-0.0859

p-value p<0.0021	Total Protein	Pre-Synaptic	Post-Synaptic	Pre/ Post	Synapsin	Synapto-physin	PSD-95	Gephyrin
PCA 1	0.0000	0.0000	0.0000	0.2149	0.0000	0.0000	0.0000	0.0000
PCA 2	0.6435	0.0496	0.0000	0.0038	0.8841	0.1822	0.0455	0.0000
PCA 3	0.5107	0.4857	0.7370	0.0000	0.0000	0.0128	0.0467	0.5983

(R=-0.6669, p<0.0001). The third principal component captured differences between pre- versus post-synaptic development (R=0.8034, p<0.0001), and Synapsin expression (R=0.6911, p<0.0001).

To visualize the developmental changes for each principal component in the 3 cortical areas we plotted each component as a function of age (Fig. 6). The first principal component was strongly correlated with total protein expression (R=0.9913, p<0.0001) and showed a progressive increase in the 3 cortical areas. The development of PCA 1 was well fit by tau decay functions that had overlapping developmental trajectories among the 3 cortical areas(visual, 3τ=44.7 +/- 18.3; R=0.85, p<0.0001; somatosensory, 3τ=49.6 +/- 14.8; R=0.94, p<0.0001; frontal, 3τ=36.5 +/- 19.0; R=0.78, p<0.001). We found no significant differences between the cortical areas for the age when PCA 1 reached adult-levels (z-test, n.s). This suggested that developmental increases in expression of these 4 synaptic proteins occurred in unison across these cortical areas. We then plotted the development of total protein expression (Fig. 7A) and found that adult-levels were reached at similar ages (P33-P42) (z-test, n.s) in the 3 cortical areas (visual, 3τ=42.0 +/-

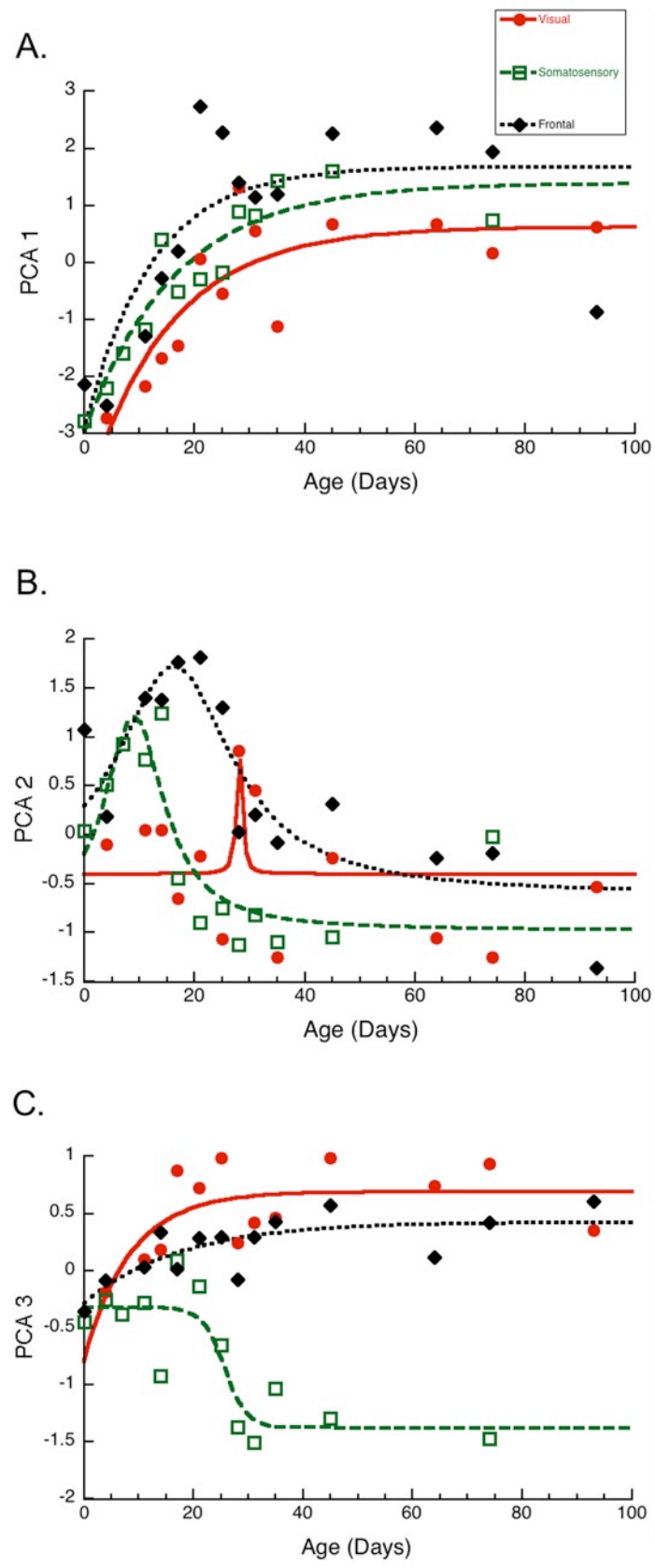

Figure 6.
Developmental changes in the three principal components in visual (red dots, solid line), somatosensory (green squares, dashed lines), and frontal (black diamonds, dotted line) cortex. (A) Principal component 1. Exponential decay functions were fit to the data for each areas, adult levels are defined as 3τ. Principal component 1 reached adult levels in visual at P45 (3τ=44.7 +/- 18.3; R=0.85, p<0.0001), somatosensory at P50 (3τ=49.6 +/- 14.8; R=0.94, p<0.0001), and frontal at P37 (3τ=36.5 +/- 19.0; R=0.78, p<0.001). (B) Principal component 2. Peak functions were fit to the data, and the timing of the peak was determined. Principal component 2 reached a peak in visual at P28 (Peak=28.1 +/- 0.6; R=0.55, p<0.05), somatosensory at P9 (Peak=9.0 +/- 1.2; R=0.86, p<0.0001), and frontal at P16 (Peak=16.3 +/- 1.9; R0.87, p<0.0001). (C) Principal component 3. Exponential decay functions were fit to the data for visual, and frontal cortex, and adult levels were defined as 3τ. A sigmoid function was fit to the data for somatosensory cortex, and the timing of the inflection point was determined. Principal component 3 reached adult levels in visual at P26 (3τ=25.5 +/- 16.8; R=0.69, p<0.01), and frontal at P53 (3τ=52.5 +/- 28.2; R=0.78, p<0.001). The inflection point in somatosensory cortex occurred at P26 (Inflection Point=25.7 +/- 2.1; R=0.87, p<0.0001).

17.6; R=0.84, p<0.0001; somatosensory, 3τ=41.6 +/- 13.8; R=0.92, p<0.0001; frontal, 3τ=32.9 +/- 17.8; R=0.77, p<0.001).

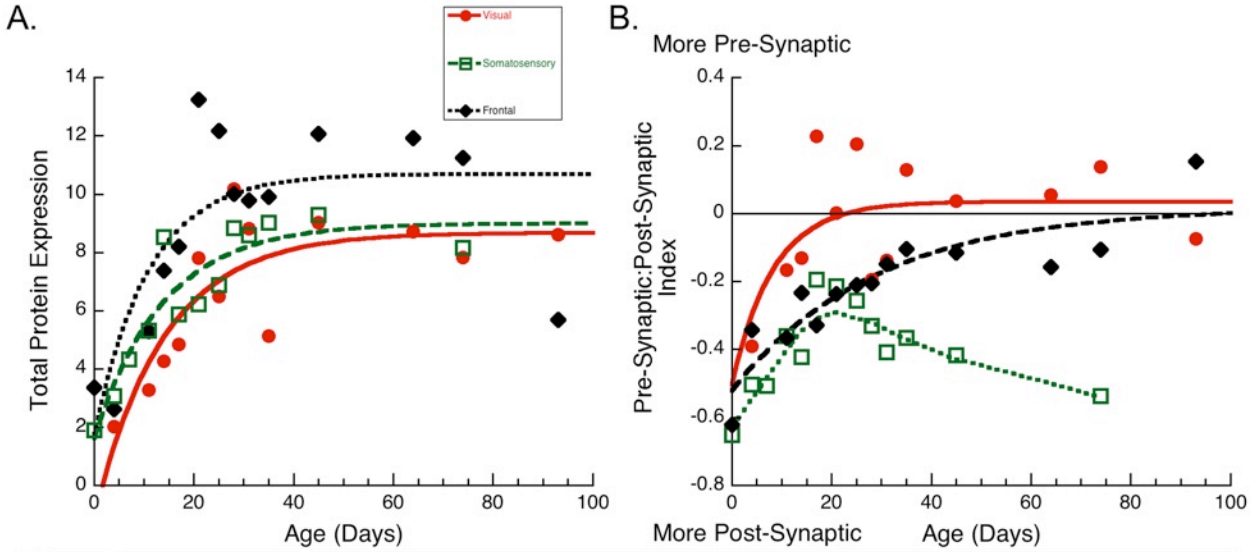

Figure 7.
Developmental changes in total protein expression (A) and the Pre-Synaptic:Post-Synaptic Index in visual (red dots, solid line), somatosensory (green squares, dashed lines), and frontal (black diamonds, dotted line) cortex. (A) Exponential decay functions were fit to the data for each area, adult levels were defined as 3τ. Total protein expression reached adult levels in visual at P42 (3τ=42.0 +/- 17.6; R=0.84, p<0.0001), in somatosensory at P42(3τ=41.6 +/- 13.8; R=0.92, p<0.0001), and in frontal cortex at P33 (3τ=32.9 +/- 17.8; R=0.77, p<0.001). (B) Exponential decay functions were fit to the Pre-Synaptic:Post-Synaptic index in visual and frontal cortex, adult levels were defined as 3τ. Pre-Synaptic:Post-Synaptic index reached adult levels in visual at P25 (3τ=25.0 +/- 15.0; R=0.64, p<0.05), and in frontal cortex at P86 (3τ=86.2 +/- 35.0; R=0.89, p<0.0001). A weighted average curve was fit to somatosensory cortex.

The second principal component (Fig. 6B) captured changes in the expression of both Gephyrin (R=0.7594, p<0.0001) and the post-synaptic index (E-I balance; R=0.7594, p<0.0001). The early phase (P0-P30) of PCA 2 development had a peak in each area. The peak occurred first in somatosensory (Peak=9.0 +/- 1.2; R=0.86, p<0.0001), second in fontal (Peak=16.3 +/- 1.9; R0.87, p<0.0001), and third in visual cortex (Peak=28.1 +/- 0.6; R=0.55, p<0.05). The timing of the peak was significantly earlier in somatosensory versus frontal cortex (z-test, p<0.0001), and frontal versus visual cortex (z-test, p<0.0001). The later phase (>P30) of PCA 2 had a separation between somatosensory cortex and the other areas, reflecting the shift in

the E-I balance to relatively more PSD-95 in somatosensory cortex (Fig. 3F). The PCA 2 results suggest a 2 stage developmental process involving an early bump in Gephyrin occuring at slightly different ages in these areas (somatosensory, P9; frontal, P16; visual, P28), and a prolonged shift in the E-I balance that is greater in somatosensory cortex.

The third principal component (Fig. 6C) was correlated with the differences between pre- and post-synaptic proteins ($R=0.8034$, $p<0.0001$) and Synapsin ($R=0.6911$, $p<0.0001$). The development of PCA 3 expression started at a similar level for the 3 areas but then diverged by P20, with somatosensory cortex taking a different trajectory from either visual or frontal cortex (Fig. 6C). The development of PCA 3 in visual and frontal cortex was well fit by tau decay functions with adult levels (3τ) reached at P26 in visual cortex ($3\tau=25.5$ +/- 16.8; $R=0.69$, $p<0.01$) and at P53 in frontal cortex ($3\tau=52.5$ +/- 28.2; $R=0.78$, $p<0.001$). These ages, however, were not significantly different because of variability in visual and frontal cortex. PCA 3 for somatosensory cortex turned away from the other areas at about P20, reached the falling inflection point at P26 (Inflection Point=25.7 +/- 2.1; $R=0.87$, $p<0.0001$), and the minimum at about P30. The final level of PCA 3 in somatosensory cortex was different from either visual (Tukey's, $p<0.0001$) or frontal cortex (Tukey's, $p<0.0001$). We plotted the index of pre-synaptic:post-synaptic difference in protein expression to visualize the developmental changes in this measure (Fig. 7B). Both visual and frontal cortex developed to reach roughly equivalent expression of the pre- and post-synaptic proteins, and there was a trend (z-test, $p=0.055$) towards later maturation in frontal cortex. In contrast, the mature somatosensory cortex had much greater expression of post-synaptic proteins (Fig. 7B). These analyses of PCA 3 and the pre-

synaptic:post-synaptic index uncovered a divergence in development of the synaptic proteome in somatosensory cortex.

Discussion

Results support an integrated network of development

By measuring a set of pre- and post-synaptic proteins and using a neuroinformatics approach to analyze expression levels we found that the pattern of maturation reflects three underlying components with clear links to the development of individual proteins and the balances between sets of synaptic proteins. First, an integrated network among the 3 cortical areas describes the largest part of development. We found substantial overlap among the 3 cortical areas in the timing of development for both individual proteins and the total expression of the 4 synaptic proteins (PCA 1). Furthermore, the principle component analysis showed that the overlapping trajectories among visual, somatosensory and frontal cortex accounted for 64% of the variance in development of the synaptic proteins. Second, each cortical area had an early wave of development linked with a transient bump in Gephyrin expression and the later tail that was the gradual emergence of an E-I between PSD-95 and Gephyrin expression (PCA 2). The wave in frontal cortex overlapped with both somatosensory and visual cortex, so there was not an obvious hierarchical sequence of development among the cortical areas. We did, however, find that the wave was broader in frontal cortex and there was significantly later maturation of both the pre- and post-synaptic balances, which together support later maturation of frontal cortex. Third, somatosensory cortex diverged from both visual and frontal cortex during maturation of the balance between pre- and post-synaptic proteins (PCA 3). Somatosensory cortex was strongly dominated by the expression of the post-synaptic proteins, while visual and frontal cortex reached a balance. Together, our results show that multiple factors, dominated by largely

overlapping trajectories underlie development of these pre- and post-synaptic proteins in rat visual, somatosensory, and frontal cortex.

Pre-Synaptic Development

The rate of development of the pre-synaptic proteins, Synapsin and Synaptophysin, was similar among the cortical areas providing support for an integrated network of pre-synaptic development. The balances between Synapsin and Synaptophysin is tied to the potential for functional synaptic vesicle cycling, since low levels of Synapsin and Synaptophysin reduce pre-synaptic functioning and transmitter release (Hopf et al., 2002). We are the first to quantify development of the balance between Synapsin and Synaptophysin expression and found very tight developmental trajectories in each cortical area. Initially, there was more Synapsin expression in rat cortex, followed by a rapid increase in Synaptophysin until balanced or slightly more Synaptophysin expression was reached. Interestingly, the pre-synaptic balance matured later in frontal cortex suggesting slower functional development. Synapsin is found at all glutamatergic and GABAergeric synapses but Synaptophysin expression is low levels at GABAergic synapses (Gronborg et al., 2010; Micheva et al., 2010). The early expression of Synapsin may reflect earlier development of GABAergic synapses in rat cortex (Ben-Ari et al., 2007) and be linked with our finding of early expression of Gephyrin. Synapsin maintains the abundance and organization of vesicles at the pre-synaptic terminal (Bykhovskaia, 2011), and the phosphorylation state regulates the pool of vesicles available for exocytosis (Bahler et al., 1990). Synaptophysin interacts with Synaptobrevin to regulate synaptic vesicle retrieval and endocytosis (Gordon et al., 2011). Development of the pre-synaptic balance suggests early maturation of vesicle exocytosis mechanisms, with a slight lag in development of endocytosis

mechanisms. This balance is likely an important mechanism affecting vesicle cycling and contributing to activity-dependent processes that rely on the physiological maturation of neuronal responsiveness from from weak and sluggish, to strong and sustained firing patterns needed for efficient synaptic transmission (Lu et al., 2006; Rust et al., 2002).

Post-Synaptic Development

On the post-synaptic side, we examined expression of PSD-95 and Gephyrin, the scaffolding proteins for GluA/GluN and $GABA_A$ receptors, respectively. We found substantial overlap among the 3 cortical areas in the rate of development of PSD-95, while the peaks for Gephyrin expression progressed from somatosensory to frontal to visual cortex. The post-synaptic balance between PSD-95 and Gephyrin followed tight developmental trajectories in each area shifting from much more Gephyrin and then an increase in PSD-95 to reach balanced expression. The time course of this shift in somatosensory and visual cortex matches development of the physiological E-I balance that has been measured for rat auditory cortex (Dorrn et al., 2010). But in frontal cortex the post-synaptic shift was later. The PSD-95:Gephyrin balance provides an indication of the relative number of excitatory versus inhibitory synapses that will contribute to the physiological E-I balance. Importantly, interactions between these 2 scaffolding proteins influence both the relative number of excitatory and inhibitory synapses and the physiological E-I balance (Keith and El-Husseini, 2008). Over expression of Gephyrin clusters during synapse formation causes a reduction in PSD-95 expression without reducing the total number of synapses, suggesting that Gephyrin interacts with PSD-95 to control the balance between excitatory and inhibitory synapses (Lardi-Studler et al., 2007). In addition, PSD-95 over expression enhances the size of excitatory synapses and

reduces the number of inhibitory contacts leading to a physiological shift in the E-I balance (Prange et al., 2004). Very early in development of the visual cortex, the physiological E-I balance favors excitation, then an increase in inhibition shifts the balance to trigger the onset of the critical period (Maffei & Turrigiano, 2008; Morishita & Hensch, 2008). Our finding of more Gephyrin early on might seem counter to those physiological findings, but initially $GABA_A$ receptors are depolarizing due to an abundance of the immature chloride co-transporter NKCC1. The developmental switch to the mature chloride co-transporters, KCC2, causes hyperpolarization upon activation of $GABA_A$ receptors (Ben-Ari, 2002), and the hyperpolarizing effect of $GABA_A$ receptors becomes apparent in visual cortex at P10 (Ikeda et al., 2003). Thus, our finding of early expression of Gephyrin relative to PSD-95 means that when KCC2 is expressed there can be a very rapid switch from excitation to inhibition, that could re-set the physiological E-I balance and trigger the critical period. In addition, the later maturation of the post-synaptic index in frontal cortex suggests slower development of the E-I balance in that area.

Emergence of Synaptophysin and PSD-95 expression coincide with the switch to functional synapses

Using a small number of synaptic proteins our study complements and extends previous work on synaptic development in rat cortex by providing a rich picture of the developmental changes in these building blocks for synapses. Analysis of the total expression of the synaptic proteins showed highly overlapping development among the cortical areas. Moreover, the links between the set of proteins and synaptic function suggests that these developmental trajectories will be helpful as a framework for connecting with physiological results and guiding future studies of synaptic development. For example, a significant event in synaptic development is the

switch from silent to functional synapse and it requires the formation of both pre- and post-synaptic components (Isaac et al., 1995; Liao et al., 1995; Durand et al., 1996). That switch occurs at P9-11 in visual (Rumpel et al., 1998) and P8-9 in somatosensory cortex (Isaac et al., 1997), ages that are similar to when we found the onset of Synaptophysin and PSD-95 expression. Furthermore, maturation of pre-synaptic transmission is required for the switch from silent to functional synapses (Renger et al., 2001), suggesting that appropriate levels of Synapsin and Synaptophysin are needed to support vesicle exo- and endocytosis to sustain neural activity. In addition, PSD-95 plays a critical role in the conversion of synapses from silent to functional, since PSD-95 knock-out mice have an increased proportion of silent synapses (Beique et al., 2006). Surprisingly, those silent synapses are located on morphologically mature spines, showing that the anatomical presence of a mature spine is not indicative of a functional synapse (Beique et al., 2006). Perhaps the balance between pre- and post-synaptic proteins will become a helpful tool to complement physiological studies of the emergence of functional synapses. For example, development of the balance between pre- and post-synaptic proteins took a different trajectory in somatosensory cortex from either visual or frontal cortex, raising the possibility of functional differences.

Increased protein expression is associated with synaptic stabilization

The synaptic proteins that we quantified are some of the most commonly used markers in imaging studies to visualize the dynamic nature of developing synapses. Imaging to track vesicle turnover has shown that Synapsin and Synaptophysin are required to stabilize the position and efficacy of pre-synaptic boutons (Hopf et al., 2002). This raises the possibility that the rapid development of a balance between these pre-synaptic proteins contributes to early

stabilization of pre-synaptic function and underlies differences in the maturation of pre-synaptic function in somatosensory and visual areas (Cheetham & Fox, 2010). On the post-synaptic side, there is a dynamic pool of PSD-95 shared by synapses within a dendrite. This motility is especially high during early stages of cortical synaptic development when PSD-95 turnover is rapid as it diffuses among neighboring spines (Gray et al. 2006). The rapid turnover is greatest during the critical period (P10-21 in barrel cortex of mice) and coincides with the time when we found that PSD-95 expression was developing rapidly. Motility of PSD-95 slows substantially by P100, and larger synaptic boutons retain PSD-95 for longer, suggesting that changes in the kinetics of PSD-95 diffusion contribute to synapse stability (Gray et al., 2006). The greatest changes in development of PSD-95 overlapped with the stages when imaging studies found the greatest dynamics for the pool of PSD-95. Furthermore, PSD-95 expression matured at about P60 in visual and somatosensory cortex, and about P50 in frontal cortex, ages that coincide with slowing of PSD-95 turnover to its constituent level and increased synapse-specific retention times (Gray et al., 2006). Together, these results suggest that the expression level of PSD-95 during development reflects the dynamic pool of PSD-95 that diffuses in dendrites among developing synapses.

The GABAergic synapse scaffolding protein Gephyrin also has significant motility, on the order of seconds to hours (Dobie & Craig, 2011). Furthermore, that motility is negatively correlated with the density of Gephyrin clusters (Kuriu et al., 2012), so that more Gephyrin equates to less motility. In the current study, we found that Gephyrin development in rat cortex goes through a brief period of increased expression similar to the period of increased density of GABAergic (type II) synapses in rat visual cortex (Blue & Parnavelas, 1983). Perhaps the bump

in Gephyrin expression imparts a period of reduced Gephyrin motility that heightens stabilization of GABAergic synapses. Interestingly, Gephyrin expression also has a bump in expression during development of human visual cortex, but it is more prolonged and extends until late childhood (Pinto et al., 2010).

This study has shown that there is substantial overlap among cortical areas in development of synaptic proteins and it provides a simple framework for future studies that aim to detail development of the cortical connectome. The developmental trajectories for the 4 synaptic proteins, and the balances among them, highlight important milestones in development that are coincident with the emergence of functional synapses, and periods of increased synaptic dynamics. Importantly, the pre- and post-synaptic indices link with both synaptic function and the E-I balance. We anticipate that these trajectories can help focus time consuming anatomical and imaging studies on critical ages in synaptic development.

Chapter 3.

Comparing development of synaptic proteins in human and rat visual cortex

Introduction

Neuroplasticity is a broadly applied term that captures the capacity for experience-dependent change as well as the mechanisms that promote structural and functional changes in the nervous system. There are many clinical applications where neuroplasticity research could improve therapies for conditions such as brain injury, neuropsychiatric disorders, neurodevelopmental disorders, and neurodegeneration and aging. A recent NIH workshop and report, about how to advance the translation of neuroplasticity research towards better clinical outcomes, highlighted the many advances in understanding the mechanisms of neuroplasticity, but noted few translations into established interventions. Basic research using animal models has traditionally focused on the synaptic mechanisms that affect maladaptive plasticity in critical periods during development, but recently, work has begun to uncover ways to promote adaptive plasticity in adults. One of the challenges for translation of neuroplasticity paradigms has been linking the plasticity observed in animal models with that found in humans, especially since the capacity for plasticity waxes and wanes across the lifespan. In particular, there is a need for parallel studies to characterize and compare expression of synaptic plasticity mechanisms in both animal and human cortex. To address this need, we have studied expression of a set of key synaptic plasticity proteins in human visual cortex across the lifespan, and determined the relationship with developing rat cortex.

Animal models, especially of visual system development, have led to many insights about the mechanisms that underlie neuroplasticity and highlighted critical periods in early development when experience can readily remodel synaptic connections. Hubel and Wiesel's (1963) studies of ocular dominance plasticity used a simple and reliable manipulation --

monocular deprivation -- to identify the critical period during development when abnormal visual experience has a profound effect on functioning of the visual system. Monocular deprivation became a standard manipulation for studying the mechanisms of neural plasticity in a variety of species and a successful model for the human amblyopia (lazy-eye). Amblyopia is one of the most prevalent neurodevelopmental disorders, affecting 0.2-5.4% of children in the western world (Kanonidou, 2011) and it is caused by abnormal visual experience during a critical period in development. Animal models have shown that experience-dependent plasticity in visual cortex is influenced by maturation of inhibition, myelination, and the E-I balance. The developmental shift in the excitatory-inhibitory (E-I) balance triggers the start of the critical period (Hensch & Fagiolini, 2005) and regulates the susceptibility of the visual cortex to abnormal visual experience (Maffei & Turrigiano, 2008; Morishita & Hensch, 2008). Furthermore, the age-related loss of orientation tuning in visual cortex is linked with changes in cortical inhibition (Leventhal et al, 2003).

Recently, animal models have been used to test a number of new treatments for amblyopia that promote recovery from early monocular deprivation by reinstating critical-period-like ocular dominance plasticity in adult animals. Interventions such as dark-rearing (He et al, 2007), chronic fluoxetine administration (Maya Vetencourt et al, 2008), environmental enrichment (Baroncelli et al, 2010), and food restriction (Spolidoro et al, 2011) have been effective in promoting plasticity in adult animals. A number of plasticity mechanisms have been linked with these interventions including decreased intracortical inhibition and a shift in the E-I balance. To facilitate translating these interventions into optimal clinical therapies we need to know more about the expression of synaptic plasticity mechanisms in human visual cortex and how they

change across the lifespan. Also, to identify important stages for neuroplasticity human development we need to know how to align the developmental trajectories for synaptic plasticity mechanisms in animal models with the age when those mechanisms are at a similar level in human visual cortex.

To address these questions we began a series of studies of human visual cortex examining early development of excitatory (NMDA) and inhibitory (GABA) receptors (Murphy et al, 2005), and changes across the lifespan for GABAergic proteins (Pinto et al, 2010) and the Angelman syndrome protein Ube3A (Williams et al, 2010). Those studies highlighted the prolonged development of human visual cortex and raised questions about how to link human developmental stages with comparable ages in the animal models. Here we expand on our previous work by quantifying the expression of a small set of pre- and post-synaptic proteins in human visual cortex and using a neuroinformatics approach to compare the developmental trajectory between rat (Pinto et al, 2013) and human visual cortex. The four synaptic proteins that we quantified are highly conserved among mammals and their development is associated with the timing of different aspects of neuroplasticity, including pre-synaptic maturation, excitatory and inhibitory development, and emergence of the E-I balance. On the pre-synaptic side, we examined the vesicle cycling proteins Synapsin and Synaptophysin; together they regulate vesicle exo- (Bahler et al, 1990) and endo-cytosis (Kwon & Chapman, 2011), respectively, and are necessary for pre-synaptic function and transmitter release (Hopf et al., 2002). On the post-synaptic side, we examined the receptor scaffolding proteins PSD-95 and Gephyrin that anchor excitatory (GluA and GluN) or inhibitory (GABAA) receptors, respectively. Interactions between PSD-95 and Gephyrin regulate the number of excitatory and

inhibitory synapses effecting the physiological E-I balance (Keith & El-Husseini, 2008; Lardi-Studler et al, 2007; Prange et al, 2004) that drives critical period plasticity.

We found that the balances between pairs of pre- and post-synaptic proteins were reached before 1 year of age, but expression of Synapsin, PSD-95, and Gephyrin developed further as children aged. We applied a neuroinformatics approach using principal component analysis (PCA) to characterize the multidimensional changes during development of these synaptic proteins. PCA showed that changes in total protein expression were the main source of variance in the data, which was also the case in a previous study that quantified the development of the same synaptic proteins in rat cortex (Pinto et al., 2013). We subsequently performed a parallel analysis of total protein expression in rat and human visual cortex, and found that the synaptic age of visual cortex is comparable for in humans from birth to 8.5 years of age, and rats from P11-P93.

Methods

Samples and Tissue

Tissue samples were obtained from the Brain and Tissue Bank for Developmental Disorders at the University of Maryland (Baltimore, MD). The samples were from the posterior pole of the left hemisphere of human visual cortex, including both superior and inferior portions of the calcarine fissure. A small piece was cut from central visual field representation of primary visual cortex (V1) according to the gyral and sulcal landmarks. The samples were from 26 individuals ranging in age from 20 days to 80 years. All samples were obtained within 23 hours postmortem, and at the Brain and Tissue Bank were fresh frozen after being sectioned coronally in 1-cm intervals, rinsed with water, blotted dry, placed in a quick-freeze bath (dry ice and isopentane), and stored frozen (-70°C). The individuals had no history of neurological or mental health disorders.

Tissue-Sample Preparation

To quantify the available pool of synaptic proteins, tissue samples (50-100 mg) were suspended in cold homogenization buffer (1 ml buffer:50 mg tissue, 0.5mM DTT, 1mM EDTA, 2 mM EGTA, 10 mM HEPES, 10mg/L leupeptin, 100nM microcystin, 0.1 mM PMSF, 50 mg/L soybean trypsin inhibitor) and homogenized in a glass-glass Dounce homogenizer (Kontes, Vineland, NJ). The homogenized sample was removed and added to 10% sodium-dodecyl-sulfate (SDS). Protein concentrations were determined using the bicinchonic acid (BCA) assay guidelines (Pierce, Rockford, IL). A control sample was made by combining a small amount of the prepared tissue sample from each of the 26 samples.

Immunoblotting

The homogenate samples (25 μg) were separated on Sodium-dodecyl-sulfide polyacrylamide gels (4-20% SDS-PAGE; Thermo Scientific, Waltham, MA) and transferred to polyvinylidene difluoride (PVDF-FL) membranes (Millipore, Billerica, MA). Each sample was run 2-4 times. Blots were pre-incubated in blocking buffer (Odyssey Blocking Buffer, Li-cor Biosciences; Lincoln, NE; 1:1 with PBS) for 1 hour, then incubated in primary antibody overnight at 4°C using the following concentrations: GAPDH, 1:4000 (Imgenex, San Diego, CA); Synapsin 1, 1:8000 (Invitrogen, Carlsbad, CA); Synaptophysin, 1:2000 (Sigma-Aldrich, St. Louis, MO); PSD-95, 1:32000 (Millipore, Billerica, MA); Gephyrin, 1:2000 (Millipore, Billerica, MA). The blots were washed with PBS containing 0.05% Tween (Sigma, St. Louis, MO) (PBS-T) (3 x 10 min), incubated for 1 hour at room temperature with the appropriate IRDye labeled secondary antibody, (Anti-Mouse, 1:8000, Anti-Rabbit, 1:10,000) (Li-cor Biosciences; Lincoln, NE), and washed in PBS-T (3 x 10 min). The bands were visualized using the Odyssey scanner (Li-cor Biosciences; Lincoln, NE). The combination of the IRDye secondary antibodies and Odyssey scanner system provides a wide linear dynamic range so that both strong and weak bands could be quantified on the same blot. We determined that both the amount of protein loaded in each well and the concentration of each antibody were within the linear range. The blots were stripped and prepared to be re-probed with additional antibodies (Blot Restore Membrane Rejuvenation kit, Chemicon International, Temecula, CA).

Analysis

To analyze the bands, we scanned the blots (Odyssey Infrared Scanner) and quantified the bands using densitometry (Licor Odyssey Software version 3.0; Li-cor Biosciences; Lincoln,

NE). The Odyssey system uses near infrared-dyes for antibody detection, providing 16-250 fold wider linear range than chemiluminescence (Schutz-Geschwender et al., 2004). Density profiles were determined by performing a subtraction of the background, integrating the pixel intensity across the area of the band, and dividing the intensity by the width of the band to control for variations in lane width. GAPDH was used as the loading control and for each sample the expression of the synaptic proteins was divided by GAPDH expression. A control sample (a mixture of all the samples) was run on all of the gels and for each blot the density of each sample was normalized relative to the control (Sample density/Control density). Finally, for each protein, expression levels across runs were normalized using the average expression of the synaptic protein.

The results were plotted in two ways to visualize the developmental trajectories of the proteins. First, changes in expression across the lifespan were plotted using scattergrams for each protein that included expression levels from all runs (light grey dots), as well as the average expression from each sample (black dots). To help quantify the patterns of change in expression, we used a model-fitting approach (Christopoulos & Lew, 2000) and determined the best curve-fit to the data (grey dots) using the online tool zunzun.com. The best fitting curve was found by least squares providing the goodness of fit (R) and statistical significance of the fit (p). Synapsin expression was well fit by a decay function ($y=a+b*\exp(-t/\tau)$), and the time constant (τ) was determined. Adult levels were defined as 3τ, a time when 87.5% of the change in protein expression had taken place. Synaptophysin was not well fit by any functions, so a simple descriptive weighted average was plotted. PSD-95 and Gephyrin expression were well fit by gaussian functions ($y=a+b*\exp(-((t-peak)^2)/c)$) since expression of both increased then

decreased. Second, to compare changes among developmental stages, samples were grouped by developmental stage (< 0.3 Years, Neonates; 0.3-1 year, Infants, 1-4 years, Young Children; 5-11 years, Older Children; 12-20 years, Teens; 21-55 years, Young Adults >55 years, Older Adults) and histograms were plotted showing the mean expression level of the synaptic protein and the standard error of the mean for each age group. Statistical comparisons between groups were made using an analysis of variance and when significant ($p<0.05$), Tukey's post-hoc comparisons were done.

We quantified the relationship between pre- and post-synaptic proteins by calculating 2 indices that measured the developmental differences between pairs of pre-synaptic (Synapsin and Synaptophysin) and post-synaptic proteins (PSD-95 and Gephyrin). The indices provide an indication of synaptic development because each pair of proteins is functionally related: Synapsin and Synaptophysin expression is required for pre-synaptic function and stabilization of pre-synaptic boutons (Hopf et al., 2002); interactions between PSD-95 and Gephyrin regulate the number of excitatory and inhibitory synapses and affect the physiological E-I balance (Keith & El-Husseini, 2008; Lardi-Studler et al., 2007; Prange et al., 2004). In addition, this type of contrast index is a common approach in signal processing to determine the quality of the signal and here provided an analysis of pre- or post-synaptic development. Pre-Synaptic Index -- [(Synapsin-Synaptophysin)/(Synapsin+Synaptophysin)], Post-Synaptic Index -- [(PSD-95-Gephyrin)/(PSD-95+Gephyrin)]. The indices were plotted as described above, and exponential decay functions were fit to the scatterplots.

Principal Component Analysis

A multivariate analysis of the expression pattern for all proteins in human visual cortex was done using principal component analysis (PCA). Protein expression was compiled into an mxn matrix. The m=4 rows represent the proteins (Synapsin, Synaptophysin, PSD-95, and Gephyrin), and the n=26 columns represent protein expression levels for each of the 26 samples. The data were centred by subtracting the mean column vector, and then a singular value decomposition (SVD) was applied to calculate the principal components in Matlab (The Mathworks, Inc., Natick, MA). The SVD represents the expression level for all proteins from one sample as a vector in high dimensional space. The PCA identifies the direction in "protein expression space" that represents the variance in all the data from the human visual cortex.

The analysis identified 4 principal components. A commonly used rule of thumb to determine how many components are significant is that it includes sequential principal components accounting for up to 80% of the cumulative variance. To be more precise, we analyzed the data using a bootstrapping method. We performed a Monte Carlo simulation with 100,000 repetitions. For each, the simulated data-set had 4 rows (proteins) and 26 columns (samples), and the simulated protein expression levels were drawn randomly from a normal distribution with the same mean and standard deviation as the original data. For each iteration, a PCA was performed and we calculated how much of the residual variance was accounted for by each of the 4 principal components. Our experimental principal components were deemed to be statistically significant if they accounted for a much greater proportion of the residual variance than would be expected from random simulation. For example, a principal components was significant with $p<0.05$ if it accounted for more of the residual variance than was observed in

95% of the simulated iterations. To determine biological links and to aid interpretation of the significant principal components, we used an approach that we developed (Beston et al., 2010) and calculated correlations between each significant principal component and several biologically relevant measures. These included: expression levels of the four proteins, the pre- and post-synaptic index, and total protein expression. The significance level for identifying potential biological correlates was adjusted to $p<0.0035$ using the Bonferroni correction for multiple comparisons. The PCA results were visualized using scatterplots and histograms as described above, with PCA coordinates on the y-axis, and age on the x-axis. To describe the pattern of change in the PCA scatterplots, we fit peak or linear functions to the data.

Transformation

Total protein expression levels were calculated for rat and human visual cortex by summing the expression levels of the four proteins for each sample. The age of each sample was converted to post-conception age, by adding 0.75 years to the age of each human sample, and 22 days to the age of each rat sample. To visualize changes in total protein expression in human and rat visual cortex, we plotted a scattergram of total protein expression as a function of post-conception age. To describe the pattern of change we fit a decay function to the rat data, and a gaussian function to the human data. To convert the rat data into human equivalent age, we transformed the rat data along the x, and y-axis. To convert along the y-axis, we multiplied the rat data by a conversion factor (Human Maximum Expression/Rat Maximum Expression), given from the curve fits. To transform along the x-axis, we used the curve-fit equations to calculate the human age that corresponds to the same total protein expression level as our 13 rat samples.

The transformed rat data was then plotted on the scattergram in human equivalent years and expression.

Results

Postmortem interval & GAPDH expression

The tissue samples were collected over a range (4-23 hours) of postmortem intervals and our first step was to determine whether there were significant correlations between postmortem interval and expression of the synaptic proteins. There were no significant ($p<0.05$) correlations between expression levels and postmortem interval for any of the four proteins (GAPDH, R=0.04; Synapsin, R=0.16; Synaptophysin, R=0.05; Gephyrin, R=0.08; PSD-95, R=0.10).

We also analyzed expression of GAPDH, the loading control for this study, to determine if it changed across the lifespan. We found that the expression levels of GAPDH was constant across the lifespan when analyzed by model-fitting (Fig. 1A), and comparison among the age groups (Fig 1B; ANOVA, p=0.87).

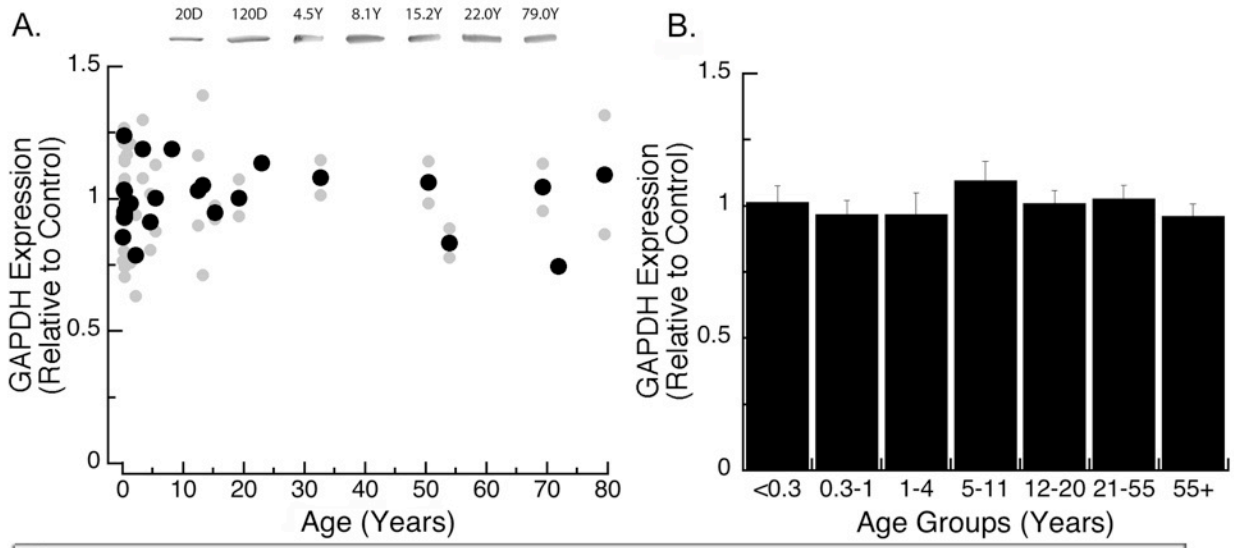

Figure 1.
Developmental changes in GAPDH expression in human visual cortex. (A) Grey dots are results from all runs, and black dots are the average for each sample. Example bands are shown above the graph. (B) Group means and standard error for each developmental group.

Pre-synaptic vesicle cycling mechanisms develop during different periods

To examine pre-synaptic development in human visual cortex across the lifespan we quantified the expression of two pre-synaptic proteins, Synapsin and Synaptophysin. Both proteins are components of the synaptic vesicle membrane and involved in different aspects of synaptic vesicle cycling. Synapsin regulates the pool of synaptic vesicles available for exocytosis (Bahler et al., 1990), and Synaptophysin regulates the kinetics of synaptic vesicle endocytosis (Kwon & Chapman, 2011). In addition, Synapsin is the most specific marker for pre-synaptic terminals (Micheva et al., 2010). Together, expression levels of Synapsin and Synaptophysin provide information about function and number of pre-synaptic terminals.

We found that expression levels of Synapsin increased during development of human visual cortex, and the changes were well fit by a τ decay function (Fig. 2A, B). Initially, Synapsin levels were very low and then rose rapidly, increasing 6-fold during the first decade of life to reach adult levels at 9 years of age (Fig. 2A; 3τ= 8.7 +/- 5.1 years; curve fit, $R=0.66$; $p<0.0001$). Analysis of the developmental stages showed a significant increase in Synapsin (Fig. 2B; ANOVA, $p<0.0001$). There was a significant increase in expression of Synapsin between Neonates (< 0.3 Years) and Older Children (5-11 Years; Tukey's, $p<0.01$), that persisted through Teens (12-20 Years; Tukey's, $p<0.001$), Young Adults (21-55 Years; Tukey's, $p<0.0001$), and Older Adults (55+ Years; Tukey's, $p<0.05$). We also found a significant increase in Synapsin expression between Infants (0.3-1 Year) and Older Children (5-11 Years; Tukey's, $p<0.05$), Teens (12-20 Years; Tukey's, $p<0.05$), and Young Adults (21-55 Years; Tukey's, $p<0.01$). In contrast, Synaptophysin expression during early development was more variable and higher than Synapsin. We did not find a significant curve-fit to the Synaptophysin expression and therefore

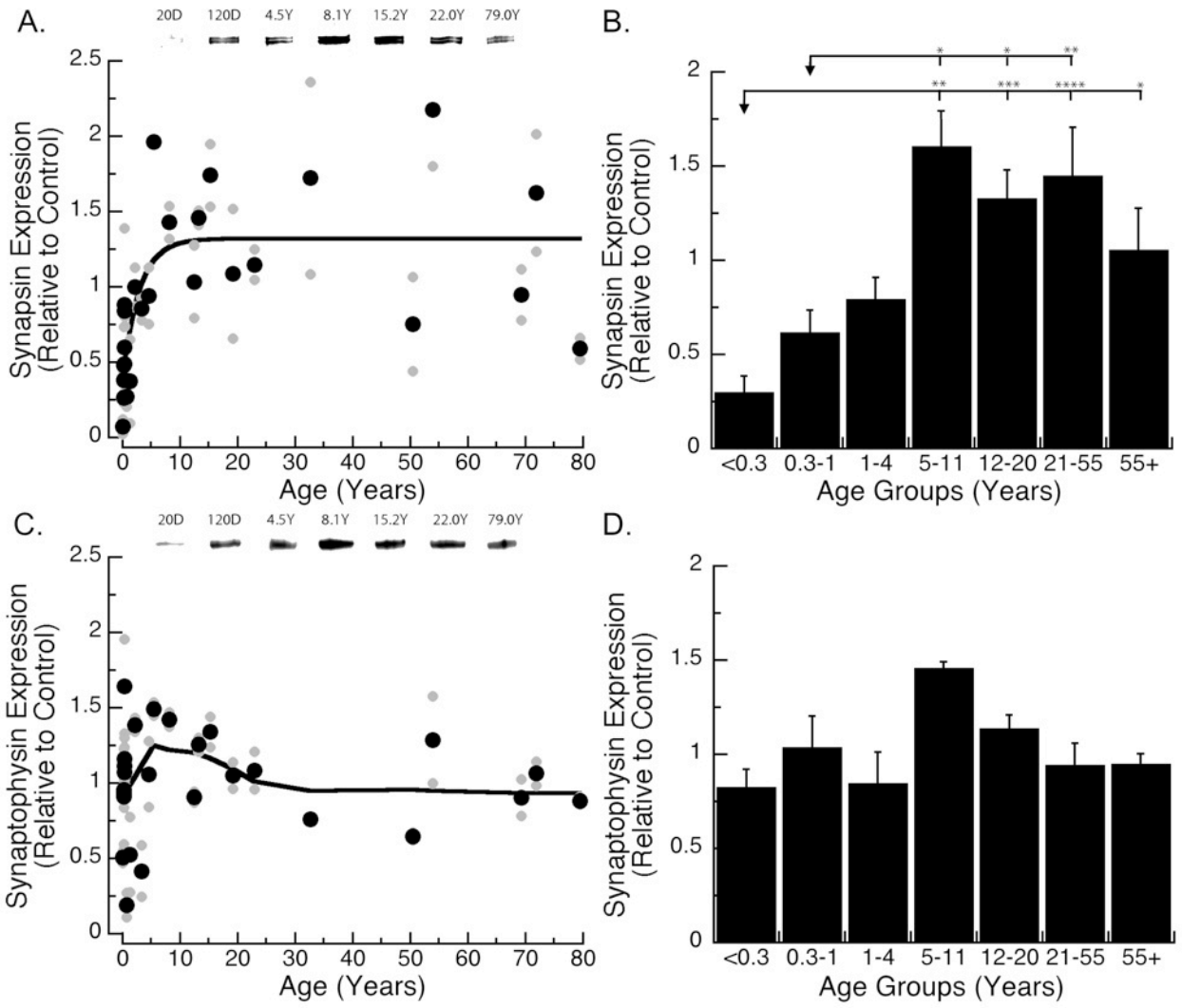

Figure 2.
Developmental changes in Synapsin (A, B) and Synaptophysin (C, D) expression in human visual cortex. (A, C) Grey dots are results from all runs, and black dots are the average for each sample. Example bands are shown above the graphs. (B, D) Group means and standard error for each developmental stage are plotted. (A) An exponential decay function was fit to all the Synapsin data points ($R=0.66$, $p<0.0001$), and adult levels are defined as 3t ($3t=8.7$ +/- 5.1 years). (B) There was a significant difference in expression of Synapsin between the groups (ANOVA, $p<0.0001$), and the statistical significance of the difference between pairs of development stages as determined by Tukey's post-hoc comparisons are plotted (* $p<0.05$; ** $p<0.01$; *** $p<0.001$; **** $p<0.0001$). (C) A weighted average fit was plotted to all of the Synaptophysin data points to describe pattern of change. (D) There was no significant difference in expression of Synaptophysin between the groups (ANOVA, $p=0.09$).

used a simple weighted average to plot a curve describing Synaptophysin expression across the lifespan (Fig. 2C). There were also no significant differences in Synaptophysin among any

developmental age groups (Fig. 2D; ANOVA, p=0.09), suggesting that it is relatively constant across the lifespan. It is important to note, however, that there was a lot of inter-individual variability in Synaptophysin expression at the younger ages (<5 years) that may have masked early developmental changes.

Post-Synaptic scaffolding proteins develop in-concert

Both excitatory and inhibitory mechanisms are involved in developmental synaptic plasticity, and the physiological E-I balance is central to the initiation of the critical period in visual cortex. We examined post-synaptic development of glutamatergic (excitatory) and GABAergic (inhibitory) systems by quantifying the expression of 2 scaffolding proteins -- PSD-95 and Gephyrin. PSD-95 anchors the excitatory GluA and GluN receptors, and is required for receptor function (Beique et al., 2006). Gephyrin anchors the inhibitory GABAA receptors, and is required for receptor stabilization (Yu et al., 2007). Together, the expression of PSD-95 and Gephyrin provides information about the development of excitatory and inhibitory synapses (Keith & El-Husseini, 2008) and the E-I balance that is crucial for ocular dominance plasticity in visual cortex (Hensch & Fagiolini, 2005).

Development of PSD-95 and Gephyrin expression followed similar developmental trajectories, with increases into late childhood and then declining into adulthood. Development of PSD-95 increased ~10-fold to reach a peak at 8 years of age (Fig. 3A; peak=8.0 +/- 0.7 years; curve fit, R=0.58; p<0.0001), and then declined ~5-fold into aging. Comparison of PSD-95 expression levels among developmental stages (Fig. 3B; ANOVA, p<0.0001) showed that it was significantly higher in Older Children (5-11 Years) relative to all other age group: Neonates (<0.3 Years; Tukey's, p<0.0001), Infants (0.3-1 Year; Tukey's, p<0.0001), Young Children (1-4 Years;

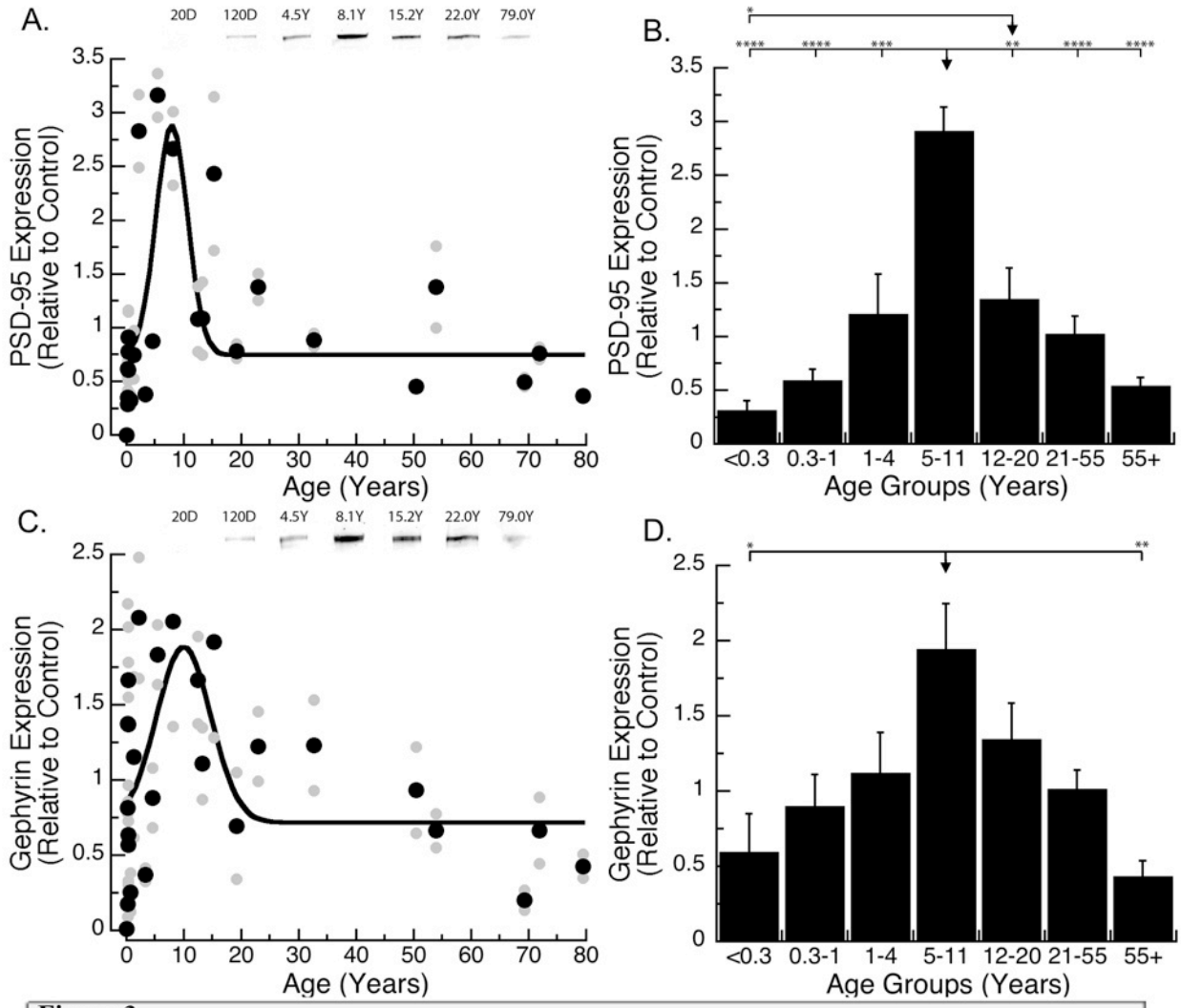

Figure 3.
Developmental changes in PSD-95 (A, B) and Gephyrin (C, D) expression in human visual cortex. (A, C) Grey dots are results from all runs, and black dots are the average for each sample. Example bands are shown above the graphs. (B, D) Group means and standard error for each developmental stage are plotted. (A) A gaussian function was fit to all the PSD-95 data points ($R=0.58$; $p<0.0001$), and a peak in expression was reached at 8 years of age (peak=8.0 +/- 0.7 years). (B) There was a significant difference in expression of PSD-95 between the groups (ANOVA, $p<0.0001$), and the statistical significance of the difference between pairs of development stages as determined by Tukey's post-hoc comparisons are plotted (* $p<0.05$; ** $p<0.01$; *** $p<0.001$; **** $p<0.0001$). (C) A gaussian function was fit to all the Gephyrin data points ($R=0.48$; $p<0.0005$), and a peak in expression was reached at 10.0 years of age. (D) There was a significant difference in expression of Gephyrin between the groups (ANOVA, $p<0.005$), and the statistical significance of the difference between pairs of development stages as determined by Tukey's post-hoc comparisons are plotted (* $p<0.05$; ** $p<0.01$; *** $p<0.001$; **** $p<0.0001$).

Tukey's, $p<0.001$), Teens (12-20 Years; Tukey's, $p<0.01$), Young Adults (21-55 Years; Tukey's,

$p<0.0001$), Older Adults (55+ Years; Tukey's, $p<0.0001$). We also found that teens (12-21 Years) had higher expression levels of PSD-95 than Neonates (<0.3 Years; Tukey's, $p<0.05$).

Gephyrin expression increased ~3-fold and model-fitting of a peak function found the maximum expression at 10 years of age (Fig. 3C; peak= 10.0 +/- 1.3 years; curve fit, $R=0.48$; $p<0.0005$), followed by a subsequent ~4-fold decline into aging. We saw a similar developmental profile of Gephyrin for the developmental age groups (Fig. 3D; ANOVA, $p<0.005$). Expression levels of Gephyrin were significantly higher in Older Children (5-11 Years), than Neonates (<0.3 Years; Tukey's, $p<0.05$), and Older Adults (55+ Years; Tukey's, $p<0.01$).

Pre- and Post-synaptic balances develop within first year in human visual cortex

Each pair of proteins interact to support functioning pre-synaptic (Synapsin and Synaptophysin) or post-synaptic (PSD-95 and Gephyrin). On the pre-synaptic side, Synapsin and Synaptophysin are both required for pre-synaptic function (Hopf et al., 2002), and the balance between the two proteins will effect the dynamics of vesicle cycling because Synapsin regulates exocytosis and Synaptophysin regulates endocytosis. On the post-synaptic side, PSD-95 and Gephyrin regulate the number of excitatory and inhibitory synapses (Keith & El-Husseini, 2008; Lardi-Studler et al., 2007; Prange et al., 2004) and together affect the physiological E-I balance. To quantify the balances between each pair of synaptic proteins we calculated 2 indices; a Pre-Synaptic Index: (Synapsin-Synaptophysin)/(Synapsin +Synaptophysin), and a Post-Synaptic Index: (PSD-95-Gephyrin)/(PSD-95+Gephyrin). The indices range from +1 to -1, positive values indicate relatively more Synapsin (Pre-Synaptic

Index) or PSD-95 (Post-Synaptic Index), while negative values indicate relatively more Synaptophysin (Pre-Synaptic Index) or Gephyrin (Post-Synaptic Index).

Both the pre- and post-synaptic indices developed very rapidly in the first year (Fig. 4). On the pre-synaptic side, there was a switch from relatively more Synaptophysin expression early, to slightly more Synapsin expression, and mature-levels were reached by 12 months of age (Fig. 4A; 3τ=11.7 +/- 4.1 months; curve fit, $R=0.67$, $p<0.0001$). We found a similar developmental profile with significant switch in expression of the pre-synaptic index among the developmental age groups (Fig. 4B; ANOVA, $p<0.0005$). Expression levels switched from more Synaptophysin in Neonates (<0.3 Years) to more Synapsin in Younger Children (1-4 Years; Tukey's, $p<0.05$) and that persisted through Older Adults (55+ Years; Tukey's, $p<0.05$). This switch in the balance between Synapsin and Synaptophysin suggests that pre-synaptic function of vesicle endo- and exo-cytosis matures within the first year.

On the post-synaptic side, we found a very rapid switch from much more Gephyrin at the youngest ages, to a balance between Gephyrin and PSD-95 by 5 months of age (Fig. 4C,D; 3τ=5.3 +/- 1.8 Months; curve fit, $R=0.54$, $p<0.0001$). The developmental stages showed a similar profile switching from more Gephyrin to a balance between the 2 proteins. The rapid switch in the first few months, however, led to greater variability in those early developmental stages so the comparison between the age groups could not capture the change (Fig. 4D; ANOVA, $p=0.18$). This switch in the post-synaptic index suggests a rapid change in the E-I balance that would trigger the start of the critical period for ocular dominance plasticity in

human visual cortex by 5 months of age.

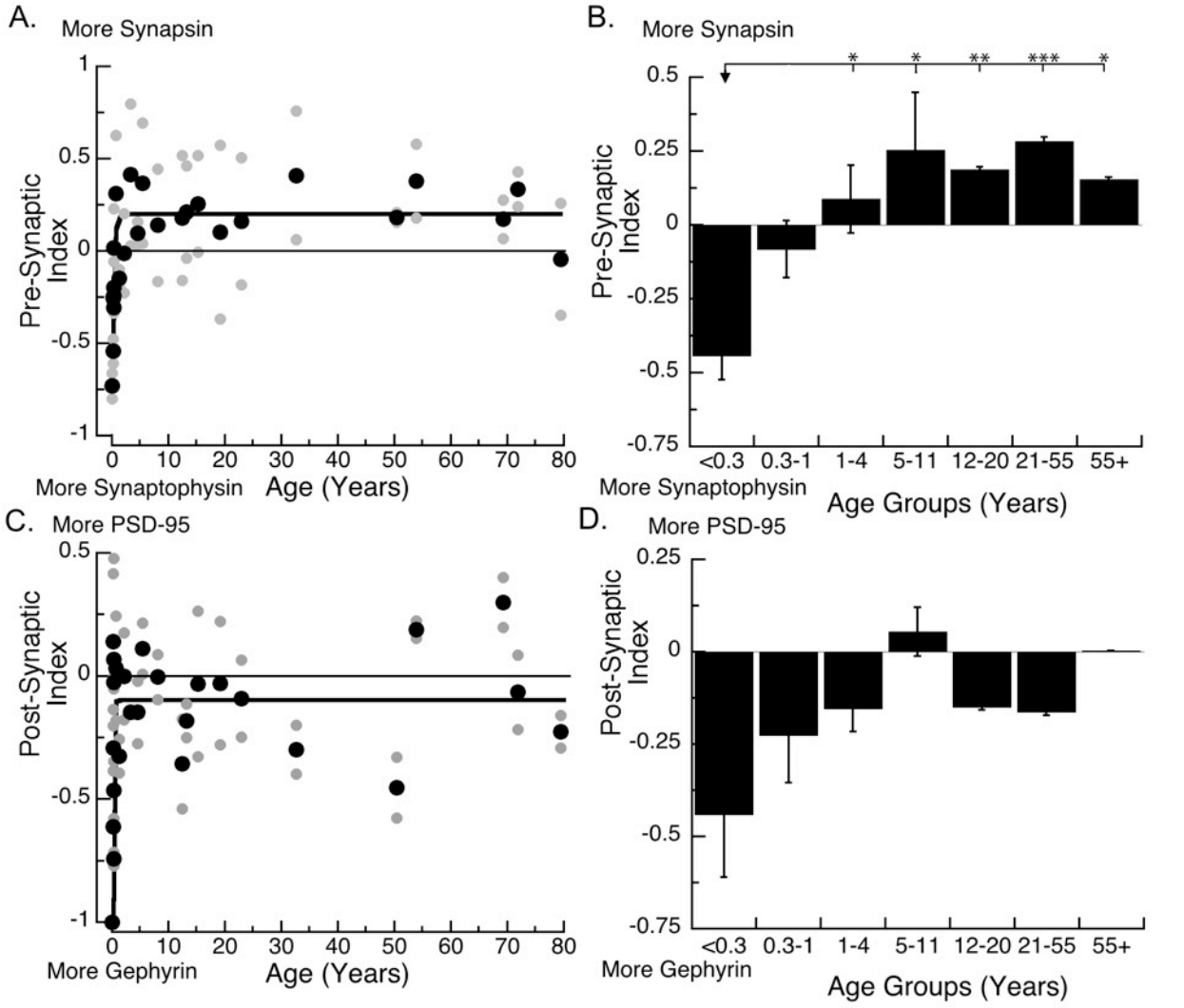

Figure 4.
Developmental changes in the pre-synaptic (A, B) and post-synaptic (C, D) index in human visual cortex. (A, C) Grey dots are results from all runs, and black dots are the average for each sample. Example bands are shown above the graphs. (B, D) Group means and standard error for each developmental stage are plotted. (A) An exponential decay function was fit to all the pre-synaptic index data points ($R=0.67$, $p<0.0001$), and adult levels are defined as 3t (3t=11.7 +/- 4.1 months). (B) There was a significant difference in expression of the pre-synaptic index between age groups (ANOVA, $p<0.0005$) and the statistical significance of the difference between pairs of development stages as determined by Tukey's post-hoc comparisons are plotted (* $p<0.05$; ** $p<0.01$; *** $p<0.001$; **** $p<0.0001$). (C) An exponential decay function was fit to all the post-synaptic index data points ($R=0.51$, $p<0.0001$), and adult levels were defined as 3t (3.5 +/- 1.8 months). (D) There were no significant differences in expression of the post-synaptic index among the developmental stages (ANOVA, $p=0.18$).

Principal Component Analysis

The synaptic proteome is a complex functional system, so to address the multidimensional nature of development for the 4 proteins, we used a data-driven approach and analyzed all of the protein expression with singular value decomposition (SVD). This allowed us to quantify the underlying principal components that explain the multidimensional data-set in human visual cortex. The SVD found 4 principal components, the first principal component (PCA 1) explained the greatest proportion of the variance (64%), the second (PCA 2) explained 20% of the variance, the third (PCA 3) explained 10%, and the fourth (PCA 4) explained 6% (Fig. 5A). Thus, the PCA 1 and PCA 2 combine to account for 84% of the variance. Furthermore, the monte-carlo simulation showed that the first principal component accounted for a significant proportion of the variance (PCA 1, $p<0.0001$), and there was a trend for the second principal component (PCA 2, $p=0.09$). Based on these 2 rules we used PCA 1 and PCA 2 for the subsequent analyses.

Each principal component represents a linear combination of the expression of the proteins and the influence that each protein had on a principal component was reflected in the relative amplitude of the basis vector (Fig. 5). Analyzing the basis vectors was an important, 2-step process, that we used to link the principal components with relevant biological mechanisms (Beston et al., 2010). First, we computed the basis vectors, this provides insights regarding the biological mechanisms driving the data. The basis vectors for PCA 1 (Fig. 5B) showed positive contributions from all 4 of the proteins, albeit a very small amount for Synaptophysin, indicating that it is driven by total protein expression. For PCA 2 (Fig. 5C) the basis vectors showed opposite directions for Synapsin and Synaptophysin, the pre-synaptic markers for vesicle

cycling, and PSD-95 and Gephyrin, the markers for excitatory and inhibitory synapses, respectively. The different directions for the pairs suggests that PCA 2 is linked with both the pre and post-synaptic indices.

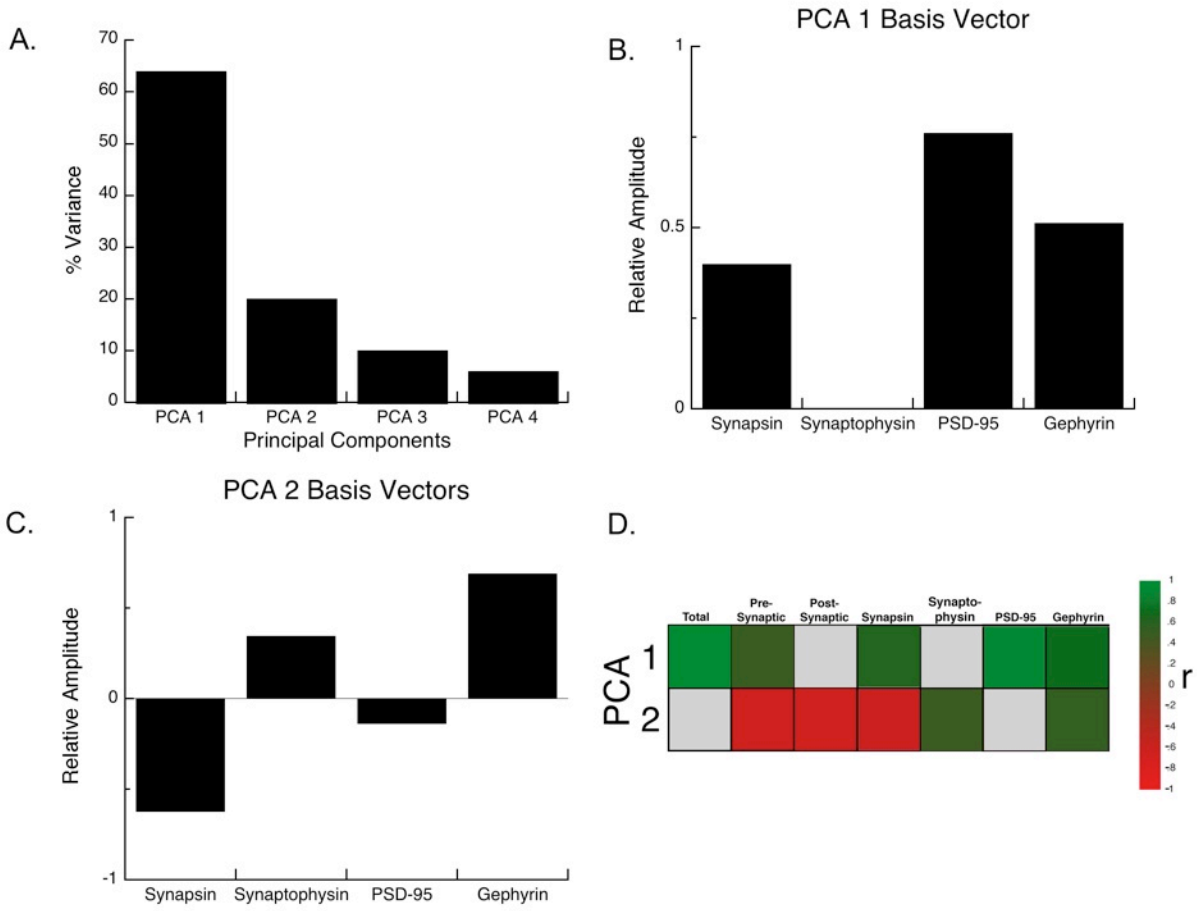

Figure 5.
Principal component analysis. (A) The percent variance captured by each component of the SVD analysis of protein expression in human visual cortex. The first 2 principal components represent 84% of the SVD. (B) The influence of each protein on the first principal component was reflected by the relative amplitude in the basis vectors. (C) The influence of each protein on the second principal component was reflected by the relative amplitude in the basis vectors. (D) Significant correlations (colored cells) between the first 2 principal components and the combinations of proteins derived from the basis vectors. The color indicates the magnitude (represented by color intensity) and direction (green indicates positive, red indicates negative) of significant correlations (Bonferroni corrected, $p<0.0035$).

For the second step, we generated a set of correlations between the two principal components (PCA 1 and PCA 2), and the 4 proteins, 2 indices, and a new measures identified in

step one (Total Protein Expression). To account for multiple comparisons, we performed a Bonferroni correction, and then displayed significant correlations between the 2 principal components and the 7 measures (Fig. 5C; green and red squares, $p<0.0035$). The pattern of correlation provided information that described the biological links for each principal component. The first principal component had the greatest correlation with total protein expression ($R=0.9764$, $p<0.0001$), and was also correlated with Synapsin ($R=0.6882$, $p<0.0001$), PSD-95 ($R=0.9486$, $p<0.0001$), Gephyrin ($R=0.7651$, $p<0.0001$), and the pre-synaptic index ($R=0.5480$, $p<0.0001$). The second principal component was correlated with changes in Synapsin ($R=-0.5944$, $p<0.0001$), Synaptophysin ($R=0.528$, $p<0.001$), and Gephyrin ($R=0.5717$, $p<0.0001$) expression, and had slightly higher correlations with the balances for the pre-synaptic ($R=-0.6105$, $p<0.0001$), and post-synaptic (E-I) ($R=-0.625$, $p<0.0001$) indices.

We plotted PCA 1 (Fig. 6A,B) and PCA 2 (Fig. 6C,D) as a function of age, and the developmental stages. The first principal component (Fig. 6A,B) was strongly correlated with total protein expression ($R=0.9764$, $p<0.0001$) and rose to a peak at about 9 years of age. The developmental of PCA 1 was well fit by a logistic function, and the peak in expression was reached at 9 years of age (Fig. 6A; Peak=9.2 +/- 0.7 years; curve-fit, $R=0.52$, $p<0.0001$). We found a similar developmental profile when comparing the age groups (Fig. 6B). There were significant differences in expression among the developmental stages (ANOVA, $p<0.0001$), with Older Children (5-11 Years) having significantly higher PCA 1 than all other age groups. Teens (12-20) also had relative higher PCA 1 when compare with Neonates (<0.3 Years; Tukey's, $p<0.01$), and Infants (0.3-1 Year; Tukey's, $p<0.05$), while Neonates (<0.3 Years) had relatively less when compare with Young Children (1-4 Years; Tukey's, $p<0.05$), and Young Adults (21-55

Years; Tukey's, p<0.05). Together, these results show a prolonged developmental increase in total expression that continues into older children, and suggests a long period of synaptic stabilization.

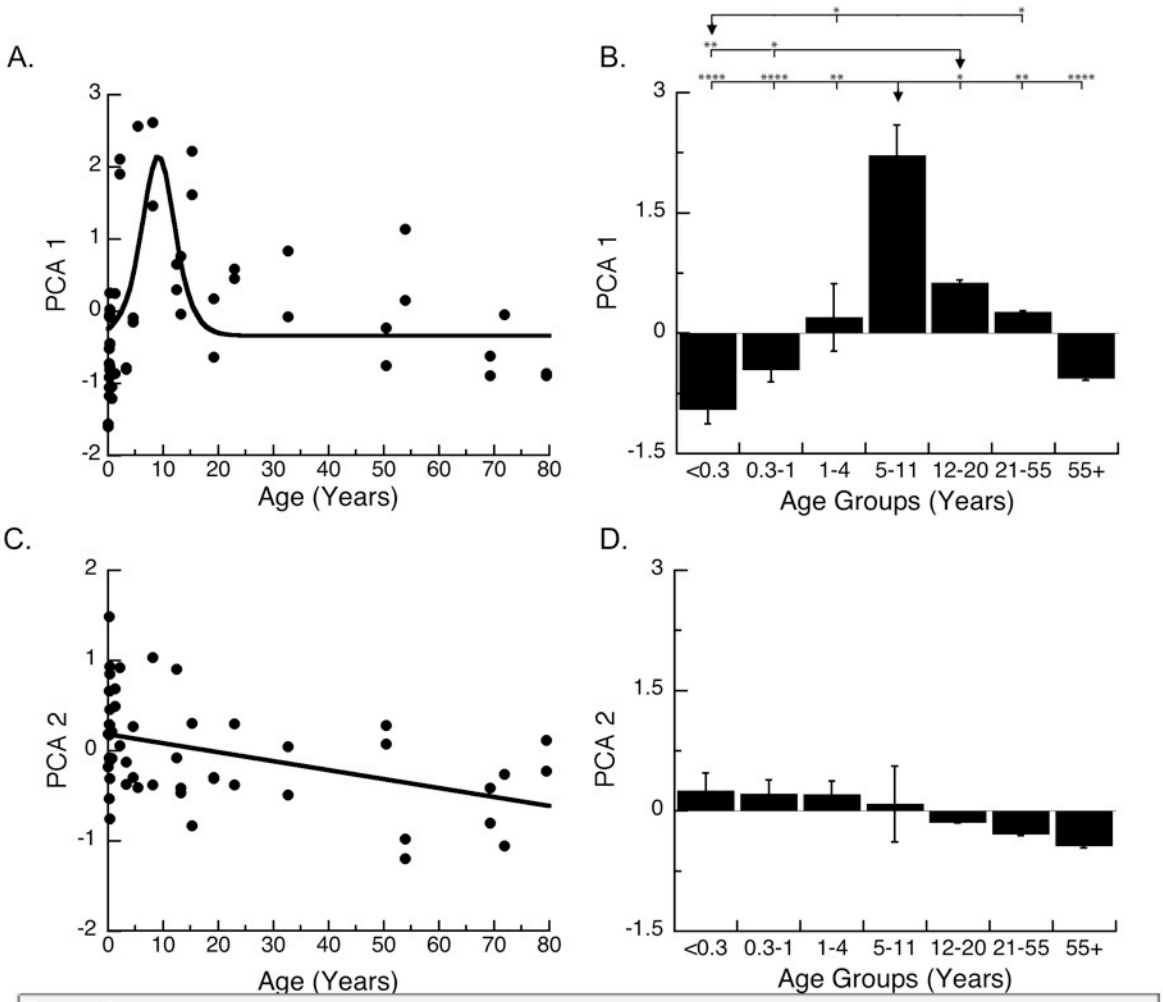

Figure 6.
Developmental changes in the principal components 1 and 2 in human visual cortex. (A) Principal component 1. A logistics function was fit to the data. Principal component 1 had a peak in expression at 9 years of age (Fig. 6; Peak=9.2 +/- 0.7 years; curve-fit, R=0.52, p<0.0001). (B) Group mean and standard error for each developmental stage are plotted and the statistical significance (ANOVA, p<0.0001) of the difference between pairs of development stages as determined by Tukey's post-hoc comparisons are plotted (* p<0.05; ** p<0.01; *** p<0.001; **** p<0.0001). (C) Principal component 2. A linear function was fit to the data (R=0.43, p<0.005). (D) Group mean and standard error for each developmental stage are plotted and there were no significant differences in expression among experimental groups (ANOVA, p=0.11).

The second principal component captured changes among a number of measures, with the strongest positive correlation being Gephyrin expression (R=0.5717, p<0.0001), and the

strongest negative correlation being the post-synaptic index (E-I balance; $R=-0.625$, $p<0.0001$). Development of PCA 2 was well fit by a linear function (Fig. 6C; $R=0.43$, $p<0.005$), and showed a very long and shallow decline. When comparing the developmental stages, it is clear that the magnitude of change in PCA 2 is small, and although there was an overall trend for a decline (Fig. 6D; ANOVA, $p=0.11$) there were no significant differences among the age groups.

Comparing human and rat total protein expression

The principal component analysis identified total expression of the 4 proteins as the main source of variance for development of human visual cortex. In another study, we quantified expression of the same synaptic proteins (Synapsin, Synaptophysin, PSD-95, and Gephyrin) in developing rat cortex, and using PCA analysis found that the largest portion of the variance was also accounted for by total protein expression (Pinto et al., 2013). Together, these data sets provide a unique opportunity to run a parallel comparison between human and rat cortical development, and determine how to translate synaptic age between these species. First, we quantified total protein expression in human visual cortex and plotted that as a function of post-conception age (Fig. 7). In human visual cortex, development of total protein expression (black dots) followed a trajectory that was well fit by a gaussian function with the peak of expression at 9 years of age (Fig. 7; curve-fit, $R=0.7376$, $p<0.0001$). Second, we plotted the development of total protein expression in rat visual cortex (Pinto et al, 2013, Fig. 7) and transformed the rat ages (P4-P93) to post-conception days. In rat visual cortex (open red dots), development of total protein expression for the range of ages followed a decay function that reached a maximum

expression at 55 days post-conception (Fig. 7; curve-fit, R=0.9215, p<0.0001).

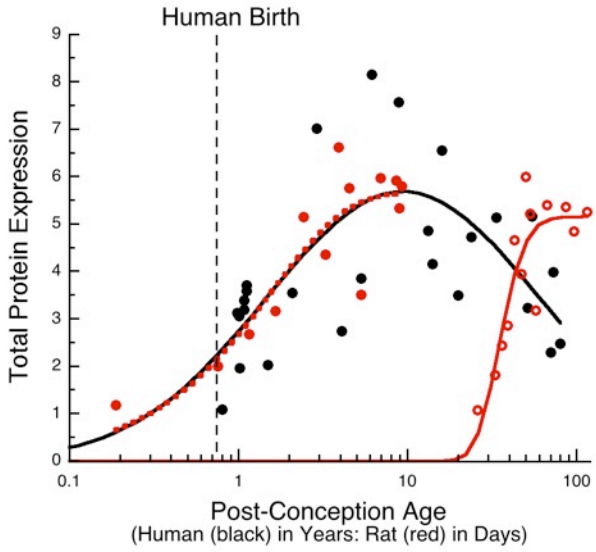

Figure 7.
Transformation of rat data to human age. Total protein expression for human (black dots), rat (open red dots), and rat transformed (red dots) data plotted as a function of post-conception age in years for human and rat transformed data and days for rat data. Human data was fit with a gaussian function (R=0.74, p<0.0001), and reached a peak in expression at 9 years of age (Peak: x-axis=9.4 years, y-axis=5.7). Rat data was fit with a decay function (R=0.92, p<0.0001), and reached maximum expression at P55 (Peak: x-axis=54.5 days, y-axis=5.2).

The process involved determining the transformation required to shift the rat curve (solid red curve) along the x- and y-axis, to match the human curve and then applying that transformation to the rat data to visualize each point in human age. To normalize the maximum expression levels, we multiplied the rat data by the quotient between the maximum for the rat and human curves (Human Expression at 9 years/Rat Expression at 55 Days=Quotient). To shift the rat along the x-axis we found the horizontal transformation necessary to match the rat and human curve of total protein expression, and then applied that transformation to each of the rat data points. The transformed rat data was plotted (red circles) in human equivalent space. This simple transformation showed similar developmental trajectories for total protein in rats (P0-P93) and humans (20d-8.5 yrs.). A large portion of those curves approximated a linear increase which facilitated a simple conversion between rat age in days and humans age in years (Rat Age (Days)=11+5.5*Human Age (Years)). Using this conversion, we made a table (Table 2) to depict the ages when protein expression was comparable between the 2 species, and highlighted known

milestones in visual system plasticity. Interestingly, there was comparable expression at human birth and rat eye opening, suggesting that total expression is driven by the initial strong visual stimuli experienced in both species. In addition, there was also comparable expression at the ages linked to the end of susceptibility for developing amblyopia in humans (~ 6 years; Keech & Kutschke, 1995), and the end of the critical period for ocular dominance plasticity in rats (P45; Fagiolini et al., 1994). Taken together, these results show the translation between rat and human synaptic development in visual cortex, and suggest that total protein expression in human and rat visual cortex reflects comparable stages of visual system development.

Table 1. Transformation of human and rat age with milestones in visual development

Human Visual Milestones	Human Age (Years)	Rat Age (Days)	Rodent Visual Milestones
	-0.6	4	
Birth	0.0	11	Eye Opening
	0.4	14	Pre-Critical Period
	0.9	17	
	1.7	21	Start of Critical Peri
	2.5	25	
	3.2	28	
	3.8	31	
	4.6	35	
End of Susceptibility for Developing Amblyopia[3]	6.2	45	End of Critical Perio
	7.8	64	
	8.2	74	
	8.5	93	

[1] Smith SL, Trachtenberg JT. 2007. Experience-dependent binocular competition in t visual cortex begins at eye opening. Nat Neurosci 10:370-5

[2] Fagiolini M, Pizzorusso T, Berardi N, Domenici L, Maffei L. 1994. Functional postnat development of the rat primary visual cortex and the role of visual experience: dark rearing and monocular deprivation. Vision Res 34:709-20

[3] Keech RV, Kutschke PJ. 1995. Upper age limit for the development of amblyopia. J Pediatr Ophthalmol Strabismus 32:89-93

Discussion

The results of this study highlight the complex nature of synaptic development in human visual cortex showing that there are both prolonged and rapid changes in synaptic proteins, and found a simple transformation to translate between synaptic age in rats and humans. We have drawn three main conclusions from the results. First, there is prolonged development of pre- and post-synaptic proteins in human visual cortex, suggesting that synaptic development and stabilization in human visual cortex extends well into the childhood years. Furthermore, expression of the pre-synaptic proteins was relatively stable into aging but there was a large loss of both post-synaptic proteins which indicates significant age-related changes in function of inhibitory and excitatory synapses. Pre-synaptically, Synaptophysin expression was relatively constant across the lifespan, while Synapsin expression increased until about 6 years of age. Both Synapsin and Synaptophysin are required for stabilization of pre-synaptic boutons (Hopf et al., 2002) and perhaps the increase in Synapsin expression during childhood promotes pre-synaptic stabilization. Post-synaptically, both PSD-95 and Gephyrin expression increased during childhood and then declined into aging. PSD-95 effects the strength of excitatory glutamatergic synapses (Schnell et al., 2002; Stein et al., 2003; Ehrlich & Malinow, 2004; Colledge et al., 2003), and nearby post-synaptic densities in a dendrite compete for the available pool of PSD-95 (Gray et al., 2006). Together, these functions for PSD-95 point to prolonged maturation of excitatory synapse functioning in human visual cortex and then age-related weakening of glutametergic synapses. On the inhibitory side, Gephyrin cluster density is negatively correlated with motility of the protein among neighboring GABAergic synapses (Kuriu et al., 2012). This function suggests that the progressive developmental increase in Gephyrin expression reflects

prolonged maturation and stabilization of inhibitory synapses followed by less stability in the aging human visual cortex. The long development trajectories for the four synaptic proteins point to slow development of synaptic stabilization in human visual cortex. Interestingly, the timing of this development coincides with clinical reports highlighting an extended period of susceptibility for developing amblyopia in children (Keech & Kutschke, 1995; Epelbaum et al., 1993).

Second, we found very rapid changes in the balances between pre- and post-synaptic proteins that are best described as switches occurring within the first year of life. The pre-synaptic proteins reached a balance at about a year of age. Since Synapsin and Synaptophysin regulate different aspects of vesicle cycling, endocytosis or exocytosis, respectively, their balance will effect the probability of transmitter release, especially with strong or sustained patterns of visually-driven activity. This rapid pre-synaptic development likely effects the maturation of neural signal-to-noise contributing to the change from weak and sluggish, to strong and sustained firing patterns. That change is necessary for both efficient synaptic transmission (Rust et al., 2002) and driving neuroplasticity mechanisms needed for development of receptive field properties (Smith & Trachtenberg, 2007). The post-synaptic E-I switch was even faster occurring at about 5 months of age with the change from more Gephyrin towards balanced expression between Gephyrin and PSD-95. This switch in the E-I balance in human visual cortex parallels the change we found for rat visual cortex at the start of the critical period for ocular dominance plasticity (Pinto et al, submitted). Perhaps the rapid change in the E-I balance reflects the onset of the period for greatest ocular dominance plasticity in human visual cortex since the relative expression of PSD-95 and Gephyrin provides an indication of the balance

between excitatory and inhibitory synapses that contribute to the physiological E-I balance (Keith & El-Husseini, 2008; Lardi-Studler et al., 2007; Prange et al., 2004). Early in development, the physiological E-I balance favors excitation, and a strong increase in inhibition is known to trigger the onset of the critical period for ocular dominance plasticity (Fagiolini & Hensch, 2000; Maffei & Turrigiano, 2008). Our finding of more Gephyrin early in development may seem counter intuitive to the physiological findings, but GABAA receptors are depolarizing early in development due to an abundance of the immature chloride co-transporters NKCC1. During development, there is a switch from NKCC1 to KCC2, which turns GABAA receptors hyperpolarizing (Ben-Ari, 2002). This switch takes place early in human cortical development, with a 3-fold reduction in NKCC1 during the first 3 months of life, and a 95% increase in KCC2 within the first year (Kirmse et al., 2011). The timing of the switch in the chloride co-transporters supports 3-5 months as the age when there is a strong increase in inhibition that could trigger the onset of the critical period. Functional aspects of binocular vision also emerge during this early developmental window (3-5 months) (Braddick et al., 1980; Braddick et al., 1983; Held et al., 1980), and the maturation of cortical binocularity in infants is driven by visual experience (Jando et al., 2012). Our results point to rapid development of the E-I balance and raise the intriguing possibility that maturation of human visual cortex has an early pre-critical period (before 5 months) when experience-dependent binocular competition drives map refinement (Smith & Trachtenberg, 2007), followed by the onset of the critical period for ocular dominance plasticity at about 5 months of age. This possibility of a pre-critical and critical period during the first year of life may be important for the development and translation of more effective neuroplasticity-based treatments for amblyopia in children.

Third, using a neuroinformatics approach we analyzed expression of all four synaptic proteins and found that total protein expression accounts for most (64%) of the variance in development of human visual cortex across the lifespan. Furthermore, the total expression of Synapsin, Synatophysin, PSD-95 and Gephyrin had a very prolonged developmental trajectory that increased until late childhood and then decreased into aging. Recently, we applied the same analysis to rat visual cortex and found that total protein expression also accounts for a surprisingly similar amount (64%) of the developmental changes in the set of synaptic proteins (Pinto et al, submitted). This strong similarity between rat and human visual cortex provided us with a measure -- total protein expression -- to determine the transformation from rat to human synaptic age. A simple transformation showed good alignment between biologically relevant stages during development of rat and human visual system. For example, total protein expression levels were similar at birth in humans and at eye opening (~P11) in rats. This is consistent with previous studies suggesting that rat cerebral cortex at P12-13 is comparable to human cerebral cortex at birth (Romijn et al., 1991), and that the initial strong visual stimulation experienced in both species drives similar increases in synaptic protein expression. In addition, total protein expression at 6 years of age in humans lined up with 45 days of age in rats. These two ages coincide with the end of susceptibility for developing amblyopia in children (Keech & Kutschke, 1995) and the end of the critical period for ocular dominance plasticity in rats (Fagiolini et al., 1994). Interestingly, the transformation that we used led to the alignment of a number of important milestones in visual system development and plasticity between rats and humans. These results suggest that the developmental trajectories for total protein expression reflect similar changes in experience-dependent neuroplasticity in both species. Furthermore, it

points to total protein expression as a good measure for aligning cortical age between species and helping to find optimal translation from animal models of neuroplasticity to human developmental stages.

Although we have effectively translated synaptic age of visual cortex between rodents and humans, a number of challenges still arise in converting detailed rodents studies to humans. Even though rodents and humans share 75% 1:1 gene orthologues (Church et al, 2009), slight differences in the genome make translation difficult (Geerts, 2009), for example, mice lack the ApoE4 gene, which is a major risk factor for Alzheimer's (Loring et al., 1996). These slight differences render animal models incomplete, making it difficult to generate functionally relevant conclusions about human disease or development. There are a number of similarities and differences in the developmental trajectories of the synaptic proteins in human and rat visual cortex. Synapsin, Gephyrin, and the post-synaptic index followed the same developmental trajectory, whereas, Synaptophysin, PSD-95, and the pre-synaptic index followed different developmental trajectories in human visual cortex as compared to previous studies of rat visual cortex (Pinto et al, Submitted). These differences in individual proteins, and the known differences in the genome between rats and humans highlight the need to conduct parallel studies to compare between the species, and the importance of quantify composite measures, such as total protein expression, that capture comparable changes between the species.

Previous studies of human visual cortex development used anatomical techniques (e.g. electron microscopy) to count synapses and found a peak in the number of synapses at about 8-11 months of age (Huttenlocher et al., 1982). The timing of that peak is around the ages when the pre- and post-synaptic balances were reached, however, we found that maturation of protein

expression continued for a number of years until later childhood (about 8-10 years of age). The electron microscopy (EM) studies defined a synapse as the presence of synaptic vesicles, as well as a pre- and post-synaptic density (Huttenlocher et al., 1982), perhaps the pre- and post-synaptic balances used in this study are tied to initial presence of a full synaptic complement. There is a peak in the number of dendritic spines at 5 months of age, with adult levels reached at 2 years of age (Michel & Garey, 1984) which is similar to our results for maturation of the E-I balance. It is important to note that quantifying expression of synaptic proteins is different from using EM to count synapses, and this difference may contributed to why the peaks from counting synapses and quantifying protein expression do not line-up. Answering this issue will require application of new anatomical techniques, such and array tomography (Micheva & Smith, 2007), that have high enough resolution to counts synapses and label with multiple markers for synaptic proteins.

An important aspect of the developing human visual cortex is the inter-individual variability in expression of synaptic proteins, especially in children, that we observed in this and our previous studies (Murphy et al., 2005; Pinto et al., 2010; Williams et al., 2010). This developmental variability is greater than what we have found when studying synaptic proteins in various animal models (Beston et al., 2010; Williams et al., 2010; Murphy et al., 2011) and points to the need for extra care when interpreting results of human cortical development from small sample sizes. Anatomical studies of human cortex are very time consuming and technically challenging because of the need to collect the postmortem tissue samples, for example, Huttenlocher et al, (1982) had just 6 samples between 4 months and 11 years of age. Perhaps the greater number of samples in the current study helped to reveal the large variability

throughout childhood and resulted in developmental trajectories that were less effected by an individual spike in expression.

A growing number of studies are finding complex patterns of change across the lifespan in human cortex for expression of synaptic proteins (Murphy et al, 2005; Pinto et al, 2010; Williams et al, 2010) and the genes that encoding synaptic proteins (Duncan et al., 2010). For example, expression of the Angelman Syndrome protein -- Ube3A -- is relatively steady throughout development, and then has a large loss of expression in aging (Williams et al, 2010). Since Ube3A is tied to trafficking of the GluA containing excitatory receptors that studies provides additional support for an age-related loss of function at glutamatergic synapses. GABAergic proteins exhibit a very complex pattern with some increasing (e.g. GABAaa1), others decreasing (e.g. VGAT), and Gephyrin following a rise then fall of expression (Pinto et al., 2010). It is clear that more studies, with even more samples than we have used, are needed to address the issue of inter-individual variability in developing human cortex.

Full characterization of the changing synaptic proteome in human cortex is an important goal for future studies to identify key stages of human cortical development when neuroplasticity driven by disease can cause maladaptive change and when neuroplasticity driven by new treatments can promote adaptive change. The results from this study provide a basis for aligning maturation of cortical synapses in animals and humans, an important step in the development of optimal neuroplasticity based therapies. Recent advances in the development of neuroplasticity therapies have shown that a number of interventions (e.g. dark rearing, fluoxetine, environmental enrichment, food restriction) can promote recovery from abnormal early visual experience in adult (P100) rats (Baroncelli et al, 2010; He et al, 2007; Maya Vetencourt et al, 2008; Spolidoro

et al, 2011). Rats at P100 are typically describes as "adults" due to their early sexual maturity (Quinn, 2005). However, the relationship between sexual maturity and cortical maturity is not the same in rats and humans, and using sexual maturity has led to misalignment of cortical developmental stages between the species. Thus, it is an open question whether newly developed neuroplasticity interventions for P100 rats can be effectively translated to treat amblyopia or other visual disorder in adult humans. Additional parallel studies of neuroplasticity using animal models and humans will be key to identifying age-appropriate therapies that can be effectively translated to provide optimal treatment for human visual diseases.

Chapter 4.

Development of GABAergic mechanisms in human visual cortex across the lifespan

Introduction

Functional maturation of the visual cortex is linked with dynamic changes in synaptic expression of GABAergic signaling mechanisms. Even small changes in the relative amounts of excitation and inhibition can dramatically alter experience-dependent plasticity (Hensch et al., 1998; Iwai et al., 2003; Kirkwood & Bear, 1994). During development, specific components of the GABAergic signaling affect ocular dominance plasticity (Hensch et al., 1998; Hensch, 2005; Fagiolini et al., 2004) and orientation selectivity (Fagiolini et al.,2004; Tsumoto & Sato, 1985). Furthermore, the emergence of normal binocular visual function depends on interocular inhibition that is mediated by GABAergic inhibitory circuitry in visual cortex (Sengpiel & Vorobyov, 2005). In adult visual cortex, activity regulates $GABA_A$ receptor expression (Hendry et al., 1994) and during aging the loss of orientation tuning in visual cortical receptive fields (Leventhal et al., 2003) and changes in visual perception (Betts et al., 2005) have been linked with an overall loss of GABA.

When GABAergic signaling in visual cortex is manipulated to shift the excitatory-inhibitory balance, the effect can either enhance or reduce experience-dependent plasticity (Maffei et al., 2004; Hensch & Fagiolini, 2005; Iwai et al., 2003; Kirkwood & Bear, 1994). This approach has been extended in a series of recent studies using pharmacological manipulations of GABA signaling, such as fluoxetine, to reinstate ocular dominance plasticity in adult visual cortex and facilitate recovery from amblyopia (Maya Vetencourt et al., 2008; Harauzov et al., 2010). Taken together, these studies are providing a better understanding for the role of GABAergic signaling in the maturation and function of the visual cortex, and have opened the

door for the development of new treatments for neurodevelopmental disorders such as amblyopia.

The GABAergic synapse is a complex structure with a large set of pre- and post-synaptic proteins, many of which have been linked with experience-dependent plasticity in the cortex. On the pre-synaptic side these include: the 2 isoforms of the GABA synthesizing enzyme glutamic acid decarboxylase (GAD), GAD65 and GAD67; the CB1 receptor that modulates GABA release; and the vesicular transporter VGAT that is responsible for loading GABA into synaptic vesicles (McIntire et al., 1997; Sagne et al., 1997). GAD65 is localized in the axon terminals and synthesizes the on-demand pool of GABA, while GAD67 is located in the cell body and synthesizes the basal pool of GABA (Feldblum et al., 1993; Feldblum et al., 1995). Knocking out GAD65 leads to a loss of critical period ocular dominance plasticity, however, it can be rescued by infusion of diazepam (Iwai et al., 2003). Activation of CB1 receptors is involved in regulating activity-dependent synaptic plasticity (Sjöström et al., 2003; Jiang et al., 2010) and blocking CB1 receptors during the critical period alters activity patterns (Bernard et al., 2005). Finally, VGAT contributes to an efficient up- and down-regulation of vesicular GABA content that effects postsynaptic currents and the fine-tuning of inhibitory strength (Engel et al., 2001).

On the post-synaptic side many components of the ionotropic $GABA_A$ receptor complex contribute to experience-dependent plasticity. Gephyrin is the $GABA_A$ receptor anchoring protein. Gephyrin clusters $GABA_A$ receptors (Essrich et al., 1998; Kneussel et al., 1999), and it seems to fulfill a modulator role for changes in synaptic activity and structure. Furthermore, expression levels of Gephyrin give an indication of the total amount of $GABA_A$ receptors at a given time. The $GABA_A$ receptor is a pentameric structure and is functionally diverse, with 20

known subunits. Three subunits are of particular interest, α1, α2, and α3, because they are developmentally regulated (Chen et al., 2001; Bosman et al., 2002; Hendrickson et al., 1994), they affect receptor kinetics (Laurie et al., 1992; Gingrich et al., 1995), and the α subunit is the interface for binding GABA (Smith & Olsen, 1995) and benzodiazepine (Sigel, 2002). Both α1 and α2 subunits play key functional roles, with α2 involved in regulating cell firing, and α1 necessary for critical period plasticity (Fagiolini et al., 2004). The α1 subunit also has high-affinity for binding GABA and benzodiazepine receptor ligands (Pritchett et al., 1989).

Although there have been many animal studies of developmental and aging changes in expression of GABAergic signaling components in visual cortex (e.g. Guo et al., 1997; Hendrickson et al., 1994; Hornung & Fritschy, 1996; Shaw et al., 1991; Minelli et al., 2003; Leventhal et al., 2003), there have been relatively few studies of human visual cortex (Murphy et al., 2005). This poses a challenge when considering how to translate GABAergic drug treatments for amblyopia from animal models to human trials. To fill this gap, we have carried out a comprehensive study of changes in the expression of a collection of pre- and post-synaptic GABAergic signaling mechanisms in human visual cortex across the lifespan. Using Western blot analysis we quantified the developmental trajectories for 4 pre- and 4 post-synaptic components of GABA signaling. These results show a complex pattern of different developmental trajectories among the GABA signaling mechanisms in human visual cortex. Many of the changes are prolonged, highlighting a long time course for the development of GABA signaling in human visual cortex, much longer than would be predicted from animal studies. Furthermore, there are 3 transition stages when there are rapid switches in the relative amounts of the different components, indicating that functioning of the GABAergic system must

change as the visual cortex develops and ages. A portion of these data has been presented previously (Pinto et al., 2008).

Methods

Samples and Tissue

Tissue samples were obtained from the Brain and Tissue Bank for Developmental Disorders at the University of Maryland (Baltimore MD). The samples were from the posterior pole of the left hemisphere of human visual cortex, including both superior and inferior portions of the calcarine fissure where the central visual field is represented in primary visual cortex (V1) according to the gyral and sulcal landmarks. The samples were from 28 individuals ranging in age from 20 days to 80 years (Table 1). All samples were obtained within 23 hours postmortem, and at the Brain and Tissue Bank were fresh frozen after being sectioned coronally in 1-cm intervals, rinsed with water, blotted dry, placed in a quick-freeze bath (dry ice and isopentane), and stored frozen (-70°C). The individuals had no history of neurological or mental health disorders.

Tissue-Sample Preparation

Tissue samples (50-100 mg) were cut from the frozen block of V1 and suspended in cold homogenization buffer (1 ml buffer:50 mg tissue, 0.5mM DTT, 1mM EDTA, 2 mM EGTA, 10 mM HEPES, 10mg/L leupeptin, 100nM microcystin, 0.1 mM PMSF, 50 mg/L soybean trypsin inhibitor). The tissue samples were homogenized in a glass-glass Dounce homogenizer (Kontes, Vineland, NJ). A subcellular fractionation procedure (synaptoneurosomes) (Hollingsworth et al., 1985; Titulaer & Ghijsen, 1997; Quinlan et al., 1999) was performed to obtain protein samples that were enriched for synaptic proteins. The synaptoneurosome was obtained by passing the

homogenized sample through a coarse (100µm) pore nylon-mesh filter followed by a fine (5µm) pore hydrophilic mesh filter (Millipore, Bedfored, MA), then centrifuged at x1,000g for 10 min

Table 1. Human Tissue Samples. The age group, age, postmortem interval and cause of death for each of the human cortical tissue samples.

Age Group	Age	Postmortem Interval (hours)	Sex	Cause of death
Neonates	20 days	14	F	pneumonia
Neonates	86 days	23	F	not known
Neonates	96 days	12	M	bronchopneumonia
Neonates	98 days	16	M	cardiovascular disorder
Neonates	119 days	22	M	bronchopneumonia
Neonates	120 days	23	M	pneumonia
Neonates	133 days	16	M	accidental
Neonates	136 days	11	F	pneumonia
Neonates	273 days	10	M	sudden infant death syndrome
Infants	1.34 years	21	M	dehydration
Infants	2.16 years	21	F	cardiovascular disorder
Infants	2.21 years	11	F	accidental
Young Children	3.34 years	11	F	drowning
Young Children	4.56 years	15	M	accidental
Young Children	4.71 years	17	M	drowning
Older Children	5.40 years	17	M	accidental
Older Children	8.14 years	20	F	accidental
Older Children	8.59 years	20	F	cardiovascular disorder
Teens	12.45 years	22	M	cardiovascular disorder
Teens	13.27 years	5	M	asphyxia
Teens	15.22 years	16	M	multiple injuries
Young Adults	22.98 years	4	M	multiple injuries
Young Adults	32.61 years	13	M	cardiovascular disorder
Young Adults	50.43 years	8	M	cardiovascular disorder
Young Adults	53.90 years	5	F	cardiovascular disorder
Older Adults	69.30 years	12	M	cardiovascular disorder

Age Group	Age	Postmortem Interval (hours)	Sex	Cause of death
Older Adults	71.91 years	9	F	multiple medical disorders
Older Adults	79.50 years	14	F	drug overdose

to obtain the synaptic fraction of the membrane. The synaptic pellet was resuspended in boiling 1% sodium-dodecyl-sulfate (SDS) and stored at -80 C. Protein concentrations were determined using the bicinchonic acid (BCA) assay guidelines (Pierce, Rockford, IL). A control sample was made by combining a small amount of the prepared tissue sample from each of the cases.

Immunoblotting

The samples (20 µg) were separated on Sodium-dodecyl-sulfide polyacrylamide gels (SDS-PAGE) and transferred to polyvinylidene difluoride (PVDF-FL) membranes (Millipore, Billerica, MA). Each sample was run multiple times. Blots were pre-incubated in blocking buffer (Odyssey Blocking Buffer 1:1 with PBS) for 1 hour (Li-cor Biosciences; Lincoln, NE), then incubated in primary antibody overnight at 4°C using the following concentrations: GAD65, 1:500 (Chemicon, Temecula, CA); GAD67, 1:1000 (Chemicon, Temecula, CA); VGAT, 1:1000 (Synaptic Systems, Goettingen, GER); CB1, 1:1000 (Cayman, Ann Arbor, MI); Gephyrin, 1:500 (Chemicon, Temecula, CA); $GABA_A$ α1, 1:500 (Imgenex, San Diego, CA); $GABA_A$ α2, 1:1000 (Imgenex, San Diego, CA); $GABA_A$ α3, 1:1000 (Imgenex, San Diego, CA). The blots were washed with phosphate buffer saline containing 0.05% Tween (Sigma, St. Louis, MO) (PBS-T) (3 x 10 min), incubated (1 hour, room temperature) with the appropriate IRDye labeled secondary antibody, (Anti-Mouse, 1:8000, Anti-Rabbit, 1:10,000) (Li-cor Biosciences; Lincoln, NE), and washed in PBS-T (3 x 10 min). The blots were visualized using the Odyssey scanner

(Li-cor Biosciences; Lincoln, NE). The blots were stripped and prepared to be re-probed with additional antibodies (Blot Restore Membrane Rejuvenation kit, Chemicon International, Temecula, CA).

Analysis

To analyze the bands, we scanned the blots (Odyssey Infrared Scanner) and quantified the bands using densitometry (Licor Odyssey Software version 3.0; Li-cor Biosciences; Lincoln, NE). Density profiles were determined by performing a subtraction of the background, integrating the pixel intensity across the area of the band, and dividing the intensity by the width of the band to control for variations in band size. A control sample (a mixture of all the samples) was run on all of the gels and the density of each sample was measured relative to that control (sample density / control density).

To visualize changes in expression of the GABAergic signaling mechanisms, the results were plotted in 2 ways. This was done to facilitate analysis of changes between developmental stages, to describe the pattern of changes, and to be able to quantify the time course of changes. First, the samples were grouped into developmental ages (< 1 years neonates, 1-2 years infants, 3-4 years young children, 5-11 years older children, 12-20 years teens, 21-55 young adults, and >55 older adults) with 3 or more cases in each group and following the age groups used by Law et al (2003) and Duncan et al (2010). Group means and standard errors were calculated for each antibody and normalized to the mean level of expression for the youngest group. Second, we plotted scattergrams for each antibody that included both the average expression level (black symbols) for each case and every point from all runs (gray symbols). To help describe the pattern of change in expression across the lifespan, a weighted average curve was fit to each

scatter plots using the locally weighted least squares method at 50% (dotted lines). In addition, an exponential decay function (solid lines) was fit to the scattergrams when there was a clear monotonic increase or decrease in the expression across the lifespan. The goodness of fit was determined (R) and the time constant (τ) for the rise or fall of expression level was calculated from the exponential decay function. The age when adult levels were reached was defined as 3τ. This provides an objective measure, representing the age at which expression had reached 87.5% of their asymptotic level.

Four indices were calculated to quantify relative changes in expression levels of the GABAergic signaling components: maturation of receptor composition ($GABA_A\,\alpha1$: $GABA_A\,\alpha2$ [($GABA_A\,\alpha1$-$GABA_A\,\alpha2$)/($GABA_A\,\alpha1$+ $GABA_A\,\alpha2$)]; $GABA_A\,\alpha1$: $GABA_A\,\alpha3$ [($GABA_A\,\alpha1$-$GABA_A\,\alpha3$)/($GABA_A\,\alpha1$+ $GABA_A\,\alpha3$)]; changes in pre-synaptic production vs trafficking (GAD65:VGAT [(GAD65-VGAT)/(GAD65+VGAT)]); and changes in pre- vs post-synaptic GABAergic signaling (GAD65:Gephyrin [(GAD65-Gephyrin)/GAD65 + Gephyrin)]).

Statistical comparisons of differences in expression levels between the age groups were calculated using Kruskal–Wallis nonparametric analysis of variance and planned pairwise comparisons using a Tukey's HSD test ($p<0.05$).

Results

The tissue samples were collected over a range (4-23 hours) of postmortem intervals and the first step was to determine if that interval affected expression of any of the GABAergic proteins. There were no significant correlations (ps>0.1) between postmortem interval and the expression level for any of the antibodies (GAD65, R=0.26; GAD67, R=0.08; VGAT, R=0.20; $GABA_A\alpha1$, R=0.04; $GABA_A\alpha2$, R=0.25; $GABA_A\alpha3$, R=0.17; Gephyrin, R=0.17; CB1, R=0.19).

Changes in Presynaptic GABAergic Components

Expression levels of the two GABA synthesizing enzymes (GAD65 and GAD67) were quantified in human V1 across the lifespan. GAD65 is the isoform that localizes in the axon-terminals and is responsible for supplying the "on-demand" pool of GABA. GAD67 is the isoform that is predominant in the cell body and supplies the basal pool of GABA (Esclapez 1994, Feldblum 1993). Expression levels of GAD67 did not change across the lifespan (Fig. 1A, 1B). In contrast, developmental changes were found for GAD65 expression levels ($p<0.0002$) (Fig 1C, 1D). GAD65 showed a progressive 60% increase in expression levels from early in life (<4 years) to the teenage and adult years ($p<0.05$), with a slight decline into older adults (>55 years). The difference in the developmental trajectories of these two enzymes indicates that the basal pool of GABA is maintained across the lifespan, whereas the axonal pool has a time window of heightened production capacity.

To further examine how the presynaptic components of the GABAergic system change across the lifespan in human V1, we quantified the expression of two key inhibitory proteins, CB1 and VGAT (Fig. 2). CB1 is a presynaptic receptor involved in modulating GABA release (Hajos & Freund, 2002) ; over the lifespan there were significant changes in the expression of

CB1 in human V1 ($p<0.0002$). In infants (< 1 year) and pre-teens (5-11 years), CB1 expression was high, but in young children (1-2 years), adults (21-55 years), and older adults (>55 years) it was about 40% less ($p<0.05$) (Fig. 2A, 2B). The GABA vesicular transporter VGAT showed a similar pattern of expression levels across the lifespan ($p<0.002$). VGAT expression was highest in infants (<1 year) and pre-teens (5-11 years), and had about 32% less expression in adults (21-55 years) ($p<0.02$) (Fig. 2C, 2D).

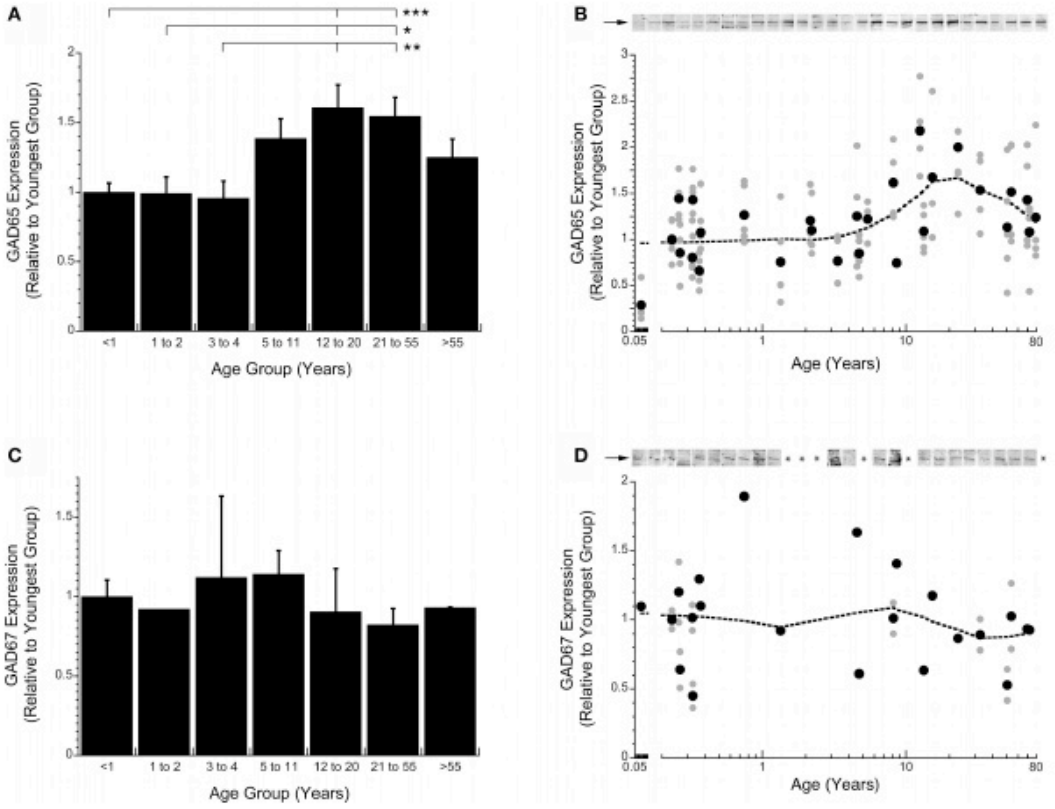

FIGURE 1 | Developmental changes in GAD65 (A,B) and GAD67 (C,D) expression in human visual cortex across the lifespan plotted relative to the youngest age group (<1 year) for the grouped means and scattergrams (• average expression for each case; ◦ all runs). Example blots for each case are presented above the scattergrams **(B,D)**. The arrow indicates the band that was quantified. A weighted average curve was fit to each scatter plots using the locally weighted least squares method at 50% (dotted line). GAD65 showed a significant change across the lifespan (Kruskal–Wallis, $p < 0.0001$) with progressive increase in expression levels into the teenage and adult years then a loss with aging **(A,B)**. There was no change in expression levels of GAD67 across the lifespan **(C,D)**. The lines above the histograms identify the groups that were significantly different (Tukey's *post hoc* HSD, $*p < 0.05$, $**p < 0.02$, $***p < 0.001$).

To quantify changes in the balance between the mechanisms that produce and traffic GABA in the presynaptic terminal, we calculated an index of GAD65:VGAT expression. There were significant changes in the balance between GAD65:VGAT across the lifespan ($p<0.0005$).

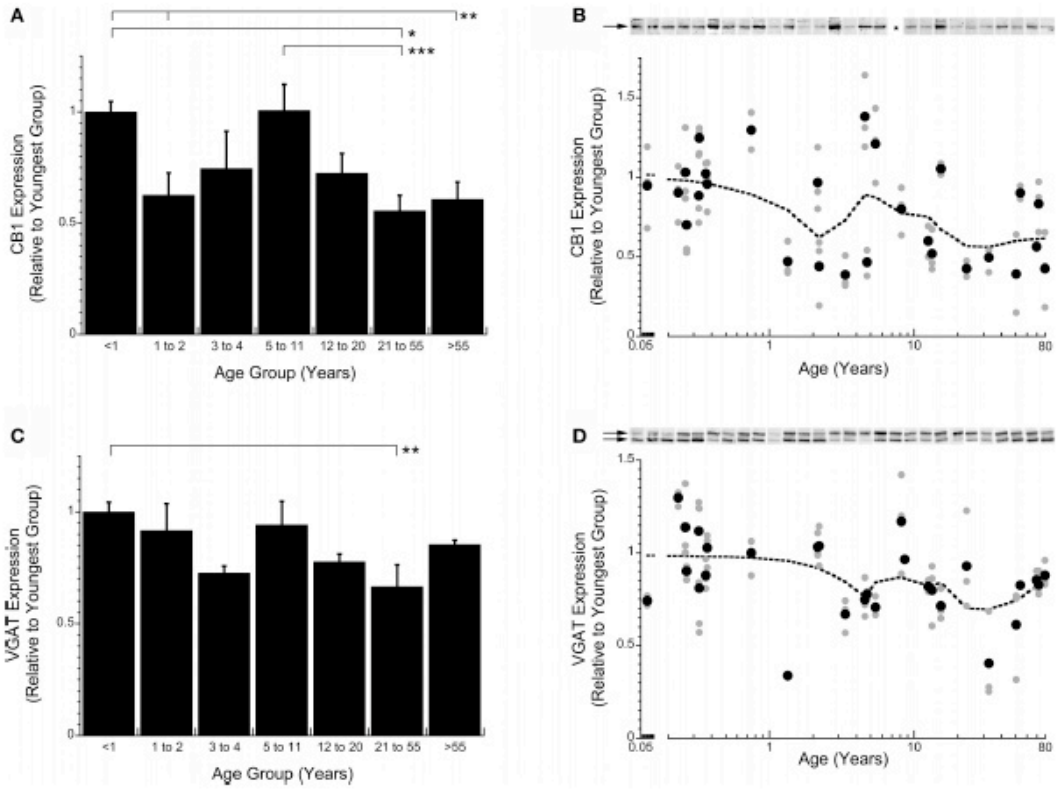

FIGURE 2 | Quantification of changes in expression levels of CB1 (A,B) and VGAT (C,D) in human visual cortex across the lifespan. The graphs follow the same conventions as described in **Figure 1**. CB1 levels are high in infants (<1 year) then fall into young children (1–2 years) before rising again in pre-teens (5–11 years) and falling again in teens (12–20 years) and leveling off (Kruskal–Wallis, $p < 0.0001$) **(A,B)**. For VGAT 2 bands were quantified (arrows at 50 and 57 kDa). VGAT levels are highest in infants (<1 year) then gradually fall into children (3–4 years) before rising again into pre-teens (5–11 years) then falling into adults (21–55 years) before finally rising again in older adults (>55 years) (Kruskal–Wallis, $p < 0.005$) **(C,D)**. The lines above the histograms identify the groups that were significantly different (Tukey's *post hoc* HSD, $*p < 0.05$, $**p < 0.02$, $***p < 0.001$) (• average expression for each case; • all runs; dotted line is the weighted average).

There was more VGAT expression in both young children (< 11 years) and older adults (>55 years) (Fig. 3). In contrast, there was an abrupt switch to much more GAD65 during the teenage ($p<0.02$) and young adult years ($p<0.001$). These shifts in the balance between GAD65 and VGAT indicate that the rate limiting component regulating GABA transmission changes across the lifespan (Fig. 3).

Postsynaptic Changes in $GABA_A$ Receptors

Expression levels for 3 subunits of the ionotropic $GABA_A$ receptor were quantified ($GABA_A\alpha1$, $GABA_A\alpha2$, $GABA_A\alpha3$). Each subunit exhibited a unique developmental trajectory

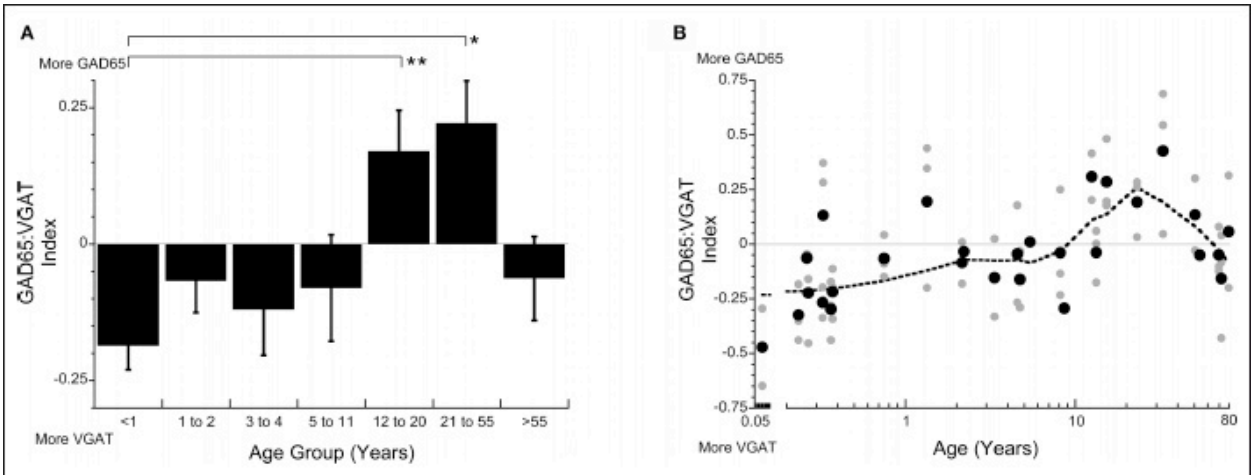

FIGURE 3 | The index of GAD65:VGAT (A,B) gives insight into the relative balance between production and trafficking of GABA. The balance is in favor of VGAT early (<11 years) and late (>55 years) in development, but there is much more GAD65 during the teenage to adult years (12–55 years) (Kruskal–Wallis, $p < 0.0002$) **(A,B)**. The lines above the histograms identify the groups that were significantly different (Tukey's *post hoc* HSD, $*p < 0.05$, $**p < 0.02$, $***p < 0.001$) (• average expression for each case; ▪ all runs; dotted line is the weighted average).

across the lifespan (Fig. 4). Quantification of $GABA_A\alpha1$ expression in human V1 showed a prolonged development profile, increasing about 75% to reach adult levels at 13.5 years of age (3τ, τ=4.50 years, R=0.67; p<0.0001; Fig. 4B). $GABA_A\alpha2$ expression changed in the opposite direction and had a slightly more rapid developmental profile, decreasing by about 65% to reach adult levels at 10 years of age (3τ, τ=3.34 years, R=0.96; p<0.0001; Fig. 4D). $GABA_A\alpha3$ had no significant change in expression levels across the lifespan (p>0.36 Fig. 4E, 4F).

The 3 $GABA_A$ receptor subunits that we quantified are classified into two categories, immature ($GABA_A\alpha2$, $GABA_A\alpha3$) and mature ($GABA_A\alpha1$), with the mature subunit conferring faster receptor decay times and great affinity for GABA compared with the immature subunits. To determine the magnitude and time-course of receptor maturation we calculated two indices ($GABA_A\alpha1$:$GABA_A\alpha2$, $GABA_A\alpha1$:$GABA_A\alpha3$). The $GABA_A\alpha1$:$GABA_A\alpha2$ balance was initially in favor of $GABA_A\alpha2$, then progressively shifted towards more $GABA_A\alpha1$ (Fig. 5). We fit a tau (τ) function to the index to quantify the time-course of the switch in receptor composition. The mature balance was reached at 4.5 years of age (3τ, τ=1.50 years, R=0.84;

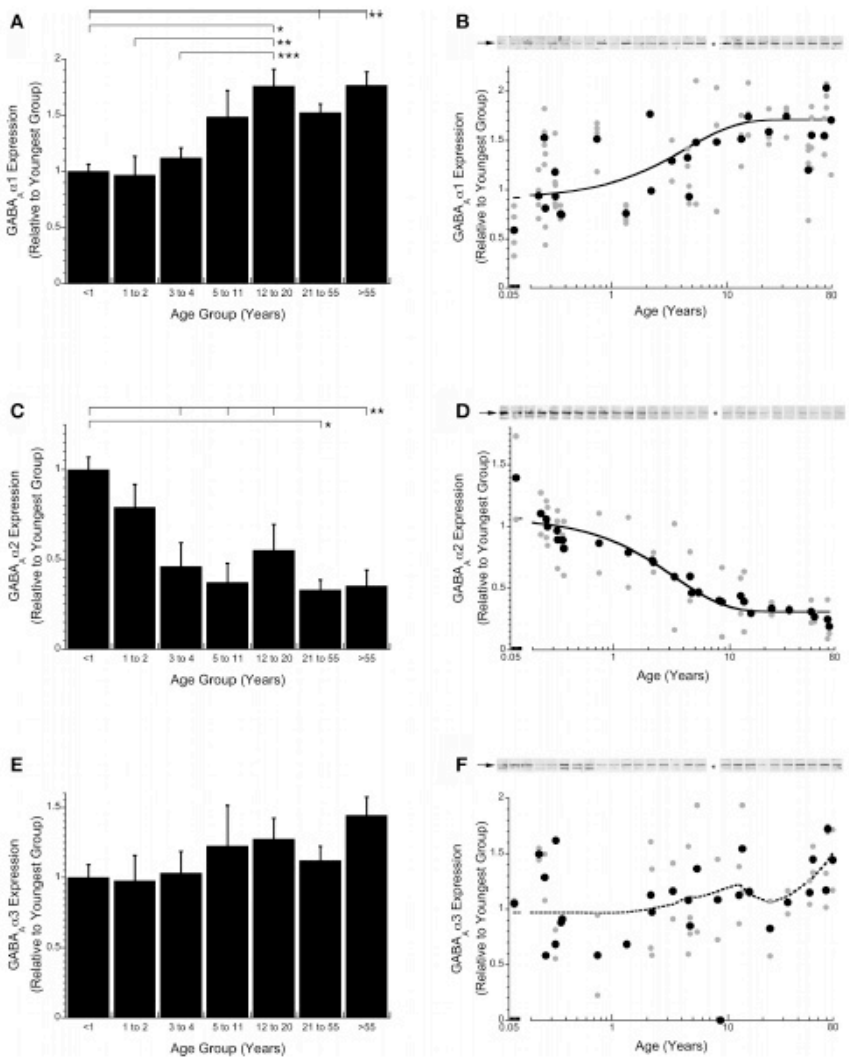

FIGURE 4 | Changes in expression of GABA$_A$ receptor subunits GABA$_A$α1 (A,B), GABA$_A$α2 (C,D), and GABA$_A$α3 (E,F) during postnatal development. An exponential decay function (solid line) was fit to the expression levels for GABA$_A$α1 and GABA$_A$α2 and the time constants (τ) were calculated with adult levels defined as 3τ. GABA$_A$α1 expression increased until early teens when it leveled off (3τ = 13.5 years, τ = 4.50 years, $R = 0.67$; $p < 0.0001$; **B**). GABA$_A$α2 expression decreased until older childhood when it leveled off (3τ = 10 years of age, τ = 3.34 years, $R = 0.96$; $p < 0.0001$; **D**). GABA$_A$α3 expression levels did not change significantly throughout the lifespan **(E,F)** (dotted line is the weighted average). The lines above the histograms identify the groups that were significantly different (Tukey's *post hoc* HSD, $^*p < 0.05$, $^{**}p < 0.02$, $^{***}p < 0.001$) (• average expression for each case; ∘ all runs).

p<0.0001; Fig. 5B). The GABA$_A$α1:GABA$_A$α3 switch was smaller in magnitude and much more abrupt. There was initially more GABA$_A$α3, but that switched within the first year to slightly more GABA$_A$α1, and reached mature levels at about 8 months of age (3τ, τ=0.23 years, R=0.65; p<0.0001; Fig. 5D). Both indices showed a shift to more GABA$_A$α1, however, there

was a greater change for the shift from more $GABA_A\alpha2$ to more $GABA_A\alpha1$.

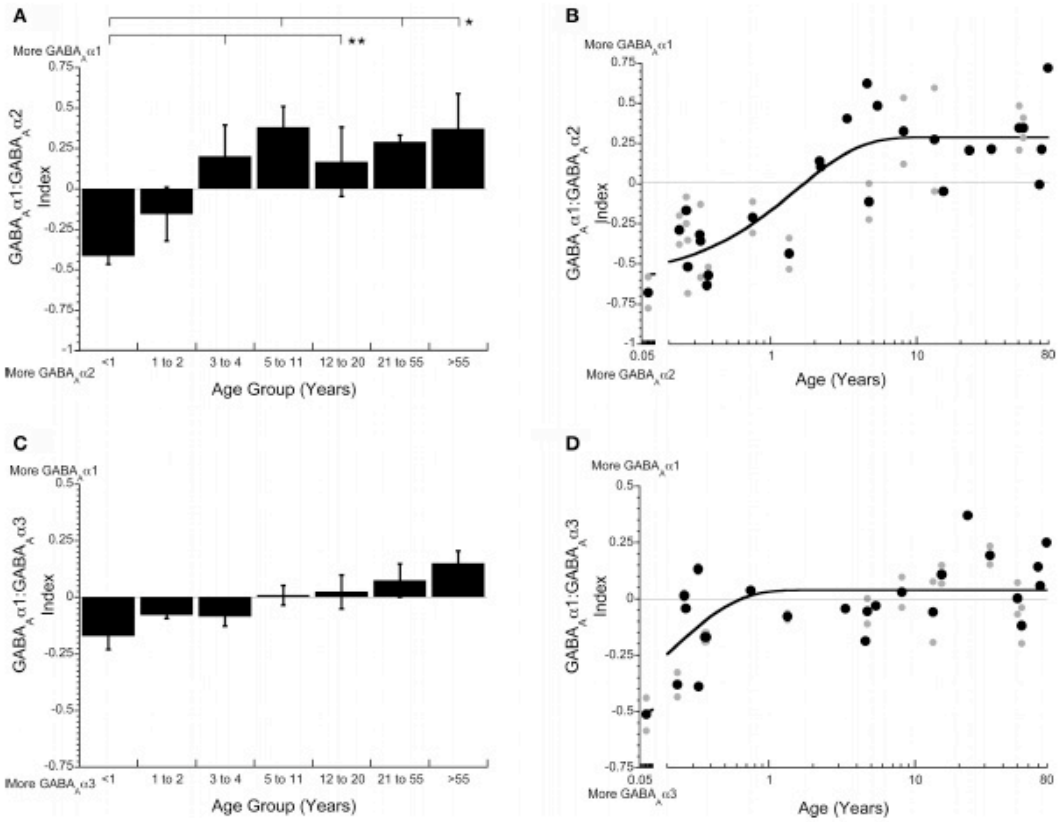

FIGURE 5 | The indices of $GABA_A\alpha1$:$GABA_A\alpha2$ (A,B) and $GABA_A\alpha1$:$GABA_A\alpha3$ (C,D) are important for determining the kinetics and maturation of the $GABA_A$ receptor. The $GABA_A\alpha1$:$GABA_A\alpha2$ index starts in favor of $GABA_A\alpha2$, then shifts to more $GABA_A\alpha1$ in children (3–4 years), reaching the adult balance in younger childhood (3τ = 4.5 years of age, τ = 1.50 years, $R = 0.84$; $p < 0.0001$; **B**). The $GABA_A\alpha1$: $GABA_A\alpha3$ index starts out with more $GABA_A\alpha3$ very early, then quickly shifts to slightly more $GABA_A\alpha1$, reaching adult levels within the first year (3τ = 0.69 years of age, τ = 0.23 years, $R = 0.65$; $p < 0.0001$; **D**). The lines above the histograms identify the groups that were significantly different (Tukey's *post hoc* HSD, $^*p < 0.05$, $^{**}p < 0.02$, $^{***}p < 0.001$) (• average expression for each case; • all runs; solid lines are exponential decay functions).

To examine the overall levels of $GABA_A$ receptors in human V1, we quantified the expression of Gephyrin across the lifespan. Gephyrin is the $GABA_A$ receptor anchoring protein and these expression levels provide an indication of total $GABA_A$ receptor expression. There were significant changes in Gephyrin expression across the lifespan ($p<0.002$). Early in development (<1 year) and for older adults (>55 years), the expression levels for Gephyrin were low. In contrast, during the rest of the lifespan, Gephyrin expression was significantly higher

(~120% increase) and had a peak in expression during childhood (5-11 years) ($p<0.05$; Fig. 6A).

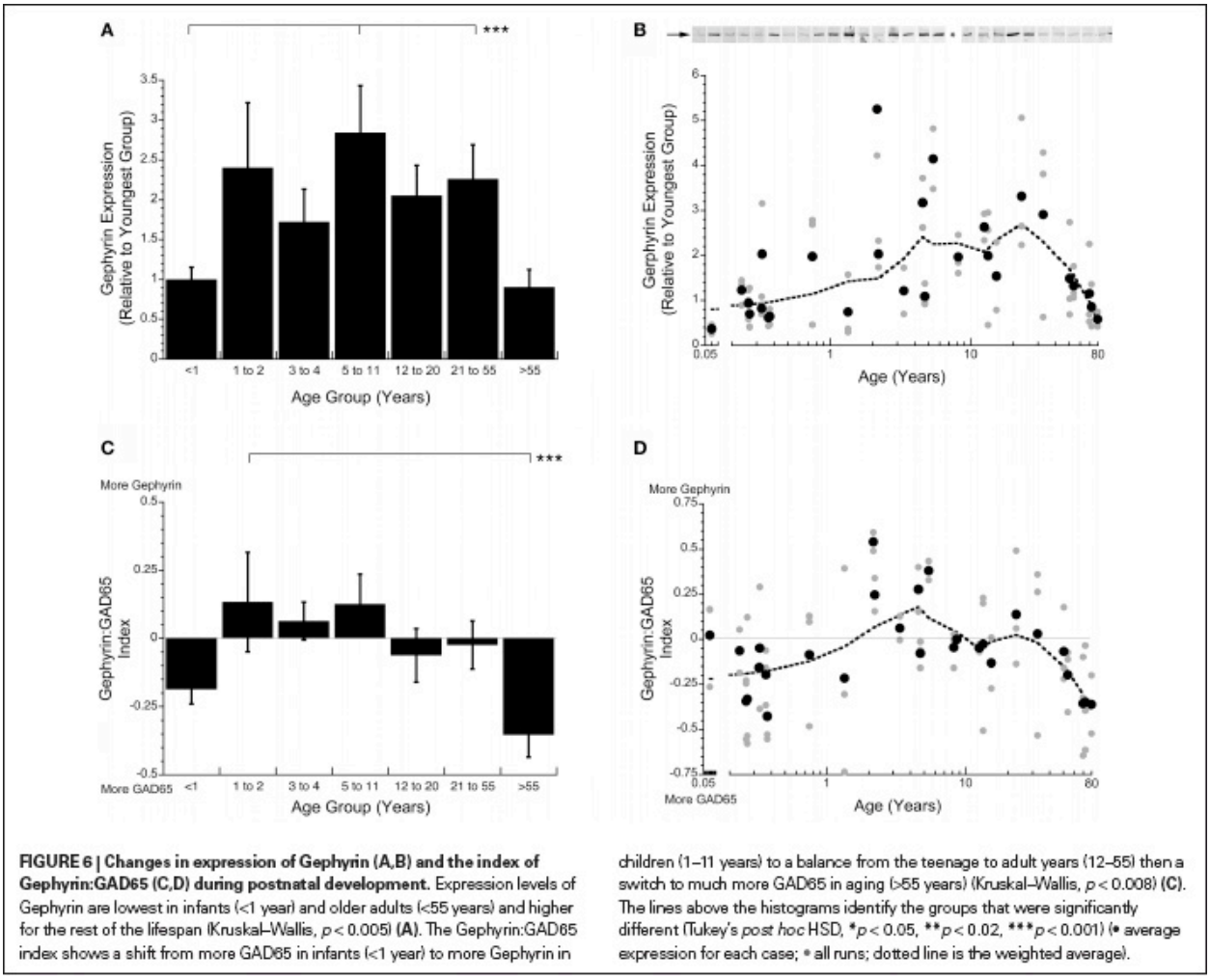

FIGURE 6 | Changes in expression of Gephyrin (A,B) and the index of Gephyrin:GAD65 (C,D) during postnatal development. Expression levels of Gephyrin are lowest in infants (<1 year) and older adults (<55 years) and higher for the rest of the lifespan (Kruskal–Wallis, $p < 0.005$) **(A)**. The Gephyrin:GAD65 index shows a shift from more GAD65 in infants (<1 year) to more Gephyrin in children (1–11 years) to a balance from the teenage to adult years (12–55) then a switch to much more GAD65 in aging (>55 years) (Kruskal–Wallis, $p < 0.008$) **(C)**. The lines above the histograms identify the groups that were significantly different (Tukey's *post hoc* HSD, $*p < 0.05$, $**p < 0.02$, $***p < 0.001$) (• average expression for each case; • all runs; dotted line is the weighted average).

Presynaptic versus Postsynaptic development

To determine the relative contribution of pre- versus post-synaptic components of GABAergic signaling across the lifespan, we calculated a index of Gephyrin:GAD65 expression (Fig. 6). In young infants (< 1 year) this pre- versus post-synaptic balance was in favor of more GAD65, the pre-synaptic side ($p<0.01$). This switched to more Gephyrin during childhood (1 to 11 years of age), then a balance during the teenage and adult years, followed by an abrupt switch to relatively more GAD65 in older adults ($p<0.05$; Fig. 6C, 6D). These changes represent a shift in GABAergic signaling mechanisms from more pre-synaptic, to more post-synaptic, to a

balance, to substantially more pre-synaptic. This index captures an important aspect of the changing nature of the pre- and post-synaptic GABAergic signaling mechanisms in human V1 across the lifespan. There is not a single balance that is maintained across the lifespan.

Discussion

Our study is the first to characterize changes in pre- and post-synaptic components of the GABAergic signaling system across the lifespan in human primary visual cortex. We found a complex pattern of different developmental trajectories among these GABAergic signaling mechanisms. Many of the changes were prolonged and continued well into into the teen, young adult, and even older adult years. For example, the peak of GAD65 expression was not reached until the teen to young adult years before falling off in aging. Thus, the potential to produce the on-demand pool of GABA, which enables repeated waves of phasic inhibition and experience-dependent plasticity, must have a very long developmental time course in human visual cortex. Changes in expression of $GABA_A$ α1 and $GABA_A$ α2 subunits were also prolonged and increased or decreased, respectively, into the teenage years. Comparing the balance between these subunits, however, showed that the switch from relatively more $GABA_A$ α2 to more $GABA_A$ α1 occurred during childhood. This switch is important for understanding changes in GABAergic signaling, since it is the relative balance of the $GABA_A$ subunits that influences the shift to more phasic inhibition (Prenosil et al., 2006). The current results extend our previous study that focused on synaptic changes during the first 5 years of life (Murphy et al., 2005). In addition, we found a number of changes in GABAergic signaling during aging. Gephyrin and GAD65 declined into aging, highlighting that there are both pre- and post-synaptic losses of GABAergic signaling in the aging visual cortex. The changes across the life span in expression of these components of GABA signaling undoubtedly affects experience-dependent plasticity (Hensch, 2005), development and tuning of cortical receptive fields (Fagiolini et al., 2004; Leventhal et al., 2003), and visual perception (Betts et al., 2005; Edden et al., 2009).

There is a heterogenous array of GABAergic neurons and circuits in primate visual cortex (Jones, 1993). The diversity of anatomical and physiological characteristics points to 14-19 different types of GABAergic neurons in the cortex (Gupta et al., 2000). They are spread across all layers of the cortex and in primate visual cortex the largest concentration is in layers II-III and IVa (Beaulieu et al., 1992). The $GABA_A$ receptor is also very diverse. This pentameric receptor has at least 20 different subunits, including α, β, γ, ρ, ε, θ, and π, that combine to make a very wide range of different $GABA_A$ receptors (Seighart, 1995; Cherubini & Conti, 2001; Rudolph et al., 2001). GABAergic interneurons make connections onto specific compartments of cortical pyramidal neurons. Synapses containing α-subunits are differentially distributed across pyramidal neurons with all types of α-subunits found at synapses on dendrites, α1 and α2 are also found on the soma, and only α2 is on the axon initial segment. This diversity of morphologies, receptor compositions, and connectivity patterns confers a wide range of specific functions to the different GABAergic circuits (Hensch, 2005). This heterogeneity poses a challenge for understanding the organization and function of GABAergic signaling.

The diversity in the GABAergic system introduces a number of sources of variability. We found substantial inter-individual variability for expression of the GABAergic proteins in human visual cortex and this probably reflects the heterogeneous nature of the GABAergic system. In addition, we also found substantial variability when measuring the expression levels of the GABAergic proteins from individuals. This measurement variability likely arises because the GABAergic system represents a smaller fraction of the total number of neurons and synapses in visual cortex compared to the excitatory system. This smaller sample size will contribute to increased measurement variability when quantifying GABAergic expression. For example,

GABAergic signaling in primate visual cortex comprises about 20% of the total number of neurons (Beaulieu et al., 1992; Jones, 1993), and an even smaller portion (17%) of the total number of synapses (Beaulieu et al., 1992). Based on the difference in proportion of excitatory versus inhibitory synapses, statistics predicts that there should be about 4.8 times more measurement variability when quantifying expression of GABAergic synaptic proteins. This is very close to the larger measurement variability that we have found when quantifying the expression of inhibitory (gephyrin) versus excitatory (PSD-95) anchoring proteins in rat cortex (Pinto & Murphy, unpublished results). Additional variability in higher mammals will arise from inter-individual differences in the number of inhibitory synapses (Beaulieu & Colonnier, 1985), and the relatively smaller number of inhibitory synapses per neuron in primates compared with rats (Beaulieu et al., 1992). Taken together, the diversity and smaller proportion of GABAergic synapses predicts that there must be substantial variability when measuring expression of GABAergic synaptic proteins. Furthermore, previous studies suggest that there is greater synaptic specialization in non-human primates (Beaulieu et al., 1992) raising the possibility of even greater diversity in human cortex. In spite of these inherent sources of variability, our large data set makes it clear that there are significant changes in GABAergic expression in human visual cortex across the lifespan.

Monyer & Markram (2004) aptly describe studying GABAergic interneurons as a daunting task because of the diverse nature of this system. They also point out that combinatorial approaches are helping to clarify the diversity of GABAergic interneurons. In our study, we used a large number of samples from human visual cortex covering the lifespan to quantify the expression and developmental trajectories of 8 components of the GABAergic system. The

number of proteins quantified allowed us to capture a unique perspective on both pre- and post-synaptic development that would be missed by studying a smaller set of synaptic proteins. Furthermore, by quantifying the expression of GABAergic proteins in a preparation enriched for synaptic proteins (Hollingsworth et al., 1985; Titulaer & Ghijsen, 1997; Quinlan et al., 1999), we are able to tie the current findings closer to functional changes at the synapse. This is especially important for changes that affect experience-dependent plasticity (Quinlan et al., 1999). This contrasts with other approaches, such as measuring mRNA expression of GABAergic components (e.g. Duncan 2010), because it is hard to make the link between mRNA expression and the level of protein expression at the synapse. Finally, the developmental trajectories that we describe reflect the average across the whole group of samples and this type of cross sectional design cannot address how the levels of these GABAergic markers change in an individual. The higher level of variability in expression that we found for older children through young adults suggests that the timing of rapid changes may vary across individuals.

The immunoblotting technique used for the current study does not allow for an analysis of developmental changes in the variety of different morphological types of GABAergic interneurons, specific intracortical inhibitory circuits, or locations of receptor subunits on different compartments of the post-synaptic neuron. It will be important for future studies to extend this work to include anatomical methods that describe and quantify laminar and morphological changes in GABAergic neurons, as well as tracing the specific locations of GABAergic synapses in cortical circuits. These will be challenging studies because of the difficulty obtaining post-mortem tissue that is both appropriate for anatomical investigations and covers a wide range of ages. Despite these obstacles they should be a priority, especially since

site-specific optimization of GABA synapses may trigger experience-dependent plasticity in visual cortex (Katagiri et al., 2007).

Transitional Stages in GABAergic Signaling

The pattern of changes in expression of the GABAergic signaling mechanisms was complex and there was not 1 or 2 key components driving these changes. Instead, each pre- and post-synaptic mechanisms followed different developmental trajectory that combine to create a complex pattern of overall changes. The expression patterns for individual proteins can be characterized as either no change (GAD67, $GABA_A$ α3), a monotonic increase or decrease ($GABA_A$ α1, $GABA_A$ α2), a biphasic increase then decrease (GAD65, Gephyrin), or multiple increases and decreases (VGAT, CB1) across the lifespan. These different developmental trajectories may be linked to functional changes and the different roles that these synaptic proteins play in GABAergic signaling. For example, the multiple increases and decreases found for CB1 may reflect the multiple roles that it has in synaptic development, plasticity, and regulating GABA release (Hajos & Freund, 2002). By calculating a series of indices to quantify the balance between the various pre- and post-synaptic GABAergic mechanisms, we found 3 transitional stages during early development, teen years, or aging when there were large switches in the relative amounts of the components of the GABAergic signaling system. The 3 distinct transitional stages in GABAergic signaling reflect important times during the lifespan when there must be significant changes in the function of GABAergic inhibition. Interestingly, these transition stages line up with time points when visual functions are changing and when the visual system is sensitive to experience-dependent change (Faubert, 2002; Lewis & Maurer, 2005; Maurer et al., 2007a; Maurer et al., 2007b).

The first stage reflects an early developmental transition between neonates/infants (< 2 years) and young children (3-5 years) when there was a switch in composition of the $GABA_A$ receptor. The relative expression switched from more of the immature subunits ($GABA_A$ α2 and $GABA_A$ α3) to more of the mature ($GABA_A$ α1) subunit. The $GABA_A$ α1 subunit has a special role in development of the visual cortex driving experience-dependent plasticity whereas $GABA_A$ α2 modulates neuronal firing (Fagioloini et al., 2004). The kinetics of the $GABA_A$ receptor speed up threefold when the $GABA_A$ α1 subunit dominates (Gingrich et al., 1995) and gamma bursts depend on circuits dominated by $GABA_A$ α1 (Cardin et al., 2009; Sohal et al., 2009). Furthermore, the switch has pharmacological implications as the α2 subunit exhibits the anxiolytic effects of benzodiazepines, whereas α1, α3, and α5 mediate the sedative and amnesic effects (Low et al., 2000, Rudolph et al., 1999). This developmental switch in $GABA_A$ receptor subunits also occurs in rats (Bosman et al., 2002), cats (Chen et al., 2001), and macaque monkeys (Hendrickson et al., 1994). For these species, however, the switch is correlated with different aspects of the critical period. In rats, the switch occurs before the start of the critical period (Heinen et al., 2004), but in cats and macaque monkeys the switch overlaps the critical period for ocular dominance plasticity (Chen et al., 2001; Hendrickson et al., 1994). The current results show that in human V1 this transitional switch in expression of $GABA_A$ receptor subunits spans the critical period, when disrupting vision can cause long lasting changing in visual acuity (Lewis & Maurer, 2005). Perhaps this first stage defines the period of ocular dominance plasticity in human V1.

In the second stage, the teenage transition was a switch from a greater capacity for trafficking GABA (more VGAT) to a greater capacity to produce the on-demand pool of GABA

(more GAD65). In addition, there was a high level of $GABA_A$ α1 expression during this stage. These suggest that in teens and young adults the pool of on-demand GABA can be readily replenished and binds with α1 containing receptors to maintain a high level of phasic inhibition. Perhaps this combination is needed for optimal coding of neural signals, especially during periods of sustained neural activity. Optimal orientation tuning of receptive fields (Leventhal et al., 2003) and perceptual performance on orientation discrimination (Edden et al., 2009) depend on the level of GABA concentration. It seems likely that the high levels of GAD65 and $GABA_A$ α1 at this stage are contributing to optimal visual performance on tasks such as orientation discrimination.

In the third stage, during the transition to older adults, there were 2 switches in the balance between components of the GABAergic signaling system: from greater capacity to produce GABA (more GAD65) to greater capacity to traffic GABA to the synapse (more VGAT); and from relatively more post-synaptic (more Gephyrin) to more pre-synaptic (more GAD65) expression. Both of these changes were large switches from those found for young adults and point to significant changes in functioning of GABAergic synapses in the aging visual cortex. Furthermore, the time course of the GABAergic changes in aging is similar to the decline of visual abilities. The changes could contribute to the loss of orientation tuning (Leventhal et al., 2003) and processing of complex visual stimuli that are particularly vulnerable during aging (Habak & Faubert, 2000; Faubert, 2002). For example, the perception of a moving stimulus in the context of a moving surround is particularly affected in aging (Betts et al, 2005) and a loss of GABA inhibition has been suggested as the mechanism underlying this perceptual loss. It seems

likely that the changes in the balance of GABAergic components at aging synapses contribute to the visual losses that accompany aging.

Links with Experience-Dependent Plasticity

Previous studies have shown that a specific excitatory-inhibitory balance and expression of the $GABA_A$ α1 subunit are required for ocular dominance plasticity in the developing rodent visual cortex (Hensch et al., 1998; Fagiolini et al., 2004). Furthermore, inhibition is abnormal in visual cortex of monocularly deprived (Burchfiel & Duffy, 1981) and strabismic cats (Singer et al., 1980). Our findings suggest that the period of ocular dominance plasticity in the human visual cortex is prolonged. If ocular dominance plasticity follows the development of $GABA_A$ α1 then it would extend through childhood into teenage and possibly even to young adult years. This idea is consistent with the prolonged period of visual changes found in children with cataracts (Lewis & Maurer 2005; Maurer et al., 2007a; Maurer et al., 2007b). Importantly, the current findings indicate that primary visual cortex continues to have the necessary balance of GABAergic signaling mechanisms to mediate experience-dependent plasticity well into the teenage years. In addition, because the development of GAD65 expression may extend into the young adult years it is possible that this affects plasticity in primary visual cortex and contributes to visual recovery promoted by perceptual learning treatment in adults with amblyopia (Levi & Li, 2009). Finally, the losses in aging may contribute to reduced synaptic plasticity and may be part of a more generalized change in the balance of synaptic proteins (Williams et al., 2010) in the aging cortex that could underlie age-related perceptual and cognitive declines.

The prolonged window of GABA changes in human visual cortex provides an opportunity to translate experimental treatments that target GABAergic signaling in the visual system into

therapeutics that may even be useful in treating amblyopia in young adults. For example, new studies have shown that fluoxetine can reinstate ocular dominance plasticity in the adult cortex by reducing intracortical inhibition (Maya Vetencourt et al., 2008; Harauzov et al., 2010). The current study provides the necessary information about GABAergic signaling in human cortex to begin the process of translating the exciting therapies being developed in animal models into effective treatments for amblyopia in humans.

Chapter 5.

Transforming adult plasticity: Changes caused by fluoxetine and altered visual experience

Introduction

The magnitude of plasticity is high during critical periods in development, and the classic critical period is characterized by a rise, peak, and fall of plasticity. Amblyopia is a neurodevelopmental disorder caused by abnormal visual experience during a critical period early in development. Abnormal visual experience during this period results in a shift in cortical responsiveness away from the deprived eye towards the non-deprived eye. Treatments for amblyopia, based primarily on our knowledge of ocular dominance plasticity in animals, require plasticity to facilitate the re-organization of cortical connections. In the western world, most visual abnormalities are corrected early in development, when the degree of plasticity is still high, and severe cases of amblyopia rarely develop. However, in the developing world, these visual abnormalities are often left untreated and manifest into severe cases of amblyopia. Recent work has shown that there is some residual plasticity in the visual system of teenagers and young adults (Ostrovsky et al., 2006), but not to the same extent seen during the critical period. Therefore, a strong need has arisen to develop interventions that re-instate critical period like ocular dominance plasticity in adult visual cortex.

Recently, a number of interventions have tested that show that they are able to re-instate critical period-like ocular dominance plasticity in adult rats. Some of these interventions include chronic fluoxetine administration (Maya Vetencourt et al., 2008), environmental enrichment (Baroncelli et al., 2010), dark rearing (He et al, 2007) and food restriction (Spolidoro et al., 2011). Fluoxetine and environmental enrichment are thought to re-instate ocular dominance plasticity by reducing intracortical inhibition, and increasing BDNF expression (Baroncelli et al., 2010; Maya Vetencourt et al., 2008), while food restriction decreased intracortical inhibition, but

has no effect on BDNF expression (Spolidoro et al., 2011). It is unclear, however, how these interventions effect the excitatory/inhibitory (E-I) balance, or structural elements of the extracellular matrix (ECM), which are the mechanisms known to facilitate, and put the brakes on ocular dominance plasticity, respectively.

The E-I balance, and structural elements of the ECM, such as myelin and perineuronal nets, are known to be the mechanisms that facilitate the onset, and closure of the critical period for ocular dominance plasticity, respectively. The E-I balance is a physiological measure that quantifies the relative contribution of excitation and inhibition. Early in development, the balance is shifted in favor of excitation, and a strong increase in inhibition sets the E-I balance, which triggers the onset of the critical period in rodents (Fagiolini & Hensch, 2000; Maffei & Turrigiano, 2008). Once the E-I balance is set, it persists throughout development and structural elements are responsible for closing the critical period. Structural elements, such as myelin and perineuronal nets close the critical period by putting the brakes on plasticity (Bavelier et al., 2010). They are thought to restrict neuronal reorganization, by inhibiting axonal outgrowth (McGee et al., 2005). These two mechanisms provide a simple view of plasticity, however, many other cellular and molecular interactions contribute to each mechanism.

A conservative set of proteins provides an excellent representation of the complex protein-protein interactions that control the mechanisms of plasticity. At the synaptic level, both pre- and post-synaptic proteins are integral for the physiological E-I balance required to facilitate the onset of the critical period. On the pre-synaptic side, Synapsin is the most specific marker for synapses, it is present at all GABAergic and glutamatergic synapses (Micheva et al., 2010). Synapsin regulates the reserve pool of synaptic vesicle available for exocytosis (Bahler et al.,

1990), and maintains the organization and abundance of synaptic vesicles at pre-synaptic terminals (Bykhovskaia, 2011). Synaptophysin is preferentially located at glutamatergic synapses (Micheva et al., 2010), it regulates the kinetics of synaptic vesicle endocytosis (Kwon & Chapman, 2011), and synaptic vesicle retrieval through its interactions with synaptobrevin (Gordon et al., 2011). Together, synapsin and synaptophysin provide information about the pre-synaptic E-I balance, and both are required for the stabilization of pre-synaptic boutons (Hopf et al., 2002). On the post-synaptic side, PSD-95 and gephyrin are the GluA/GluN and $GABA_A$ receptor scaffolding proteins, respectively. Interactions between PSD-95 and gephyrin regulate the number of excitatory and inhibitory synapses that affect the physiological E-I balance (Keith & El-Husseini, 2008, Lardi-Studler et al., 2007; Prange et al., 2004), required for facilitating the onset of the critical period (Hensch & Fagiolini, 2005; Maffei & Turrigiano, 2008). Outside the synapse, large structural proteins restrict plasticity and put an end to the critical period. Myelin basic protein (MBP) is a structural protein that maintains the compaction of myelin in the central nervous system (Readhead et al., 1990). Myelin is known to be one the main structural elements that put the brakes on plasticity, and closes the critical period for ocular dominance plasticity (Bavelier et al., 2010).

This study aims to determine how fluoxetine effects the two mechanisms known to control the critical period for ocular dominance plasticity. Western blot analysis was used to quantify changes in the expression of the available pool of synapsin, synaptophysin, PSD-95, gephyrin, and MBP. The results from this study support the E-I balance, and MBP as the mechanisms by which fluoxetine re-instates ocular dominance plasticity in adult rats. Fluoxetine facilitates the reinstatement of ocular dominance plasticity by re-setting the E-I balance to a juvenile state. It

also decreases MBP expression, thereby removing the brakes on plasticity. Taken together, fluoxetine re-instates ocular dominance plasticity in adult rats because it modulates the two mechanisms that control the onset and closure of the critical period for ocular dominance plasticity.

Methods

All treatment and surgical procedures were adapted from Maya Vetencourt et al (2010) to re-create the same experimental paradigm.

2.1 Animal treatment and Surgical Procedures

28 long-evans rats were grouped into 4 experimental conditions (Table 1). Animals were group-housed under standard conditions with a 12:12 light/dark cycle. Adult rats at P70 were systemically treated with fluoxetine (0.2 mg/ml drinking water) for 4 weeks.

To assess changes due to a shift in ocular dominance plasticity, one week of was monocular deprivation was performed through eyelid suture at P91. Animals under treatment were briefly anesthetized with isoflurane then monocularly deprived. Eyelid closure was inspected daily and a topical antibiotic was applied to prevent infection.

2.2 Tissue collection

A total of 28 tissue samples were collected from the four experimental groups (Normal, n=6; Monocular Deprivation, n=6; Fluoxetine, n=8; Fluoxetine + Monocular Deprivation, n=8) (Table 1). The rats were euthanized with Euthanol and transcardially perfused with cold 0.1 M PBS (4 ºC) until circulating fluid was cleared. The brain was quickly removed and immersed in cold PBS, a sample was cut out from primary visual cortex, in the hemisphere contralateral to MD (approx. 3 mm X 2 mm) then quickly frozen on dry ice and stored at -80 ºC.

2.3 Tissue sample preparation

Tissue samples (50-100 mg) were suspended in cold homogenization buffer (1 ml buffer:50 mg tissue, 0.5mM DTT, 1mM EDTA, 2 mM EGTA, 10 mM HEPES, 10 mg/L leupeptin, 100nM microcystin, 0.1 mM PMSF, 50 mg/L soybean trypsin inhibitor) and homogenized in a glass-

glass Dounce homogenizer (Kontes, Vineland, NJ). The homogenized sample was removed and added to 10% sodium-dodecyl-sulfate (SDS). Protein concentrations were determined using the bicinchonic acid (BCA) assay guidelines (Pierce, Rockford, IL). A control sample was made by combining a small amount of the prepared tissue sample from each of the 28 samples.

2.4 Immunoblotting

The samples (25 μg) were separated on Sodium-dodecyl-sulfide polyacrylamide gels (SDS-PAGE) and transferred to polyvinylidene difluoride (PVDF-FL) membranes (Millipore, Billerica, MA). Each sample was run multiple times. Blots were pre-incubated in blocking buffer (Odyssey Blocking Buffer 1:1 with PBS) for 1 hour (Li-cor Biosciences; Lincoln, NE), then incubated in primary antibody overnight at 4°C using the following concentrations: GAPDH, 1:4000 (Imgenex, San Diego, CA); Synapsin 1, 1:8000 (Invitrogen, Carlsbad, CA); Synaptophysin, 1:2000 (Sigma-Aldrich, St. Louis, MO); PSD-95, 1:32000 (Millipore, Billerica, MA); Gephyrin, 1:2000 (Millipore, Billerica, MA); Myelin Basic Protein, 1:4000 (Abcam, Cambridge, MA). The blots were washed with phosphate buffer saline containing 0.05% Tween (Sigma, St. Louis, MO) (PBS-T) (3 x 10 min), incubated (1 hour, room temperature) with the appropriate IRDye labeled secondary antibody, (Anti-Mouse, 1:8000, Anti-Rabbit, 1:10,000) (Li-cor Biosciences; Lincoln, NE), and washed in PBS-T (3 x 10 min). The blots were visualized using the Odyssey scanner (Li-cor Biosciences; Lincoln, NE). The combination of the IRDye secondary antibodies and Odyssey scanner system provides a wide linear dynamic range (16-250X chemiluminescence, Schutz-Geschwender et al., 2004) so that both strong and weak bands could be quantified on the same blot. The blots were stripped and prepared to be re-

probed with additional antibodies (Blot Restore Membrane Rejuvenation kit, Chemicon International, Temecula, CA).

2.5 Analysis

To analyze the bands, we scanned the blots (Odyssey Infrared Scanner) and quantified the bands using densitometry (Licor Odyssey Software version 3.0; Li-cor Biosciences; Lincoln, NE). Density profiles were determined by performing a subtraction of the background, integrating pixel intensity across the area of the band, and dividing the intensity by the width of the band to control for variations in lane width. GAPDH normalization was used as the loading control and for each sample the expression of the synaptic proteins was divided by GAPDH expression. The control sample (Mixture of all samples) was run on all gels, and the density of each sample was measured relative to that control.

To visualize changes in the expression between experimental groups, we plotted histograms with the mean and standard error of the mean for each group. The groups were named and color coded as follows -- Normal (Normal, Black); Monocular Deprivation (MD, Red), Fluoxetine (Drug, Grey); Fluoxetine and Monocular Deprivation (Drug+MD, Green). To determine overall changes in expression a one-way ANOVA was performed, and when significant 4 planned pairwise post-hoc comparisons between groups (Normal and MD, Normal and Drug, Normal and Drug+MD, Drug and Drug+MD) were made using an unpaired equal variance student's t-test.

We quantified the relationship between pre- and post-synaptic proteins by calculating 2 indices that measured the changes between the pairs of pre-synaptic (Synapsin and Synaptophsyin) and post-synaptic proteins (PSD-95 and Gephyrin). The indices provide an indication of synaptic function because each pair of proteins is related: Synapsin and

Synaptophysin expression is required for pre-synaptic function and stabilization of pre-synaptic boutons (Hopf et al., 2002); interactions between PSD-95 and Gephyrin regulate the number of excitatory and inhibitory synapses and affect the physiological E-I balance (Keith & El-Husseini, 2008; Lardi-Studler et al., 2007; Prange et al., 2004). In addition, this type of contrast index is a common approach in signal processing to determine the quantity of the signal and here provided an analysis of pre- or post-synaptic function. Pre-Synaptic Index -- [(Synapsin-Synaptophysin)/(Synapsin+Synaptophysin)], Post-Synaptic Index -- [(PSD-95-Gephyrin)/(PSD-95+Gephyrin)]. To determine overall changes in expression a one-way ANOVA was performed, and when significant post-hoc comparisons between groups were made using an unpaired equal variance students t-test.

Results

3.1 GAPDH as Loading Control

We used GAPDH expression as our loading control in this study and examined its expression across the 4 experimental groups. GAPDH is a ubiquitous housekeeping protein involved in glycolysis. We found that there were significant changes in GAPDH expression across the experimental groups (ANOVA: $p<0.0005$). Monocular deprivation significantly reduced GAPDH expression relative to normals (Fig. 1; Student's t-test, $p<0.005$). It was important to normalize our data to GAPDH to ensure all subsequent differences in protein expression reflect actual changes in protein expression, not overall changes in cortical metabolic activity.

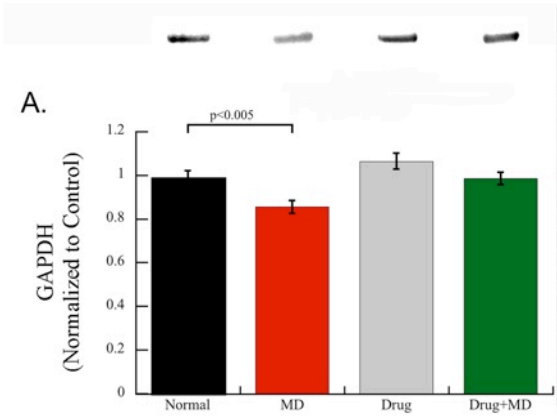

Figure 1.
Expression levels of GAPDH among the experimental groups; Normal (Normal, Black), Monocular Deprivation (MD, Red), Fluoxetine (Drug, Grey), Fluoxetine + Monocular Deprivation (Drug+MD, Green). Example bands for each group are shown above the plot. Mean and standard error of the mean are presented for each experimental group. There were significant differences in GAPDH expression between experimental groups (ANOVA, $p<0.0005$). Monocular deprivation significantly reduced GAPDH expression relative to normally reared animals (Students t-test, $p<0.05$).

3.2 Fluoxetine does not effect pre-synaptic vesicle cycling mechanisms

To examine pre-synaptic changes we quantified the expression of Synapsin and Synaptophysin. Synapsin is the most specific marker for pre-synaptic terminals (Micheva et al., 2010), present at all GABAergic and Glutamategic synapses. Synapsin regulates the reserve pool of synaptic vesicle available for exocytosis (Bahler et al., 1990), and maintains the organization and abundance of synaptic vesicles at pre-synaptic terminals (Bykhovskaia, 2011).

Synaptophysin is preferentially located at glutamatergic synapses (Micheva et al., 2010), it regulates the kinetics of synaptic vesicle endocytosis (Kwon & Chapman, 2011), and synaptic vesicle retrieval through interactions with synaptobrevin (Gordon et al., 2011).

There were no significant changes in Synapsin (Fig. 2A; ANOVA: p=0.99), or Synaptophysin (Fig. 2B; ANOVA: p=0.79) expression between the experimental groups. This suggests that adult plasticity, facilitated by fluoxetine, is not mediated by pre-synaptic vesicle cycling mechanisms.

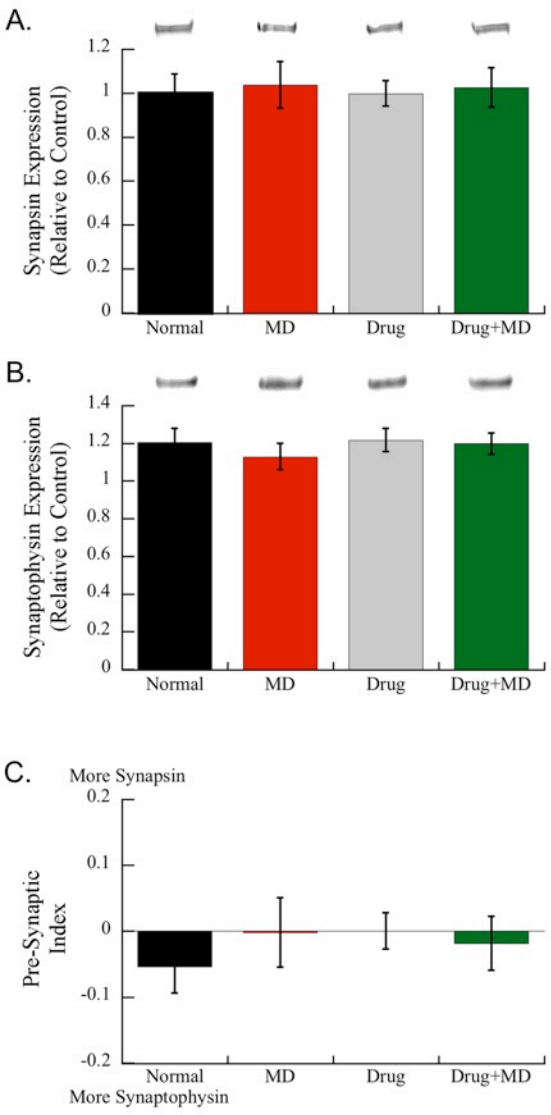

Figure 2.
Expression levels of Synapsin (A), Synaptophysin (B), and the Pre-Synaptic Index (C) among the experimental groups; Normal (Normal, Black), Monocular Deprivation (MD, Red), Fluoxetine (Drug, Grey), Fluoxetine + Monocular Deprivation (Drug+MD, Green). Example bands for each group are shown above the plots for Synapsin (A) and Synaptophysin (B). Mean and standard error of the mean are presented for each experimental group. There were no significant differences in expression of Synapsin (ANOVA, p=0.99), Synaptophysin (ANOVA, p=0.79), or the Pre-Synaptic Index (ANOVA, p=0.77) among the experimental groups.

To address if there were any changes in the relationship between the pair of pre-synaptic proteins, we calculated an index of Synapsin and Synaptophysin expression that quantifies the balance between the pre-synaptic proteins. This index provides a measure of pre-synaptic function, since Synapsin and Synaptophysin expression is required for stabilization of pre-synaptic boutons (Hopf et al., 2002). The index ranges from +1 to -1, with positive values indicating relatively more Synapsin, and negative values indicating relatively more Synaptophysin. In normal animals, expression levels were balanced between Synapsin and Synaptophysin, which is a balance that we would be predicted from our developmental studies (Pinto et al., Submitted). There were no significant changes in expression of the pre-synaptic index between the experimental groups (Fig. 2C; ANOVA: $p=0.77$). This provides further support that pre-synaptic vesicle cycling mechanisms are not effected by fluoxetine driven plasticity in the adult visual cortex.

3.3 Fluoxetine causes robust changes in the post-synaptic density

Both glutamatergic and GABAergic mechanisms are involved in developmental synaptic plasticity, and the E-I balance is required for the initiation of the critical period in visual cortex. To examine changes in glutamatergic and GABAergic mechanisms, we quantified the expression of 2 post-synaptic scaffolding proteins, PSD-95, and Gephyrin. PSD-95 anchors the excitatory GluA and GluN receptors, and is required for receptor function (Beique et al., 2006). Gephyrin anchors the inhibitory $GABA_A$ receptors and is required for the stabilization of GABAergic synapses (Yu et al., 2007). Together, they provide information about the relative number of excitatory and inhibitory synapses (Keith & El-Husseini, 2008) that contribute to the physiological E-I balance required for ocular dominance plasticity (Hensch & Fagiolini, 2005).

We found significant differences in PSD-95 expression between the experimental groups (Fig. 3A; ANOVA: $p<0.001$). Monocular deprivation, or fluoxetine treatment alone had no significant effect on PSD-95 expression relative to normals. However, the group that received fluoxetine treatment and monocular deprivation had a trend towards 50% increased PSD-95 expression relative to normals (Fig. 3A; Student's t-test, $p=0.058$), and a significant 60% increase in expression relative to animals treated with only fluoxetine (Fig. 3A; Student's t-test, $p<0.005$). These results point to the combination of fluoxetine and a change in visual experience driving an increase in expression of excitatory, PSD-95, receptors.

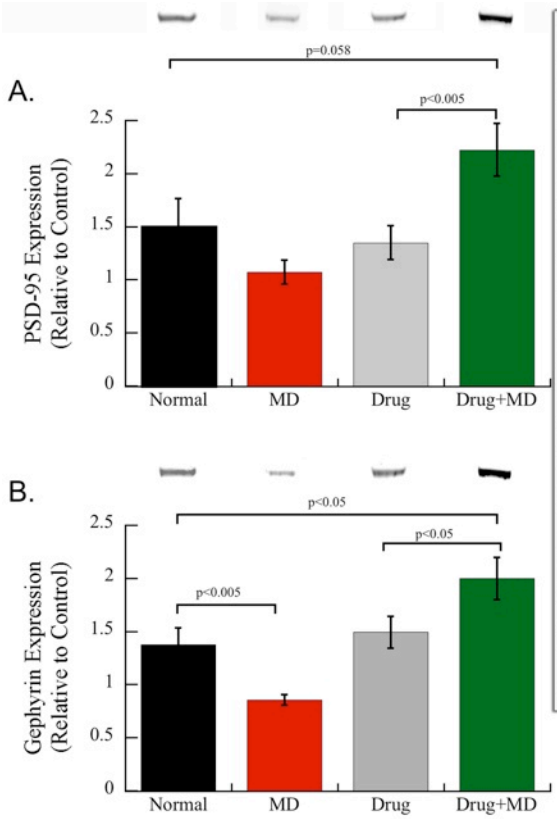

Figure 3.
Expression levels of PSD-95 (A), and Gephyrin (B) among the experimental groups; Normal (Normal, Black), Monocular Deprivation (MD, Red), Fluoxetine (Drug, Grey), Fluoxetine + Monocular Deprivation (Drug+MD, Green). Example bands for each group are shown above the plot. Mean and standard error of the mean are presented for each experimental group. A) There were significant differences in PSD-95 expression between the experimental groups (ANOVA, $p<0.001$). Fluoxetine+Monocular Deprivation increased PSD-95 expression relative to animals treated with Fluoxetine alone (Students t-test, $p<0.005$), and normally reared animals (Students t-test, $p=0.058$). B) There were significant differences in gephyrin expression between the experimental groups (ANOVA, $p<0.0001$). Monocular Deprivation reduced Gephyrin expression relative to normally reared animals (Students t-test, $p<0.005$). Fluoxetine+Monocular Deprivation increased Gephyrin expression relative to normally reared animals (Students t-test, $p<0.05$), and animals treated with Fluoxetine alone (Students t-test, $p<0.05$).

We also found significant differences in Gephyrin expression between the experimental groups (Fig. 3B; ANOVA: $p<0.0001$). Monocular deprivation significantly reduced Gephyrin expression relative to normal (Student's t-test, $p<0.005$), while fluoxetine alone had no effect.

Once again, the group that received fluoxetine treatment and monocular deprivation significantly increased Gephyrin expression relative to normals (Student's t-test, $p<0.05$), and fluoxetine alone (Student's t-test, $p<0.05$). These results provide additional evidence for a combined effect of fluoxetine and monocular deprivation on the expression of receptors. Taken together, these results show that fluoxetine alone does not expression of glutamatergic and GABAergic receptor anchoring proteins, but when combined with monocular deprivation there is a robust upregulation of both excitatory and inhibitory anchoring proteins.

3.4 Fluoxetine re-sets the E-I balance

We next wanted to address the relationship between the pair of post-synaptic proteins to determine if fluoxetine has an effect on the E-I balance. We calculated an index of PSD-95 and Gephyrin, this index provides a relative measure of the number of excitatory and inhibitory synapses that affect the physiological E-I balance (Keith & El-Husseini, 2008; Lardi-Studler et al., 2007; Prange et al., 2004). The index ranges from +1 to -1, with positive values indicating relatively more PSD-95, and negative values indicating relatively more Gephyrin. In normal animals, expression levels were balanced between PSD-95 and Gephyrin, which would be predicted from our developmental studies (Pinto et al., Submitted). There were significant changes in expression between the experimental groups (Fig. 3C; ANOVA, $p<0.005$). Monocular deprivation did not have a significant effect on the E-I balance relative to normals, but fluoxetine significantly shifted the E-I balance towards more Gephyrin expression (Student's t-test, $p<0.05$). Interestingly, the shift in the E-I balance caused by fluoxetine moves the expression level of the E-I balance towards the level seen during the peak of the critical period for ocular dominance plasticity (P25-30) in rat visual cortex (Pinto et al., Submitted). Animals

treated with monocular deprivation and fluoxetine cause a significant shift back to balanced expression relative to fluoxetine alone (Student's t-test, $p<0.02$). These results indicate that fluoxetine facilitates ocular dominance plasticity by re-setting the E-I balance back to levels seen during the critical period.

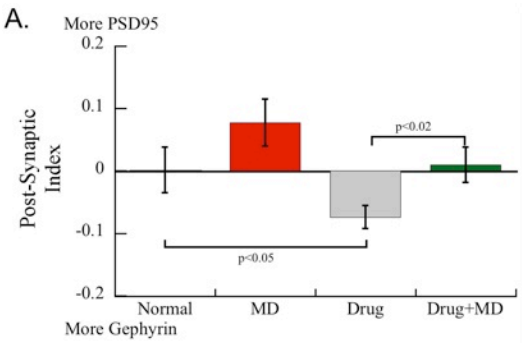

Figure 4.
Expression levels of the Post-Synaptic Index among the experimental groups; Normal (Normal, Black), Monocular Deprivation (MD, Red), Fluoxetine (Drug, Grey), Fluoxetine + Monocular Deprivation (Drug+MD, Green). Mean and standard error of the mean are presented for each experimental group. There were significant differences in expression level between the expreimental groups (ANOVA, $p<0.005$). Fluoxetine shifted the index towards Gephyrin expression relative to normally reared animals (Students t-test, $p<0.05$). Fluoxetine+Monocular Deprivation shifted the index back towards balanced expression relative to animals treated with Fluoxetine alone (Students t-test, $p<0.02$).

3.5 Fluoxetine removes the brakes on plasticity

To address the other mechanisms that control ocular dominance plasticity, the structural brakes on plasticity, we quantified expression of Myelin Basic Protein (MBP) across the experimental groups. MBP is a structural protein that maintains compaction of myelin in the central nervous system (Readhead et al., 1990), which is known to put the brakes on plasticity and close the critical period (Bavelier et al., 2010). It is thought to put the brakes on plasticity by inhibiting neurite outgrowth (McGee et al., 2005), and therefore prevent the formation of new connections. We found that there were significant differences in MBP expression between the experimental groups (Fig. 5; ANOVA: $p<0.05$). Monocular deprivation had no significant effect on MBP expression, however, fluoxetine significantly reduced MBP expression relative to normal (Fig. 5; Student's t-test, $p<0.05$). This points to fluoxetine re-instating ocular dominance

plasticity in rat adult visual cortex by removing the structural brakes on plasticity.

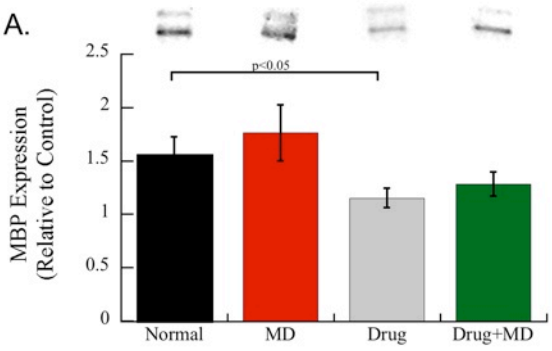

Figure 5.
Expression levels of MBP among the experimental groups; Normal (Normal, Black), Monocular Deprivation (MD, Red), Fluoxetine (Drug, Grey), Fluoxetine + Monocular Deprivation (Drug+MD, Green). Example bands for each group are shown above the plot. Mean and standard error of the mean are presented for each experimental group. There were significant differences in MBP expression among the experimental groups (ANOVA, $p<0.05$). Fluoxetine reduced MBP expression relative to normally reared animals (Students t-test, $p<0.05$).

Discussion

The results of this study support a conclusion that fluoxetine reinstates ocular dominance plasticity in adult rats by re-setting the E-I balance to juvenile levels, and reducing MBP expression. These two mechanisms have been proposed as ways to promote plasticity in adulthood (Bavelier et al., 2010). The E-I balance is known to facilitate the onset of the critical period for ocular dominance plasticity during early development. Early in development, the balance is shifted in favor of excitation, but a strong increase in inhibition bring it to a balance, and facilitates the onset of the critical period for ocular dominance plasticity. In this study, we quantified PSD-95 and Gephyrin expression, which is a measure of the relative number of excitatory and inhibitory synapses that contribute to the physiological E-I balance. Normally reared animals had balanced expression between PSD-95 and Gephyrin, and is consistent with previous measures in rats around that age (Pinto et al,. Submitted). A month of fluoxetine shifted the balance towards more Gephyrin, to a level comparable to that of a rat at P30 (Pinto et al., Submitted), the timing of the peak of the critical period for ocular dominance plasticity. This suggests that one way fluoxetine re-instates ocular dominance plasticity is by by shifting the E-I balance back in favor of Gephyrin. Structural elements of the ECM, such as myelin and perineuronal nets close the critical period by putting the brakes on plasticity. Removing these brakes on plasticity in young animals prevents the closure of the critical period (Bavelier et al., 2010). One of the primary brakes on plasticity, myelin basic protein, acts by inhibiting neurite outgrowth (McGee et al., 2005). In this study, we found the fluoxetine reduces MBP expression, thereby reducing the brakes on plasticity. Taken together, the results from this study show that

fluoxetine re-instates ocular dominance plasticity in the visual cortex of adult rats, by re-setting the E-I balance to a juvenile state, and reducing the structural brakes on plasticity.

We found increased expression levels of PSD-95 and Gephyrin in animals that received fluoxetine and monocular deprivation. Increased PSD-95 and Gephyrin expression levels are known to stabilize excitatory and inhibitory synapses, respectively. PSD-95 determines the strength of glutamatergic synapses (Schnell et al., 2002; Stein et al., 2003; Ehrlich & Malinow, 2004; Colledge et al., 2003), and post-synaptic densities compete for the available pool of PSD-95 (Gray et al., 2006). Gephyrin cluster density is negatively correlated with motility (Kuriu et al., 2012), therefore increased expression helps to stabilize Gephyrin levels at inhibitory synapses. In human visual cortex, there is an increase in expression of PSD-95 and Gephyrin in older children (Pinto et al., Submitted), which is the end of susceptibility for developing amblyopia. This suggests that one week of monocular deprivation after chronic fluoxetine administration may be sufficient to at least begin to stabilize newly formed excitatory and inhibitory connections.

Rats between the age of P70 and P100 are typically considered adults because they become sexually mature at approximately P50, in contrast, humans become sexually mature relatively later in development at about the start of the teenage years (Quinn, 2005). Recent work from our lab (Pinto et al., Submitted), has shown that rate of maturation of the visual cortex between rat and humans follows a different timeline. We found that when comparing the development of total synaptic protein expression between rat and human visual cortex, that the maturation of rat visual cortex proceeds slower than previously thought. According to our measure of total protein expression in visual cortex, the visual cortex of a rat between P70-100 is similar to a human

visual cortex between 8-9 years of age. Other studies (Romijn et al., 1991) that compared the development of the cerebral cortex between rat and humans found that across all 4 factors studied, the cerebral cortex matures slower than would be expected from the timing of sexual maturity. Therefore, the rats used for this study, and other studies that have demonstrated the re-instatement of ocular dominance plasticity in adult rats, have cerebral cortices, and more specifically, visual cortex that more closely resemble older children than adults. This suggests that these rats may have some sub-threshold level of residual plasticity when fluoxetine administration began at P70. This may explain why a number of interventions have been able to re-instate ocular dominance plasticity in rats at this age. To determine the viability of these interventions on re-instating ocular dominance plasticity in the visual cortex of adult humans, it may be useful to recreate these paradigms in older rats.

The results from this study have shown how fluoxetine re-instates ocular dominance plasticity in the visual cortex of adult rats by altering the two mechanisms that control the critical period. This study concludes that fluoxetine affects the relative balance between the number of excitatory and inhibitory synapses, however, it does not address what is changing within these synapses. Changes within the synapse can affect functional properties that are not reflected by simply measuring the protein expression levels. Receptor subunit composition, and the relative balance between receptors and vesicles has the ability to alter the kinetics at the synapse, and susceptibility to change. For example, there is a well known developmental shift in the GluN2 subtype, from 2B to 2A, which is associated with faster receptor kinetics, a reduction in the susceptibility to change, this is known to occur during the critical period for ocular dominance plasticity. Addressing how fluoxetine affects the functioning of excitatory and inhibitory

synapses is an important next step in refining our understanding of how drugs such as fluoxetine can re-instate critical period like plasticity in adult visual cortex.

Chapter 6.

General Discussion

In this thesis, I have made significant contributions towards the understanding of how synaptic plasticity mechanisms develop across species. This thesis shows that using a conservative set of synaptic proteins provides a tremendous amount of information about cortical development. Each chapter of this thesis demonstrates how a subset of functionally relevant synaptic proteins can provide insights about the mechanisms controlling developmental synaptic plasticity. This is an important finding because it shows that proteomic studies can be hypothesis driven by using a small, conservative set of functionally relevant proteins. The second chapter of this thesis quantified expression of Synapsin, Synaptophysin, PSD-95, and Gephyrin, and demonstrated that rat cortex develops as an integrated network. The 4 proteins in this study provided a framework to compare the development among the 3 cortical areas, and was designed to address the question, does the cortex develop as a cascade or integrated network. The third chapter of this thesis quantified the same 4 synaptic proteins to quantify the development of human visual cortex, and then compared the development of visual cortex between rat and human. This study showed that the development of rat and human visual cortex can be directly compared using total protein expression, and that the composition of visual cortex of rats from P11-P93 is analogous to human visual cortex from birth to 8.5 years of age. The fourth chapter of this thesis quantified the development of GABAergic mechanisms in human visual cortex across the lifespan. The goal of this chapter was to quantify mechanisms that are known to control the critical period. GAD65 is required for ocular dominance plasticity (Iwai et al., 2003), CB1 activation regulates activity dependent synaptic plasticity (Sjostrom et al., 2003), and the GABAAa1 subunit is necessary for critical period plasticity (Fagiolini et al., 2004). We found that there were prolonged and complex patterns of change in the GABAergic mechanisms in

human visual cortex across the lifespan. The fifth chapter of this thesis quantified the expression Synapsin, Synaptophysin, PSD-95, Gephyrin, and MBP, to determine how fluoxetine affects the mechanisms that control the induction and closure of the critical period for ocular dominance plasticity. This study showed that fluoxetine re-instates plasticity in adult rat visual cortex by removing the brakes on plasticity (MBP), and re-setting the E-I balance to juvenile levels.

The significance of this thesis pushes beyond the traditional scope of the field by directly quantifying the relationship between the development of total protein expression in rat and human visual cortex. Transforming age relationships between rodents and humans has been a focus in the scientific community for a number of years. Rodents are typically used to model the human biological system, therefore, it is vital to understand the biological relationship between the species, to accurately model the human condition. Transforming age between the species is especially important in understanding developmental disorders such as amblyopia, and developmental process, such as synaptic plasticity. There are two previous studies (Quinn, 2005; Romijn et al., 1991), that aimed to translate age between rodent and human, by using evidence from previous studies. Both studies focused on determining how many rat days equate to one human year, given a number of biological factors. What these studies neglect to account for is differences, or changes in the rate of development. The comparison by Quinn (2005), looked at 6 biological factors of development to determine how many rat days equate to one human year: total lifespan (13.8 days), nursing period (42.4 days), prepubescent period (4.3 days), adolescent period (10.5 days), reproductive senescence (11.8 days), and post-senescence (17.1 days). The range of comparisons from this study indicates that a rat at P100 is equivalent to a human from 2.4-23.3 years, depending on the measure. The comparison by Romijn et al, (1991), looked at 4

factors of cerebral cortex development to determine when rats were equivalent to humans at birth; synapse formation at P14.9, GAD activity at P8.2, cholineacetyltransferase at P20.4, and electrical activity P12.5. Extrapolating these factors, indicates that a rat at P100 has a cerebral cortex that is equivalent to humans from 4.9-12.2 years of age. If we take into account all the measures from Quinn (2005), and Romijn et al., (1991), except prepubescent period, we find that a rat at P100 is child-like. This is an important point, since the majority of experimental paradigms working on re-instating ocular dominance plasticity in "adult rats", use rats in the P70-100 age range. The rational for using rats in this age range comes from comparative studies on sexual maturity (prepubescent period). Sexual maturity is reached in rats at P50, and humans at 11.5 years, therefore it is assumed that a rat at P100 is adult-like. This signifies the importance of comparing between these species on a systems by systems basis, which is exactly what I have done in chapter 3 of this thesis. Using total protein expression as the metric, I have shown that rat and human visual cortex is comparable at visually relevant milestone in development. The transformation showed that visual cortex of rats between P70-100 are comparable to older children, which suggests their visual cortices are not "adult-like". This is a significant contribution to the field of neuroscience, since the visual system of rodents has provided tremendous amounts of information on neuroplasticity. This transformation of visual cortex age between rats and humans will serve as a framework for developing future therapies that aim to more effectively treat neuroplasticity based disorders, such as amblyopia.

There are strengths and limitations associates with all scientific research. There are two main methodological strengths associated with work completed as part of this thesis. The first major strength is the technique used, Western blotting. This technique quantifies protein

expression levels, which are the functional units at the synapse. It is also a technique that is quite robust and allowed for quantification of a number of samples, and is easily translatable across species. The second major strength is the model fitting approach, which provides the optimal mathematical relationship between variables, and provides a strong basis for comparison among variables, studies, and species. There are also some limitations that the techniques used in this thesis provide. First, our measure of the E-I balance is a proxy for the physiological E-I balance that is known to facilitate the onset of the critical period for ocular dominance plasticity. Second, Western blotting does not provide any information regarding where the synaptic changes are occurring, such as neuron type, or cortical layer, which could be addressed by anatomical studies.

The work completed as part of this thesis lays the foundation for future studies that help advance the field. There are 4 distinct sets of studies that can branch out from this work.

The first is to perform anatomical studies, using the same markers in visual cortex to identify the location of synaptic change. This will help to elucidate the neuronal subtype and cortical layer where the changes are occurring, and further our understanding of developmental synaptic plasticity.

The second would be to study the same set of 4 synaptic proteins (Synapsin, Synaptophysin, PSD-95, and Gephyrin) in rat aging, to determine if total protein expression is comparable in rat and human aging. Chapter 2 only extended until P93, which is fairly early in the lifespan of the rat, and it is worth evaluating whether total protein expression in rat visual cortex declines in aging as it does in humans. This will help to clarify if rat and human visual

cortex truly follows the same trajectory throughout the lifespan, or if their paths diverge after early development.

The third would be to translate the developmental trajectories of the markers that control the brakes on plasticity, such as MBP and other extra-cellular matrix proteins. This is a complimentary set of proteins known to play a significant role in developmental synaptic plasticity, that will help to determine if another subset of proteins can translate as well between the species.

The fourth is to determine if the paradigms that have shown they can re-instate ocular dominance plasticity in rats from P70-100, can re-instate ocular dominance plasticity in rats with adult-like visual cortices. One of the paradigms, environmental enrichment, has shown that it is effective in re-instating ocular dominance plasticity in older rats (22-23 month; Scali et al., 2012). This raises the possibility that the other paradigms could have the same efficacy, and should be thoroughly tested before these paradigms are applied to humans. The work from this thesis has provided a strong foundation, and members of the lab are already pursuing some of the branches mentioned above.

References

Akbarian S, Huntsman MM, Kim JJ, Tafazzoli A, Potkin SG, Bunney WE, Jr., Jones EG (1995) GABAA receptor subunit gene expression in human prefrontal cortex: comparison of schizophrenics and controls. Cereb Cortex 5:550-560.

Akbarian S, Kim JJ, Potkin SG, Hagman JO, Tafazzoli A, Bunney WE, Jr., Jones EG (1995) Gene expression for glutamic acid decarboxylase is reduced without loss of neurons in prefrontal cortex of schizophrenics. Arch Gen Psychiatry 52:258-266.

Andersen SL (2003) Trajectories of brain development: point of vulnerability or window of opportunity? Neurosci Biobehav Rev 27:3-18.

Antonini A, Stryker MP (1993) Rapid remodeling of axonal arbors in the visual cortex. Science 260:1819-1821.

Bahler M, Benfenati F, Valtorta F, Greengard P (1990) The synapsins and the regulation of synaptic function. Bioessays 12:259-263.

Baroncelli L, Sale A, Viegi A, Maya Vetencourt JF, De Pasquale R, Baldini S, Maffei L (2010) Experience-dependent reactivation of ocular dominance plasticity in the adult visual cortex. Exp Neurol 226:100-109.

Bavelier D, Levi DM, Li RW, Dan Y, Hensch TK (2010) Removing brakes on adult brain plasticity: from molecular to behavioral interventions. J Neurosci 30:14964-14971.

Bayes A, Grant SG (2009) Neuroproteomics: understanding the molecular organization and complexity of the brain. Nat Rev Neurosci 10:635-646.

Beique JC, Lin DT, Kang MG, Aizawa H, Takamiya K, Huganir RL (2006) Synapse-specific regulation of AMPA receptor function by PSD-95. Proc Natl Acad Sci U S A 103:19535-19540.

Ben-Ari Y (2002) Excitatory actions of gaba during development: the nature of the nurture. Nat Rev Neurosci 3:728-739.

Ben-Ari Y, Gaiarsa JL, Tyzio R, Khazipov R (2007) GABA: a pioneer transmitter that excites immature neurons and generates primitive oscillations. Physiol Rev 87:1215-1284.

Benes FM, Berretta S (2001) GABAergic interneurons: implications for understanding schizophrenia and bipolar disorder. Neuropsychopharmacology 25:1-27.

Bernard C, Milh M, Morozov YM, Ben-Ari Y, Freund TF, Gozlan H (2005) Altering cannabinoid signaling during development disrupts neuronal activity. Proc Natl Acad Sci U S A 102:9388-9393.

Bettler B, Kaupmann K, Mosbacher J, Gassmann M (2004) Molecular structure and physiological functions of GABA(B) receptors. Physiol Rev 84:835-867.

Betts LR, Taylor CP, Sekuler AB, Bennett PJ (2005) Aging reduces center-surround antagonism in visual motion processing. Neuron 45:361-366.

Boeckers TM, Kreutz MR, Winter C, Zuschratter W, Smalla KH, Sanmarti-Vila L, Wex H, Langnaese K, Bockmann J, Garner CC, Gundelfinger ED (2001) Proline-rich synapse-associated protein-1/cortactin binding protein 1 (ProSAP1/CortBP1) is a PDZ-domain protein highly enriched in the postsynaptic density. Ann Anat 183:101.

Boeckers TM, Winter C, Smalla KH, Kreutz MR, Bockmann J, Seidenbecher C, Garner CC, Gundelfinger ED (1999) Proline-rich synapse-associated proteins ProSAP1 and ProSAP2 interact with synaptic proteins of the SAPAP/GKAP family. Biochem Biophys Res Commun 264:247-252.

Bosman LW, Rosahl TW, Brussaard AB (2002) Neonatal development of the rat visual cortex: synaptic function of GABAA receptor alpha subunits. J Physiol 545:169-181.

Braddick O, Atkinson J, Julesz B, Kropfl W, Bodis-Wollner I, Raab E (1980) Cortical binocularity in infants. Nature 288:363-365.

Braddick O, Wattam-Bell J, Day J, Atkinson J (1983) The onset of binocular function in human infants. Hum Neurobiol 2:65-69.

Bykhovskaia M (2011) Synapsin regulation of vesicle organization and functional pools. Semin Cell Dev Biol 22:387-392.

Cardin JA, Carlen M, Meletis K, Knoblich U, Zhang F, Deisseroth K, Tsai LH, Moore CI (2009) Driving fast-spiking cells induces gamma rhythm and controls sensory responses. Nature 459:663-667.

Cheetham CE, Fox K (2010) Presynaptic development at L4 to l2/3 excitatory synapses follows different time courses in visual and somatosensory cortex. J Neurosci 30:12566-12571.

Chen L, Yang C, Mower GD (2001) Developmental changes in the expression of GABA(A) receptor subunits (alpha(1), alpha(2), alpha(3)) in the cat visual cortex and the effects of dark rearing. Brain Res Mol Brain Res 88:135-143.

Cherubini E, Conti F (2001) Generating diversity at GABAergic synapses. Trends Neurosci 24:155-162.

Church DM et al. (2009) Lineage-specific biology revealed by a finished genome assembly of the mouse. PLoS Biol 7:e1000112.

Colledge M, Snyder EM, Crozier RA, Soderling JA, Jin Y, Langeberg LK, Lu H, Bear MF, Scott JD (2003) Ubiquitination regulates PSD-95 degradation and AMPA receptor surface expression. Neuron 40:595-607.

Collins MO, Husi H, Yu L, Brandon JM, Anderson CNG, Blackstock WP, Choudhary JS, Grant SGN (2006) Molecular characterization and comparison of the components and multiprotein complexes in the postsynaptic proteome. Journal of Neurochemistry 97:16-23.

Courage ML, Adams RJ (1990) Visual acuity assessment from birth to three years using the acuity card procedure: cross-sectional and longitudinal samples. Optom Vis Sci 67:713-718.

Dhossche D, Applegate H, Abraham A, Maertens P, Bland L, Bencsath A, Martinez J (2002) Elevated plasma gamma-aminobutyric acid (GABA) levels in autistic youngsters: stimulus for a GABA hypothesis of autism. Med Sci Monit 8:PR1-6.

Dobie FA, Craig AM (2011) Inhibitory synapse dynamics: coordinated presynaptic and postsynaptic mobility and the major contribution of recycled vesicles to new synapse formation. J Neurosci 31:10481-10493.

Dorrn AL, Yuan K, Barker AJ, Schreiner CE, Froemke RC (2010) Developmental sensory experience balances cortical excitation and inhibition. Nature 465:932-936.

Duffy FH, Burchfiel JL, Conway JL (1976) Bicuculline reversal of deprivation amblyopia in the cat. Nature 260:256-257.

Duncan CE, Webster MJ, Rothmond DA, Bahn S, Elashoff M, Shannon Weickert C Prefrontal GABA(A) receptor alpha-subunit expression in normal postnatal human development and schizophrenia. J Psychiatr Res.

Durand GM, Kovalchuk Y, Konnerth A (1996) Long-term potentiation and functional synapse induction in developing hippocampus. Nature 381:71-75.

Edden RA, Muthukumaraswamy SD, Freeman TC, Singh KD (2009) Orientation discrimination performance is predicted by GABA concentration and gamma oscillation frequency in human primary visual cortex. J Neurosci 29:15721-15726.

Ehrlich I, Malinow R (2004) Postsynaptic density 95 controls AMPA receptor incorporation during long-term potentiation and experience-driven synaptic plasticity. J Neurosci 24:916-927.

Ellemberg D, Lewis TL, Dirks M, Maurer D, Ledgeway T, Guillemot JP, Lepore F (2004) Putting order into the development of sensitivity to global motion. Vision Res 44:2403-2411.

Ellemberg D, Lewis TL, Liu CH, Maurer D (1999) Development of spatial and temporal vision during childhood. Vision Res 39:2325-2333.

Engel D, Pahner I, Schulze K, Frahm C, Jarry H, Ahnert-Hilger G, Draguhn A (2001) Plasticity of rat central inhibitory synapses through GABA metabolism. J Physiol 535:473-482.

Epelbaum M, Milleret C, Buisseret P, Dufier JL (1993) The sensitive period for strabismic amblyopia in humans. Ophthalmology 100:323-327.

Esclapez M, Tillakaratne NJ, Kaufman DL, Tobin AJ, Houser CR (1994) Comparative localization of two forms of glutamic acid decarboxylase and their mRNAs in rat brain supports the concept of functional differences between the forms. J Neurosci 14:1834-1855.

Essrich C, Lorez M, Benson JA, Fritschy JM, Luscher B (1998) Postsynaptic clustering of major GABAA receptor subtypes requires the gamma 2 subunit and gephyrin. Nat Neurosci 1:563-571.

Fagiolini M, Fritschy JM, Low K, Mohler H, Rudolph U, Hensch TK (2004) Specific GABAA circuits for visual cortical plasticity. Science 303:1681-1683.

Fagiolini M, Hensch TK (2000) Inhibitory threshold for critical-period activation in primary visual cortex. Nature 404:183-186.

Fagiolini M, Pizzorusso T, Berardi N, Domenici L, Maffei L (1994) Functional postnatal development of the rat primary visual cortex and the role of visual experience: dark rearing and monocular deprivation. Vision Res 34:709-720.

Fatemi SH, Halt AR, Stary JM, Kanodia R, Schulz SC, Realmuto GR (2002) Glutamic acid decarboxylase 65 and 67 kDa proteins are reduced in autistic parietal and cerebellar cortices. Biol Psychiatry 52:805-810.

Faubert J (2002) Visual perception and aging. Can J Exp Psychol 56:164-176.

Feldblum S, Dumoulin A, Anoal M, Sandillon F, Privat A (1995) Comparative distribution of GAD65 and GAD67 mRNAs and proteins in the rat spinal cord supports a differential regulation of these two glutamate decarboxylases in vivo. J Neurosci Res 42:742-757.

Feldblum S, Erlander MG, Tobin AJ (1993) Different distributions of GAD65 and GAD67 mRNAs suggest that the two glutamate decarboxylases play distinctive functional roles. J Neurosci Res 34:689-706.

Filiou MD, Bisle B, Reckow S, Teplytska L, Maccarrone G, Turck CW (2010) Profiling of mouse synaptosome proteome and phosphoproteome by IEF. Electrophoresis 31:1294-1301.

Fox K (1992) A critical period for experience-dependent synaptic plasticity in rat barrel cortex. J Neurosci 12:1826-1838.

Geerts H (2009) Of mice and men: bridging the translational disconnect in CNS drug discovery. CNS Drugs 23:915-926.

Gillberg C, Billstedt E (2000) Autism and Asperger syndrome: coexistence with other clinical disorders. Acta Psychiatr Scand 102:321-330.

Gingrich KJ, Roberts WA, Kass RS (1995) Dependence of the GABAA receptor gating kinetics on the alpha-subunit isoform: implications for structure-function relations and synaptic transmission. J Physiol 489 (Pt 2):529-543.

Goldberg MC, Maurer D, Lewis TL, Brent HP (2001) The influence of binocular visual deprivation on the development of visual-spatial attention. Dev Neuropsychol 19:53-81.

Gordon SL, Leube RE, Cousin MA (2011) Synaptophysin is required for synaptobrevin retrieval during synaptic vesicle endocytosis. J Neurosci 31:14032-14036.

Gray NW, Weimer RM, Bureau I, Svoboda K (2006) Rapid redistribution of synaptic PSD-95 in the neocortex in vivo. PLoS Biol 4:e370.

Gronborg M, Pavlos NJ, Brunk I, Chua JJ, Munster-Wandowski A, Riedel D, Ahnert-Hilger G, Urlaub H, Jahn R (2010) Quantitative comparison of glutamatergic and GABAergic synaptic vesicles unveils selectivity for few proteins including MAL2, a novel synaptic vesicle protein. J Neurosci 30:2-12.

Guo Y, Kaplan IV, Cooper NG, Mower GD (1997) Expression of two forms of glutamic acid decarboxylase (GAD67 and GAD65) during postnatal development of the cat visual cortex. Brain Res Dev Brain Res 103:127-141.

Habak C, Faubert J (2000) Larger effect of aging on the perception of higher-order stimuli. Vision Res 40:943-950.

Hanover JL, Huang ZJ, Tonegawa S, Stryker MP (1999) Brain-derived neurotrophic factor overexpression induces precocious critical period in mouse visual cortex. J Neurosci 19:RC40.

Harauzov A, Spolidoro M, DiCristo G, De Pasquale R, Cancedda L, Pizzorusso T, Viegi A, Berardi N, Maffei L Reducing intracortical inhibition in the adult visual cortex promotes ocular dominance plasticity. J Neurosci 30:361-371.

He HY, Ray B, Dennis K, Quinlan EM (2007) Experience-dependent recovery of vision following chronic deprivation amblyopia. Nat Neurosci 10:1134-1136.

Heinen K, Bosman LW, Spijker S, van Pelt J, Smit AB, Voorn P, Baker RE, Brussaard AB (2004) GABAA receptor maturation in relation to eye opening in the rat visual cortex. Neuroscience 124:161-171.

Held R, Birch E, Gwiazda J (1980) Stereoacuity of human infants. Proc Natl Acad Sci U S A 77:5572-5574.

Hendrickson A, March D, Richards G, Erickson A, Shaw C (1994) Coincidental appearance of the alpha 1 subunit of the GABA-A receptor and the type I benzodiazepine receptor near birth in macaque monkey visual cortex. Int J Dev Neurosci 12:299-314.

Hendry SH, Jones EG (1986) Reduction in number of immunostained GABAergic neurones in deprived-eye dominance columns of monkey area 17. Nature 320:750-753.

Henne WM, Boucrot E, Meinecke M, Evergren E, Vallis Y, Mittal R, McMahon HT (2010) FCHo proteins are nucleators of clathrin-mediated endocytosis. Science 328:1281-1284.

Hensch TK (2005) Critical period mechanisms in developing visual cortex. Curr Top Dev Biol 69:215-237.

Hensch TK, Fagiolini M (2005) Excitatory-inhibitory balance and critical period plasticity in developing visual cortex. Prog Brain Res 147:115-124.

Hensch TK, Fagiolini M, Mataga N, Stryker MP, Baekkeskov S, Kash SF (1998) Local GABA circuit control of experience-dependent plasticity in developing visual cortex. Science 282:1504-1508.

Hicks SP, D'Amato CJ (1968) Cell migrations to the isocortex in the rat. Anat Rec 160:619-634.

Hikosaka O, Wurtz RH (1985) Modification of saccadic eye movements by GABA-related substances. I. Effect of muscimol and bicuculline in monkey superior colliculus. J Neurophysiol 53:266-291.

Hollingsworth EB, McNeal ET, Burton JL, Williams RJ, Daly JW, Creveling CR (1985) Biochemical characterization of a filtered synaptoneurosome preparation from guinea pig cerebral cortex: cyclic adenosine 3':5'-monophosphate-generating systems, receptors, and enzymes. J Neurosci 5:2240-2253.

Hopf FW, Waters J, Mehta S, Smith SJ (2002) Stability and plasticity of developing synapses in hippocampal neuronal cultures. J Neurosci 22:775-781.

Hornung JP, Fritschy JM (1996) Developmental profile of GABAA-receptors in the marmoset monkey: expression of distinct subtypes in pre- and postnatal brain. J Comp Neurol 367:413-430.

Hubel DH, Wiesel TN (1962) Receptive fields, binocular interaction and functional architecture in the cat's visual cortex. J Physiol 160:106-154.

Hubel DH, Wiesel TN (1963) Receptive Fields of Cells in Striate Cortex of Very Young, Visually Inexperienced Kittens. J Neurophysiol 26:994-1002.

Hubel DH, Wiesel TN (1970) The period of susceptibility to the physiological effects of unilateral eye closure in kittens. J Physiol 206:419-436.

Huntsman MM, Munoz A, Jones EG (1999) Temporal modulation of GABA(A) receptor subunit gene expression in developing monkey cerebral cortex. Neuroscience 91:1223-1245.

Huttenlocher PR (1990) Morphometric study of human cerebral cortex development. Neuropsychologia 28:517-527.

Huttenlocher PR, Dabholkar AS (1997) Regional differences in synaptogenesis in human cerebral cortex. J Comp Neurol 387:167-178.

Huttenlocher PR, de Courten C (1987) The development of synapses in striate cortex of man. Hum Neurobiol 6:1-9.

Huttner WB, Schiebler W, Greengard P, De Camilli P (1983) Synapsin I (protein I), a nerve terminal-specific phosphoprotein. III. Its association with synaptic vesicles studied in a highly purified synaptic vesicle preparation. J Cell Biol 96:1374-1388.

Ikeda M, Toyoda H, Yamada J, Okabe A, Sato K, Hotta Y, Fukuda A (2003) Differential development of cation-chloride cotransporters and Cl- homeostasis contributes to

differential GABAergic actions between developing rat visual cortex and dorsal lateral geniculate nucleus. Brain Res 984:149-159.

Isaac JT, Crair MC, Nicoll RA, Malenka RC (1997) Silent synapses during development of thalamocortical inputs. Neuron 18:269-280.

Isaac JT, Nicoll RA, Malenka RC (1995) Evidence for silent synapses: implications for the expression of LTP. Neuron 15:427-434.

Issa NP, Trachtenberg JT, Chapman B, Zahs KR, Stryker MP (1999) The critical period for ocular dominance plasticity in the Ferret's visual cortex. J Neurosci 19:6965-6978.

Iwai Y, Fagiolini M, Obata K, Hensch TK (2003) Rapid critical period induction by tonic inhibition in visual cortex. J Neurosci 23:6695-6702.

Jackson Alexander C, Nicoll Roger A (2011) The Expanding Social Network of Ionotropic Glutamate Receptors: TARPs and Other Transmembrane Auxiliary Subunits. Neuron 70:178-199.

Jacob TC, Bogdanov YD, Magnus C, Saliba RS, Kittler JT, Haydon PG, Moss SJ (2005) Gephyrin regulates the cell surface dynamics of synaptic GABAA receptors. J Neurosci 25:10469-10478.

Jahn R, Schiebler W, Ouimet C, Greengard P (1985) A 38,000-dalton membrane protein (p38) present in synaptic vesicles. Proc Natl Acad Sci U S A 82:4137-4141.

Jando G, Miko-Barath E, Marko K, Hollody K, Torok B, Kovacs I (2012) Early-onset binocularity in preterm infants reveals experience-dependent visual development in humans. Proc Natl Acad Sci U S A 109:11049-11052.

Jones EG (1993) GABAergic neurons and their role in cortical plasticity in primates. Cereb Cortex 3:361-372.

Kanonidou E (2011) Amblyopia: a mini review of the literature. Int Ophthalmol 31:249-256.

Katagiri H, Fagiolini M, Hensch TK (2007) Optimization of somatic inhibition at critical period onset in mouse visual cortex. Neuron 53:805-812.

Katona I, Sperlagh B, Sik A, Kafalvi A, Vizi ES, Mackie K, Freund TF (1999) Presynaptically located CB1 cannabinoid receptors regulate GABA release from axon terminals of specific hippocampal interneurons. J Neurosci 19:4544-4558.

Keech RV, Kutschke PJ (1995) Upper age limit for the development of amblyopia. J Pediatr Ophthalmol Strabismus 32:89-93.

Keith D, El-Husseini A (2008) Excitation Control: Balancing PSD-95 Function at the Synapse. Front Mol Neurosci 1:4.

Kern JK, Trivedi MH, Grannemann BD, Garver CR, Johnson DG, Andrews AA, Savla JS, Mehta JA, Schroeder JL (2007) Sensory correlations in autism. Autism 11:123-134.

Kirkwood A, Bear MF (1994) Hebbian synapses in visual cortex. J Neurosci 14:1634-1645.

Kirmse K, Witte OW, Holthoff K (2011) GABAergic depolarization during early cortical development and implications for anticonvulsive therapy in neonates. Epilepsia 52:1532-1543.

Kneussel M, Brandstatter JH, Laube B, Stahl S, Muller U, Betz H (1999) Loss of postsynaptic GABA(A) receptor clustering in gephyrin-deficient mice. J Neurosci 19:9289-9297.

Kornau HC, Schenker LT, Kennedy MB, Seeburg PH (1995) Domain interaction between NMDA receptor subunits and the postsynaptic density protein PSD-95. Science 269:1737-1740.

Kovacs I, Kozma P, Feher A, Benedek G (1999) Late maturation of visual spatial integration in humans. Proc Natl Acad Sci U S A 96:12204-12209.

Kuriu T, Yanagawa Y, Konishi S (2012) Activity-dependent coordinated mobility of hippocampal inhibitory synapses visualized with presynaptic and postsynaptic tagged-molecular markers. Mol Cell Neurosci 49:184-195.

Kwon Sung E, Chapman Edwin R (2011) Synaptophysin Regulates the Kinetics of Synaptic Vesicle Endocytosis in Central Neurons. Neuron 70:847-854.

Lang T, Jahn R (2008) Core proteins of the secretory machinery. Handb Exp Pharmacol:107-127.

Lardi-Studler B, Smolinsky B, Petitjean CM, Koenig F, Sidler C, Meier JC, Fritschy JM, Schwarz G (2007) Vertebrate-specific sequences in the gephyrin E-domain regulate cytosolic aggregation and postsynaptic clustering. J Cell Sci 120:1371-1382.

Law AJ, Weickert CS, Webster MJ, Herman MM, Kleinman JE, Harrison PJ (2003) Expression of NMDA receptor NR1, NR2A and NR2B subunit mRNAs during development of the human hippocampal formation. Eur J Neurosci 18:1197-1205.

LeBlanc JJ, Fagiolini M Autism: a "critical period" disorder? Neural Plast 2011:921680.

Levartovsky S, Oliver M, Gottesman N, Shimshoni M (1995) Factors affecting long term results of successfully treated amblyopia: initial visual acuity and type of amblyopia. Br J Ophthalmol 79:225-228.

Leventhal AG, Wang Y, Pu M, Zhou Y, Ma Y (2003) GABA and its agonists improved visual cortical function in senescent monkeys. Science 300:812-815.

Levi DM, Li RW (2009) Perceptual learning as a potential treatment for amblyopia: a mini-review. Vision Res 49:2535-2549.

Lewis TL, Maurer D (2005) Multiple sensitive periods in human visual development: evidence from visually deprived children. Dev Psychobiol 46:163-183.

Liao D, Hessler NA, Malinow R (1995) Activation of postsynaptically silent synapses during pairing-induced LTP in CA1 region of hippocampal slice. Nature 375:400-404.

Lidow MS, Goldman-Rakic PS, Rakic P (1991) Synchronized overproduction of neurotransmitter receptors in diverse regions of the primate cerebral cortex. Proc Natl Acad Sci U S A 88:10218-10221.

Liu D, Diorio J, Tannenbaum B, Caldji C, Francis D, Freedman A, Sharma S, Pearson D, Plotsky PM, Meaney MJ (1997) Maternal care, hippocampal glucocorticoid receptors, and hypothalamic-pituitary-adrenal responses to stress. Science 277:1659-1662.

Liu X, Somel M, Tang L, Yan Z, Jiang X, Guo S, Yuan Y, He L, Oleksiak A, Zhang Y, Li N, Hu Y, Chen W, Qiu Z, Paabo S, Khaitovich P (2012) Extension of cortical synaptic development distinguishes humans from chimpanzees and macaques. Genome Res 22:611-622.

Loring JF, Paszty C, Rose A, McIntosh TK, Murai H, Pierce JE, Schramm SR, Wymore K, Lee VM, Trojanowski JQ, Peterson KR (1996) Rational design of an animal model for Alzheimer's disease: introduction of multiple human genomic transgenes to reproduce AD pathology in a rodent. Neurobiol Aging 17:173-182.

Low K, Crestani F, Keist R, Benke D, Brunig I, Benson JA, Fritschy JM, Rulicke T, Bluethmann H, Mohler H, Rudolph U (2000) Molecular and neuronal substrate for the selective attenuation of anxiety. Science 290:131-134.

Maffei A, Nelson SB, Turrigiano GG (2004) Selective reconfiguration of layer 4 visual cortical circuitry by visual deprivation. Nat Neurosci 7:1353-1359.

Maffei A, Turrigiano G (2008) The age of plasticity: developmental regulation of synaptic plasticity in neocortical microcircuits. Prog Brain Res 169:211-223.

Marco EJ, Hinkley LB, Hill SS, Nagarajan SS Sensory processing in autism: a review of neurophysiologic findings. Pediatr Res 69:48R-54R.

Maurer D, Mondloch CJ, Lewis TL (2007) Effects of early visual deprivation on perceptual and cognitive development. Prog Brain Res 164:87-104.

Maurer D, Mondloch CJ, Lewis TL (2007) Sleeper effects. Dev Sci 10:40-47.

Maya Vetencourt JF, Sale A, Viegi A, Baroncelli L, De Pasquale R, O'Leary OF, Castren E, Maffei L (2008) The antidepressant fluoxetine restores plasticity in the adult visual cortex. Science 320:385-388.

McGee AW, Yang Y, Fischer QS, Daw NW, Strittmatter SM (2005) Experience-driven plasticity of visual cortex limited by myelin and Nogo receptor. Science 309:2222-2226.

McIntire SL, Reimer RJ, Schuske K, Edwards RH, Jorgensen EM (1997) Identification and characterization of the vesicular GABA transporter. Nature 389:870-876.

Meaney MJ (2001) Maternal care, gene expression, and the transmission of individual differences in stress reactivity across generations. Annu Rev Neurosci 24:1161-1192.

Micheva KD, Busse B, Weiler NC, O'Rourke N, Smith SJ (2010) Single-synapse analysis of a diverse synapse population: proteomic imaging methods and markers. Neuron 68:639-653.

Minelli A, Alonso-Nanclares L, Edwards RH, DeFelipe J, Conti F (2003) Postnatal development of the vesicular GABA transporter in rat cerebral cortex. Neuroscience 117:337-346.

Monroy E, Hernández-Torres E, Flores G (2010) Maternal separation disrupts dendritic morphology of neurons in prefrontal cortex, hippocampus, and nucleus accumbens in male rat offspring. Journal of Chemical Neuroanatomy 40:93-101.

Morishita H, Hensch TK (2008) Critical period revisited: impact on vision. Curr Opin Neurobiol 18:101-107.

Mower GD (1991) The effect of dark rearing on the time course of the critical period in cat visual cortex. Brain Res Dev Brain Res 58:151-158.

Murphy KM, Beston BR, Boley PM, Jones DG (2005) Development of human visual cortex: a balance between excitatory and inhibitory plasticity mechanisms. Dev Psychobiol 46:209-221.

Murphy KM, Mitchell DE (1986) Bilateral amblyopia after a short period of reverse occlusion in kittens. Nature 323:536-538.

Murphy KM, Mitchell DE (1991) Vernier acuity of normal and visually deprived cats. Vision Res 31:253-266.

Naisbitt S, Kim E, Tu JC, Xiao B, Sala C, Valtschanoff J, Weinberg RJ, Worley PF, Sheng M (1999) Shank, a novel family of postsynaptic density proteins that binds to the NMDA receptor/PSD-95/GKAP complex and cortactin. Neuron 23:569-582.

Olsen RW, Sieghart W (2009) GABA A receptors: subtypes provide diversity of function and pharmacology. Neuropharmacology 56:141-148.

Olson CR, Freeman RD (1980) Profile of the sensitive period for monocular deprivation in kittens. Exp Brain Res 39:17-21.

Ostrovsky Y, Andalman A, Sinha P (2006) Vision following extended congenital blindness. Psychol Sci 17:1009-1014.

Pearse BM (1976) Clathrin: a unique protein associated with intracellular transfer of membrane by coated vesicles. Proc Natl Acad Sci U S A 73:1255-1259.

Pinto JG, Hornby KR, Jones DG, Murphy KM (2010) Developmental changes in GABAergic mechanisms in human visual cortex across the lifespan. Front Cell Neurosci 4:16.

Pinto JG, Jones DG, Murphy KM (2013) Comparing development of synaptic proteins in rat visual, somatosensory, and frontal cortex.

Pizzorusso T, Medini P, Landi S, Baldini S, Berardi N, Maffei L (2006) Structural and functional recovery from early monocular deprivation in adult rats. Proc Natl Acad Sci U S A 103:8517-8522.

Prajneshu (1998) A nonlinear statistical model for aphid population growth. J Indian Soc Agric Statist 51.

Prange O, Wong TP, Gerrow K, Wang YT, El-Husseini A (2004) A balance between excitatory and inhibitory synapses is controlled by PSD-95 and neuroligin. Proc Natl Acad Sci U S A 101:13915-13920.

Pritchett DB, Sontheimer H, Shivers BD, Ymer S, Kettenmann H, Schofield PR, Seeburg PH (1989) Importance of a novel GABAA receptor subunit for benzodiazepine pharmacology. Nature 338:582-585.

Pucadyil TJ, Schmid SL (2009) Conserved functions of membrane active GTPases in coated vesicle formation. Science 325:1217-1220.

Quinlan EM, Olstein DH, Bear MF (1999) Bidirectional, experience-dependent regulation of N-methyl-D-aspartate receptor subunit composition in the rat visual cortex during postnatal development. Proc Natl Acad Sci U S A 96:12876-12880.

Quinn R (2005) Comparing rat's to human's age: how old is my rat in people years? Nutrition 21:775-777.

Readhead C, Takasashi N, Shine HD, Saavedra R, Sidman R, Hood L (1990) Role of myelin basic protein in the formation of central nervous system myelin. Ann N Y Acad Sci 605:280-285.

Renger JJ, Egles C, Liu G (2001) A developmental switch in neurotransmitter flux enhances synaptic efficacy by affecting AMPA receptor activation. Neuron 29:469-484.

Romijn HJ, Hofman MA, Gramsbergen A (1991) At what age is the developing cerebral cortex of the rat comparable to that of the full-term newborn human baby? Early Hum Dev 26:61-67.

Rumpel S, Hatt H, Gottmann K (1998) Silent synapses in the developing rat visual cortex: evidence for postsynaptic expression of synaptic plasticity. J Neurosci 18:8863-8874.

Rust NC, Schultz SR, Movshon JA (2002) A reciprocal relationship between reliability and responsiveness in developing visual cortical neurons. J Neurosci 22:10519-10523.

Sagne C, El Mestikawy S, Isambert MF, Hamon M, Henry JP, Giros B, Gasnier B (1997) Cloning of a functional vesicular GABA and glycine transporter by screening of genome databases. FEBS Lett 417:177-183.

Schnell E, Sizemore M, Karimzadegan S, Chen L, Bredt DS, Nicoll RA (2002) Direct interactions between PSD-95 and stargazin control synaptic AMPA receptor number. Proc Natl Acad Sci U S A 99:13902-13907.

Schutz-Geschwender A, Yonghong Z, Holt T, McDermitt D, Olive DM. 2004. Quantitative, Two-Color Western Blot Detection With Inrared Fluorescence. LI-COR Biosciences.

Sengpiel F, Vorobyov V (2005) Intracortical origins of interocular suppression in the visual cortex. J Neurosci 25:6394-6400.

Shatz CJ, Stryker MP (1978) Ocular dominance in layer IV of the cat's visual cortex and the effects of monocular deprivation. J Physiol 281:267-283.

Shaw C, Cameron L, March D, Cynader M, Zielinski B, Hendrickson A (1991) Pre- and postnatal development of GABA receptors in Macaca monkey visual cortex. J Neurosci 11:3943-3959.

Sieghart W (1995) Structure and pharmacology of gamma-aminobutyric acidA receptor subtypes. Pharmacol Rev 47:181-234.

Sigel E (2002) Mapping of the benzodiazepine recognition site on GABA(A) receptors. Curr Top Med Chem 2:833-839.

Sillito AM (1974) Proceedings: Modification of the receptive field properties of neurones in the visual cortex by bicuculline, a GABA antagonist. J Physiol 239:36P-37P.

Simmons DR, Robertson AE, McKay LS, Toal E, McAleer P, Pollick FE (2009) Vision in autism spectrum disorders. Vision Res 49:2705-2739.

Sjostrom PJ, Turrigiano GG, Nelson SB (2003) Neocortical LTD via coincident activation of presynaptic NMDA and cannabinoid receptors. Neuron 39:641-654.

Skoczenski AM, Norcia AM (2002) Late maturation of visual hyperacuity. Psychol Sci 13:537-541.

Smith GB, Olsen RW (1995) Functional domains of GABAA receptors. Trends Pharmacol Sci 16:162-168.

Smith SL, Trachtenberg JT (2007) Experience-dependent binocular competition in the visual cortex begins at eye opening. Nat Neurosci 10:370-375.

Sohal VS, Zhang F, Yizhar O, Deisseroth K (2009) Parvalbumin neurons and gamma rhythms enhance cortical circuit performance. Nature 459:698-702.

Song H, Ming G, Fon E, Bellocchio E, Edwards RH, Poo M (1997) Expression of a putative vesicular acetylcholine transporter facilitates quantal transmitter packaging. Neuron 18:815-826.

Spolidoro M, Baroncelli L, Putignano E, Maya-Vetencourt JF, Viegi A, Maffei L (2011) Food restriction enhances visual cortex plasticity in adulthood. Nat Commun 2:320.

Stein V, House DR, Bredt DS, Nicoll RA (2003) Postsynaptic density-95 mimics and occludes hippocampal long-term potentiation and enhances long-term depression. J Neurosci 23:5503-5506.

Stern EA, Maravall M, Svoboda K (2001) Rapid development and plasticity of layer 2/3 maps in rat barrel cortex in vivo. Neuron 31:305-315.

Suudhof TC (2008) Neurotransmitter release. Handb Exp Pharmacol:1-21.

Takamori S et al. (2006) Molecular anatomy of a trafficking organelle. Cell 127:831-846.

Tiihonen J, Kuikka J, Rasanen P, Lepola U, Koponen H, Liuska A, Lehmusvaara A, Vainio P, Kononen M, Bergstrom K, Yu M, Kinnunen I, Akerman K, Karhu J (1997) Cerebral benzodiazepine receptor binding and distribution in generalized anxiety disorder: a fractal analysis. Mol Psychiatry 2:463-471.

Traub LM (2003) Sorting it out: AP-2 and alternate clathrin adaptors in endocytic cargo selection. J Cell Biol 163:203-208.

Tretter V, Revilla-Sanchez R, Houston C, Terunuma M, Havekes R, Florian C, Jurd R, Vithlani M, Michels G, Couve A, Sieghart W, Brandon N, Abel T, Smart TG, Moss SJ (2009) Deficits in spatial memory correlate with modified {gamma}-aminobutyric acid type A receptor tyrosine phosphorylation in the hippocampus. Proc Natl Acad Sci U S A 106:20039-20044.

Trinidad JC, Thalhammer A, Specht CG, Lynn AJ, Baker PR, Schoepfer R, Burlingame AL (2008) Quantitative analysis of synaptic phosphorylation and protein expression. Mol Cell Proteomics 7:684-696.

Tsumoto T, Sato H (1985) GABAergic inhibition and orientation selectivity of neurons in the kitten visual cortex at the time of eye opening. Vision Res 25:383-388.

Tyagarajan SK, Fritschy JM GABA(A) receptors, gephyrin and homeostatic synaptic plasticity. J Physiol 588:101-106.

Ungewickell E, Ungewickell H, Holstein SE, Lindner R, Prasad K, Barouch W, Martin B, Greene LE, Eisenberg E (1995) Role of auxilin in uncoating clathrin-coated vesicles. Nature 378:632-635.

Vaegan, Taylor D (1979) Critical period for deprivation amblyopia in children. Trans Ophthalmol Soc U K 99:432-439.

Volk DW, Austin MC, Pierri JN, Sampson AR, Lewis DA (2000) Decreased glutamic acid decarboxylase67 messenger RNA expression in a subset of prefrontal cortical gamma-aminobutyric acid neurons in subjects with schizophrenia. Arch Gen Psychiatry 57:237-245.

Wang BS, Sarnaik R, Cang J Critical period plasticity matches binocular orientation preference in the visual cortex. Neuron 65:246-256.

Wiedenmann B, Franke WW (1985) Identification and localization of synaptophysin, an integral membrane glycoprotein of Mr 38,000 characteristic of presynaptic vesicles. Cell 41:1017-1028.

Wiesel TN, Hubel DH (1963) Single-Cell Responses in Striate Cortex of Kittens Deprived of Vision in One Eye. J Neurophysiol 26:1003-1017.

Williams K, Irwin DA, Jones DG, Murphy KM (2010) Dramatic Loss of Ube3A Expression during Aging of the Mammalian Cortex. Front Aging Neurosci 2:18.

Witkin JM, Tzavara ET, Nomikos GG (2005) A role for cannabinoid CB1 receptors in mood and anxiety disorders. Behav Pharmacol 16:315-331.

Wojcik SM, Rhee JS, Herzog E, Sigler A, Jahn R, Takamori S, Brose N, Rosenmund C (2004) An essential role for vesicular glutamate transporter 1 (VGLUT1) in postnatal development and control of quantal size. Proc Natl Acad Sci U S A 101:7158-7163.

Yan XX, Zheng DS, Garey LJ (1992) Prenatal development of GABA-immunoreactive neurons in the human striate cortex. Brain Res Dev Brain Res 65:191-204.

Yu W, Jiang M, Miralles CP, Li RW, Chen G, de Blas AL (2007) Gephyrin clustering is required for the stability of GABAergic synapses. Mol Cell Neurosci 36:484-500.